AD-777 496

PREDICTION OF GEAR-MESH-INDUCED HIGH-FREQUENCY VIBRATION SPECTRA IN GEARED POWER TRAINS

Alston L. Gu, et al

Mechanical Technology, Incorporated

Prepared for:

Army Air Mobility Research and Development Laboratory

January 1974

DISTRIBUTED BY:

NTIS

National Technical Information Service
U. S. DEPARTMENT OF COMMERCE
5285 Port Royal Road, Springfield Va. 22151

Unclassified
Security Classification

AD 777496

DOCUMENT CONTROL DATA - R & D

(Security classification of title, body of abstract and indexing annotation must be entered when the overall report is classified)

1. ORIGINATING ACTIVITY (Corporate author) Mechanical Technology Incorporated 968 Albany-Shaker Road Latham, New York 12110	2a. REPORT SECURITY CLASSIFICATION Unclassified 2b. GROUP

3. REPORT TITLE

PREDICTION OF GEAR-MESH-INDUCED HIGH-FREQUENCY VIBRATION SPECTRA IN GEARED POWER TRAINS

4. DESCRIPTIVE NOTES (Type of report and inclusive dates)
Technical Report

5. AUTHOR(S) (First name, middle initial, last name)

Alston L. Gu
Robert H. Badgley

6. REPORT DATE	7a. TOTAL NO. OF PAGES	7b. NO. OF REFS
January 1974	92	13

8a. CONTRACT OR GRANT NO. DAAJ02-72-C-0040	9a. ORIGINATOR'S REPORT NUMBER(S) USAAMRDL Technical Report 74-5
b. PROJECT NO. 1G162207AA72	
c.	9b. OTHER REPORT NO(S) (Any other numbers that may be assigned this report) MTI Report 73TR28
d.	

10. DISTRIBUTION STATEMENT

Approved for public release; distribution unlimited.

11. SUPPLEMENTARY NOTES	12. SPONSORING MILITARY ACTIVITY Eustis Directorate U.S. Army Air Mobility Research and Development Laboratory, Fort Eustis, Va.

13. ABSTRACT Characteristics of vibration spectra induced by gear meshes in both single gear reductions and planetary gear reductions have been investigated. Methods have been developed to analyze the planet-pass induced vibrations which exist in normal planetary gear reduction systems. It is found that the planet-pass vibration sideband frequencies occur both below and above the base signal at integer multiples of planet-pass frequency and that the sideband amplitudes may exceed that of the base signal. The effect of planet pair phasing on the vibration sideband spectra has been determined for the CH-47 helicopter forward rotor drive transmission first-stage planetary reduction. A computer-implemented analysis has been established for predicting vibration sidebands produced by variations in centerline distance, tooth transmitted force, and tooth support discontinuities for single gear mesh systems. The sidebands are normally found at mesh frequency harmonics plus and minus integer multiples of the frequency of variation of the gear parameters. The sideband amplitudes depend on the magnitude of variation of the gear parameters. The vibration sideband spectra produced by spiral bevel gear shaft runout, externally-imposed tooth mesh force variation, and a decrease in support stiffness over a number of consecutive ring gear teeth have been obtained for gear meshes in the CH-47 helicopter forward rotor drive transmission. The sideband analysis is useful both for designing low-vibration gear systems by properly controlling various gear parameters, and for identifying the existence of several types of gear problems such as gear runout, high dynamic tooth force, and tooth cracks.

Reproduced by
NATIONAL TECHNICAL
INFORMATION SERVICE
U S Department of Commerce
Springfield VA 22151

DD FORM 1 NOV 65 1473 REPLACES DD FORM 1473, 1 JAN 64, WHICH IS OBSOLETE FOR ARMY USE.

Unclassified
Security Classification

Unclassified
Security Classification

14. KEY WORDS	LINK A		LINK B		LINK C	
	ROLE	WT	ROLE	WT	ROLE	WT
GEAR-MESH-INDUCED VIBRATIONS						
PLANET-PASS EXCITATION IN REDUCTION GEARS						
VIBRATION SPECTRA OF GEAR SYSTEMS						
DESIGN OF GEAR SYSTEMS						
DIAGNOSIS OF GEAR SYSTEMS						

Unclassified
Security Classification

ia

DEPARTMENT OF THE ARMY
U. S. ARMY AIR MOBILITY RESEARCH & DEVELOPMENT LABORATORY
EUSTIS DIRECTORATE
FORT EUSTIS, VIRGINIA 23604

The research described herein was conducted by Mechanical Technology Incorporated under the terms of Contract DAAJ02-72-C-0040. The work was performed under the technical management of Mr. Leroy T. Burrows, Technology Applications Division, Eustis Directorate.

During the past decade, vibration and noise measurements and data reduction procedures have improved to the point where it can be (and has been) clearly shown that noise and vibration are directly relatable to each other. Moreover, many noise components have been shown to be directly relatable to the gear mesh frequencies in such drive trains, and analytical methods have been formulated to help understand and control them. These methods deal with the mechanical vibrations of the gearbox components. Other significant signals that are present, however, are not directly relatable to the mesh frequencies. Some of these signals, called "sidebands", have been found to occur in tests of helicopter rotor-drive gearboxes.

The major aims of this study were as follows:

1. Using existing measured and calculated CH-47 ring gear acceleration data together with sideband amplitude prediction methods presently under development, the contractor was (a) to investigate CH-47 lower planetary mesh planet-pass sideband amplitudes for several lower planet-to-ring gear mesh relationships in order to determine sensitivity of sidebands to planet phasing, (b) to identify other design parameters expected to be useful in controlling planet-pass sidebands and describe their effects and importance, and (c) to draw conclusions concerning mechanisms producing planet-pass sidebands.

2. The computer program entitled GEARO, which is in the possession of the contractor and the Government, was to be modified and extended.

Appropriate technical personnel of this directorate have reviewed this report and concur with the conclusions contained herein.

Project 1G162207AA72
Contract DAAJ02-72-C-0040
USAAMRDL Technical Report 74-5
January 1974

PREDICTION OF GEAR-MESH-INDUCED HIGH-FREQUENCY VIBRATION SPECTRA IN GEARED POWER TRAINS

MTI Report 73TR28

By

Alston L. Gu
Robert H. Badgley

Prepared by

Mechanical Technology Incorporated
Latham, New York

for

EUSTIS DIRECTORATE
U.S. ARMY AIR MOBILITY RESEARCH AND DEVELOPMENT LABORATORY
FORT EUSTIS, VIRGINIA

Approved for public release;
distribution unlimited.

SUMMARY

Users of geared power trains have begun to recognize the importance of the high-frequency vibrations which are present in virtually all operating gearboxes: these vibrations are the key to understanding the gearbox condition in real time, a problem of considerable current importance. An immediate outward indication of the presence of such vibrations is the noise produced by a gearbox. Even the untrained ear can distinguish the presence of signals which arise in the gearbox. (Sensors are of course required to obtain information of the quality required for engineering purposes.)

During the past decade, vibration and noise measurements and data reduction procedures have improved to the point where it can be (and has been) clearly shown that noise and vibration are directly relatable to each other. Moreover, many noise components have been shown to be directly relatable to the gear mesh frequencies in such drive trains, and analytical methods have been formulated to help understand and control them. These methods deal with the mechanical vibrations of the gearbox components.

Other significant signals which are present, however, are not directly relatable to the mesh frequencies. Some of these signals, called "sidebands", have been found to occur in tests of helicopter rotor-drive gearboxes. As originally conceived, this investigation had the rather limited objective of providing the designer of geared power trains with an analytical tool which could be used to predict, and thus control, the frequencies and amplitudes at which vibration sidebands are produced by operating gearboxes. As the work progressed, however, it became apparent that the analyses and associated understanding could also have a significant and far-reaching impact on the more general problem of on-line monitoring. It is important, therefore, that the results of this study be viewed in the context of their potential impact on this technology area, as well as upon the area of gearbox noise reduction.

The major aims of this study were as follows:

1. Development of an engineering understanding of, and methods for predicting, geometrically-induced planet-pass vibration sidebands which accompany normal planetary gear reduction operation; and

2. Development of an engineering understanding of, and new analytical methods for treating, the vibration sidebands which are produced by undesirable gear characteristics, such as tooth support discontinuities (cracks), gear runout, and variations in tooth transmitted forces.

These objectives have been achieved. Sidebands as a second major category of geared drive train vibration signals can now be described and discussed directly in terms of hardware condition. An engineering understanding of the mechanisms which cause many of the kinds of vibrations produced by gear meshes thus exists.

The payoffs from such an understanding can be enormous. First, gear train

designers now have important vibration analysis tools for minimizing, at the time of design, the disturbances produced by gear meshes. This will not only make gear trains quieter, but will also reduce their internal forces, with significant improvements in lifetimes of all components.

Second, when properly exploited by joint technologist/manufacturer teams, the high-frequency vibration analysis tools will permit real-time condition monitoring to be approached on an individual signal component basis in which the precise meaning of each component is well understood, rather than on the multiple component basis associated with usual signature analysis techniques. The engineering application of the vibration analysis tools permits specific signal components to be explained on a detailed basis. This removes the uncertainty associated with the use of signal level ratio techniques and the need for lengthy test-bed study programs involving failure implants.

Extension of the gear mesh analysis techniques to high-contact-ratio gearing is now in order, as is an extension of the torsional response analysis to coupled torsional-lateral-axial vibrations.

FOREWORD

Dr. Robert H. Badgley of Mechanical Technology Incorporated served as Program Manager for the efforts reported herein. The contract was carried out under the technical cognizance of Mr. R. Burrows, Eustis Directorate, U. S. Army Air Mobility Research and Development Laboratory, Fort Eustis, Virginia.

Special credit is due to Mrs. L. Cziglenyi of MTI, who programmed the computer program modifications and who conducted the calculations.

TABLE OF CONTENTS

LIST OF ILLUSTRATIONS

LIST OF ILLUSTRATIONS (CONCLUDED)

LIST OF TABLES

INTRODUCTION

Geared power train vibrations can occur at many different frequencies. The most common of these vibrations may be found at the mesh frequencies, and their integer multiples, of particular gear meshes in the train. These are known to be caused by the mesh properties of the gear teeth. Less well understood are vibrations which occur at the foregoing frequencies plus and minus integer multiples of other frequencies. Such components are called sidebands. While methods had been developed for predicting the levels of the vibration components at the mesh frequency and its integer multiples [1 through 7],* these methods were not capable of treating the sideband components. Unfortunately, high acoustic noise levels can be produced by both types of components.

In addition, there is increasing recognition of the fact that vibrations which produce noise also carry information about the dynamic behavior of the drive train [8 through 11], in effect, information from which the condition of the drive train components may be inferred. Such vibrations are known to be present in virtually all geared systems, and they have been recorded and monitored for diagnostic purposes for many years by many people. However, a detailed engineering understanding of the meanings of the shapes and amplitudes of the measured spectra has not proceeded in company with the development of methods for sensing and displaying these spectra.

Sidebands are produced during normal operation of gearboxes which employ planetary reductions. Such sidebands normally occur at the planetary mesh frequency plus and minus the planet-pass frequency. (They may also be similarly distributed about twice mesh frequency, three times mesh frequency, etc.) It must be stressed that their presence is due simply to the kinematics of the planetary reduction, wherein the planets physically pass any stationary point. The presence of each planet in turn changes the vibration properties of the gearbox structure, both from an impedance viewpoint and also more importantly from the amount of excitation applied to the structure by the moving mesh. This change is periodic at planet-pass frequency.

Sidebands are also produced during normal operation of gearboxes with gear meshes at more than one frequency. These sidebands are normally found at one mesh frequency plus and minus integer multiples of the other mesh frequencies (and of course at other frequency combinations as mentioned above). Such sidebands are caused primarily by the dynamic properties of the drive train components (i.e., coupled torsional-lateral-axial vibrations), which permit dynamic tooth force variations to occur in one mesh at frequencies of other meshes.

Other sources of sidebands do, of course, exist, but these are for the most part associated with the presence of undesirable component behavior. Perhaps the best-known sideband source is that due to runout of a gear because of machining or assembly inaccuracies. This type of sideband, which the

*Numbers in brackets refer to literature cited at the end of this report.

analysis described herein can predict, is typically found at mesh frequency plus and minus shaft rotation frequency. It can be produced by runout not only of pinion or gear in a simple mesh, but also of a planet gear relative to its bearings on a planet carrier.

Other undesirable effects can also produce sidebands. For instance, variation of tooth support stiffness around the circumference of a gear can alter the mesh properties in a manner which repeats at gear running speed, and which can have many forms depending on the circumferential distribution of the stiffness variation. A typical cause of such sidebands would be a cracked gear web, which the analysis described herein can treat.

DESCRIPTION OF PROGRAM

In this study, the characteristics of vibration sidebands produced by gear meshes in both single gear meshes and planetary gear reductions were investigated. The study was conducted in two tasks, the details of which are described below.

During the course of earlier test efforts, it became obvious that gearbox vibration and noise signal components were being produced at frequencies which corresponded to those at which various sideband signals were expected. It was recognized that these signals would have to be explained analytically before they could be dealt with properly. Hence the decision was made to treat the signals at their sources, i.e., the gear mesh itself.

Since earlier analytical efforts had yielded a computer-implemented analysis for predicting the vibration excitation properties of normal gear meshes, the decision was made to upgrade this computer program to incorporate the new analyses. The upgraded computer program was modularized so as to permit future inclusion of other gear types and effects. A schematic diagram of the computer program's capabilities is presented and discussed later in the report (as Figure 11). The analyses described herein have been included in this program.

TASK I – INVESTIGATION OF PLANETARY MESH PLANET-PASS SIDEBANDS

As a result of earlier studies, predicted dynamic behavior of the CH-47 forward rotor drive gearbox ring gear was available. This predicted data was used to study the complex vibrations existing at a preselected point on the ring gear (corresponding to a location where measured data had been taken).

These studies produced radial vibration levels versus time, and corresponding vibration spectra, for various planet phasing relationships in the lower stage planetary reduction. Planet phasing is under the control of the gear designer, and thus it can be altered to modify and thus reduce mesh frequency vibration sidebands.

TASK II – ANALYSIS OF GEAR-MESH-INDUCED HIGH-FREQUENCY VIBRATION SPECTRA AND CALCULATIONS

This phase of the study treated both the spiral bevel and lower stage planetary planet-to-ring gear meshes. Spiral bevel gear shaft runout and externally-imposed tooth mesh force variations were studied, and gear mesh excitation spectra produced by these effects were predicted.

In the case of the planet-to-ring mesh, planet runout and externally-imposed tooth mesh force variations were considered, and excitation spectra caused by these effects were predicted. In addition, the mesh excitation spectrum resulting from the condition where a number of consecutive ring gear teeth have relatively soft support stiffness (such as could be caused by a local crack) was predicted.

INVESTIGATION OF PLANETARY MESH PLANET-PASS SIDEBANDS

ANALYSIS OF PLANET-PASS INDUCED VIBRATION

A schematic of the planetary gear system to be analyzed is shown in Figure 1. The ring gear is stationary and the sun gear rotates with speed ω_s. The four planets rotate about their own centers with a speed of ω_o (relative to the planet carrier), and the planet carrier rotates with speed ω_b (planet orbiting speed). Depending on the numbers of teeth on the component gears, the four planets are, in general, not equally spaced. In the particular case considered herein, δ is the angular offset of the pair (C,D) with respect to the pair (A,B).

In this analysis the ring gear is considered as an elastic shell-type structure. At a given location, the ring gear experiences a dynamic tooth mesh force each time a planet passes. This mesh force is associated with the tooth mesh frequency resulting from the transfer of load from one pair of teeth to the other. In this calculation, it is assumed that the dynamic tooth mesh force has a rectangular pulse form whose magnitude varies sinusoidally with the mesh frequency (see below). This oscillating force produces an oscillating deformation. It is this planet-pass induced vibration of the ring gear that is treated in this analysis.

In a coordinate frame fixed with the planet carrier, both sun and ring gears rotate as shown in the upper diagram of Figure 2. The sun gear rotates with a speed of $\omega_s - \omega_b$, while the ring gear moves in the opposite direction with the planet orbiting speed ω_b. In this reference frame, the forces acting on the ring gear due to the planet-ring gear meshes occur at fixed angular locations of $\theta = 0, \pi/2 - \delta, \pi, 3\pi/(2) - \delta$, corresponding to the locations of planets A, D, B and C respectively.

Since planets A and B are in phase, the dynamic force per unit area due to gear meshes at these two locations can be approximately expressed as

$$F_{AB}(\theta,t) = P_{AB}(\theta) \cos f_M t \tag{1}$$

where t is the time, P_{AB} the normal pressure due to normal tooth mesh forces, and f_M the tooth mesh frequency defined by

$$f_M = \omega_o N_p = \omega_b N_r \tag{2}$$

In the above, N_p and N_r are the numbers of teeth on the planet and ring gear respectively. It may be assumed that P consists of two identical rectangular pulses occurring at the locations of planets A and B, and that the width of each pulse is one tooth spacing, as shown in the lower diagram of Figure 2. The magnitude of the rectangular pulse P_o is related to common gear parameters as follows:

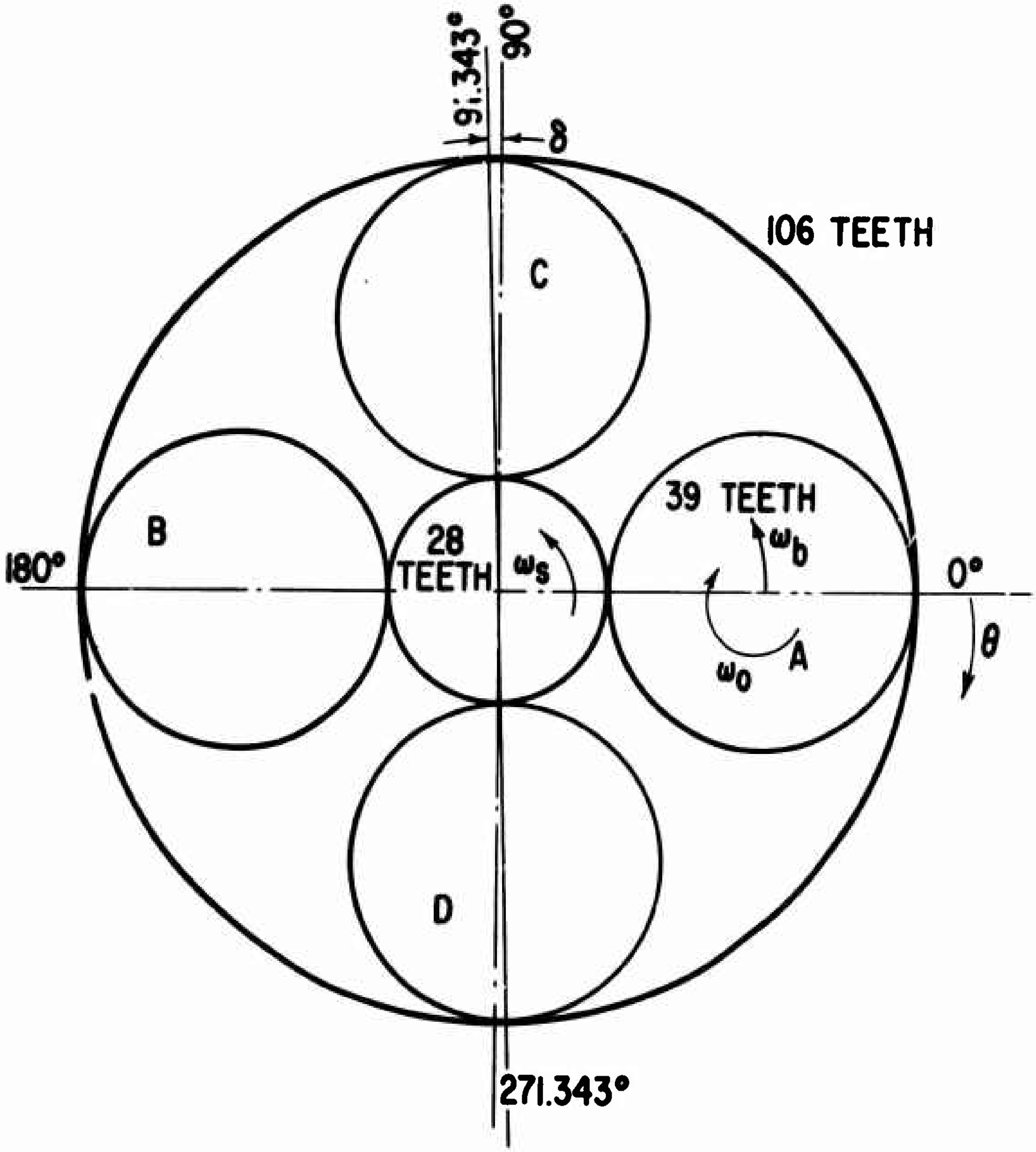

Figure 1. CH-47 Forward Rotor-Drive Gearbox Lower Planetary Gear System.

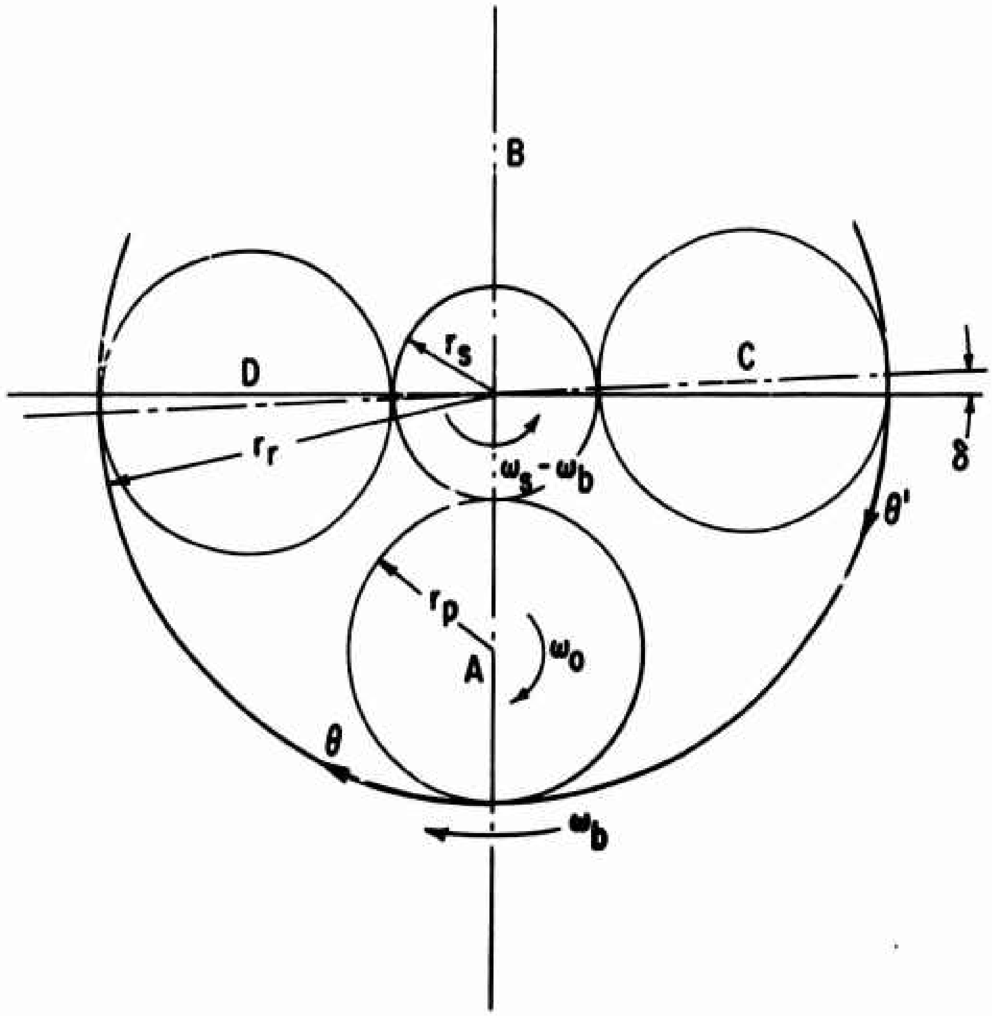

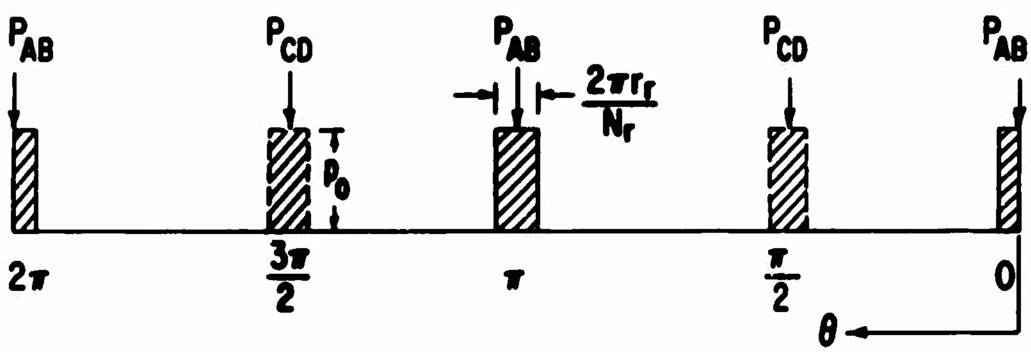

Figure 2. Gear System in a Planet-Fixed Frame and Corresponding Force Diagram.

$$P_o = \frac{F_t \tan \phi}{\frac{2\pi r_r}{N_r} L} \qquad (3)$$

where F_t is the tangential tooth force, ϕ the pressure angle, r_r the pitch radius of ring gear, and L the tooth face width.

As a result of the angular offset δ, there exists a temporal phase difference between the dynamic forces at planets C and D and those at A and B. Since rotation of the sun gear over one tooth spacing corresponds to one full cycle in gear meshing, it can be shown that the temporal phase lag of the tooth meshes of planets C and D relative to those of A and B is

$$\Psi = \delta \cdot N_s \qquad (4)$$

where N_s is the number of teeth of the sun gear. The dynamic forces at planets C and D can be thus expressed as

$$F_{CD} (\theta, t) = P_{CD} (\theta) \cos (f_M t - \Psi) \qquad (5)$$

where P_{CD} is similar to P_{AB} and is shown in the lower diagram of Figure 2.

There exist radial displacement response functions for the ring gear shell due to the dynamic forces F_{AB} and F_{CD}. These response functions depend on the elastic characteristics of the shell-type ring gear structure. Neglecting ring gear inertia (valid for shell-type structures), the response function due to the meshing of planets A and B is in phase with its forcing function F_{AB}. It may in general be written as

$$b_{AB} (\theta, z) \cos f_M t \qquad (6)$$

where z is the axial coordinate, designated for the general case that the ring gear shell is nonuniform axially. Similarly, the response function due to the meshing of planets C and D is

$$b_{CD} (\theta, z) \cos (f_M t - \Psi) \qquad (7)$$

The total response function for the ring gear shell is the sum of Equations (6) and (7), i.e.,

$$w (\theta, z, t) = b_{AB} \cos f_M t + b_{CD} \cos (f_M t - \Psi) \qquad (8)$$

where w represents the dynamic radial response at a location whose coordinates are (θ, z) on the ring gear casing.

After some manipulations, Equation (8) becomes

$$w(\theta,z,t) = A(\theta,z)\cos f_M t + B(\theta,z)\sin f_M t \tag{9}$$

where

$$A(\theta,z) = b_{AB} + b_{CD}\cos \Psi \tag{10}$$

$$B(\theta,z) = b_{CD}\sin \Psi \tag{11}$$

If the ring gear is axially symmetric, both b_{AB} and b_{CD} are even functions in θ and have a periodicity of π in θ, and so do the functions $A(\theta,z)$ and $B(\theta,z)$. Therefore, the latter may be expanded in terms of Fourier series, i.e.,

$$A(\theta,z) = \frac{a_o(z)}{2} + \sum_{n=1}^{\infty} a_{2n}(z)\cos 2n\theta \tag{12}$$

and

$$B(\theta,z) = \frac{b_o(z)}{2} + \sum_{n=1}^{\infty} b_{2n}(z)\cos 2n\theta \tag{13}$$

Let θ_o be the angular coordinate of a fixed point on the ring gear. Since the ring gear rotates clockwise with speed ω_b (see Figure 2),

$$\theta_o(t) = \theta_i + \omega_b t \tag{14}$$

where θ_i is the coordinate of the fixed point at $t = 0$. Setting $\theta_i = 0$,

$$\theta_o(t) = \omega_b t \tag{15}$$

Thus, the fixed point on the ring gear travels clockwise starting from the position of $\theta = 0$ in the frame fixed with the planet carrier.

To calculate the vibration at a fixed point on the ring gear, Equation (15) is substituted for θ into the total response function, Equation (9). This yields

$$w_o(t) = w(\omega_b t, z_o, t) = A(\omega_b t, z_o)\cos f_M t + B(\omega_b t, z_o)\sin f_M t \tag{16}$$

where z_o is the axial coordinate of the fixed point.

Using the Fourier representations of Equations (12) and (13),

$$w_o(t) = \frac{a_o}{2}\cos f_M t + \frac{b_o}{2}\sin f_M t$$

$$+ \frac{1}{2}\sum_{n=1}^{\infty} a_{2n}\left[\cos(f_M + 2n\,\omega_b)\,t + \cos(f_M - 2n\,\omega_b)\,t\right]$$

$$+ \frac{1}{2}\sum_{n=1}^{\infty} b_{2n}\left[\sin(f_M + 2n\,\omega_b)\,t + \sin(f_M - 2n\,\omega_b)\,t\right] \qquad (17)$$

The above equation represents the planet-pass induced vibration amplitude history at a fixed point on the ring gear. At $t = 0$, planet A is at the location of this fixed point; and as time goes on, planets D, B, and C pass the point in sequence.

From Equation (17), the vibration amplitude at gear tooth mesh frequency is

$$M_o = \frac{1}{2}\left(a_o^2 + b_o^2\right)^{1/2} \qquad (18)$$

The amplitudes at various sidebands about the mesh frequency are

$$M_n = \frac{1}{2}\left(a_{2n}^2 + b_{2n}^2\right)^{1/2} \quad \text{for } n = 1,2,3\ldots \qquad (19)$$

Since there are four planets, the planet-pass frequency is

$$f_p = 4\,\omega_b \qquad (20)$$

The sidebands occur at $f_M \pm n\,\frac{f_p}{2}$ with $n = 1,2,3,\ldots$. In the case of zero offset ($\delta = 0$), sidebands would appear only at $f_M \pm n\,f_p$, because the function A and B would have a periodicity of $\pi/2$ instead of π. Physically it means that at the fixed observation point, the pass of planets C and D is identical to that of planets A and B.

Equation (17) gives the amplitude-time relationship of the planet-pass induced vibration as observed at a fixed point on the ring gear. The amplitude-frequency spectrum of the vibration is presented by Equations (18) and (19).

PLANET-PASS INDUCED VIBRATION AND SIDEBAND AMPLITUDE CALCULATIONS

The gear parameters for the CH-47 lower planetary gear system and the operating conditions used in the calculations are as follows:

Number of sun gear teeth $N_s = 28$

Number of planet gear teeth $N_p = 39$

Number of ring gear teeth $N_r = 106$

Pitch radius of sun gear $r_s = 2.8$ in.

Pitch radius of planet gear $r_p = 3.9$ in.

Pitch radius of ring gear $r_r = 10.6$ in.

Pressure angle $\varphi = 25^o$

Ring gear tooth face width $L = 1.25$ in.

Angular offset of planets C and D $\delta = 1.343^o$

Planet-ring mesh frequency $f_M = 1482$ Hz

Tangential tooth force at planet-ring mesh = 159.2 lb

The planet orbiting speed ω_b is 14 Hz, and the planet-pass frequency is therefore 56 Hz. Due to the angular offset δ, the temporal phase lag of planets C and D relative to A and B is 37.6 degrees.

The cross section of the ring gear casing, which is considered as the vibrating elastic body, is depicted in Figure 3. In the dynamic response calculation, this ring gear casing is modeled as a composite cylindrical shell with variable thickness (see Figure 3). Both ends of the casing are assumed to be "simply supported," i.e., no linear translation but free to rotate. The MTI general shell dynamic response computer program was used to obtain the response functions $b_{AB}(\theta,z)$ and $b_{CD}(\theta,z)$ [4].

Let the vibration observation point on the ring gear be located at $z_o = 1.5$ inches. The response functions at this point for the specified tooth load are plotted in Figure 4. The small angular offset of 1.343^o for planets C and D is neglected. It is noted that both b_{AB} and b_{CD} are periodic with a periodicity of 180^o. Due to the axial symmetry of the ring-gear casing, b_{AB} and b_{CD} are completely similar but have a phase difference of 90^o.

The vibration induced by planet-pass as observed at a fixed point located at $z_o = 1.5$ inches on the ring gear was calculated by using Equation (17) and is plotted in Figure 5. The first half bump corresponds to the pass of planet A, and the next three bumps correspond to the passes of planets D, B and C, respectively. The pattern repeats itself after one full revolution of all planets. The period is 0.0714 sec, which is the reciprocal of ω_b.

The frequency spectrum of this planet-pass induced vibration is shown in the lower diagram of Figure 6. The amplitude at the mesh frequency has the largest value. However, the amplitude at the second pair of sidebands, at $f_M \pm f_p$, is quite large.

To see the effect of planet phasing on the vibration amplitudes at the selected point, the vibrations produced at three different temporal phase

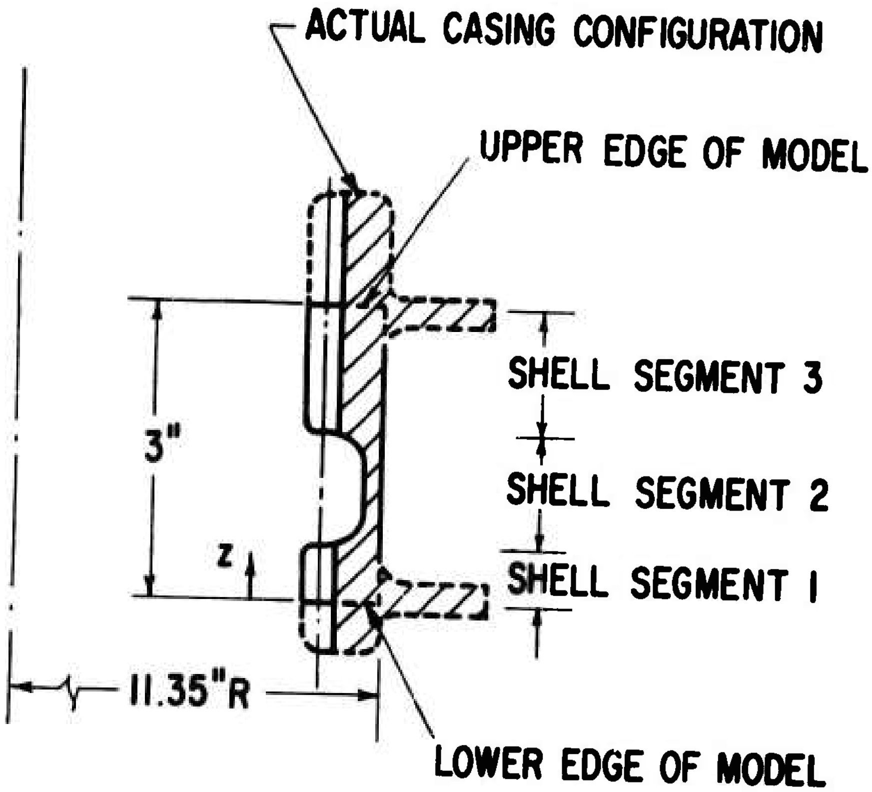

Figure 3. Dynamic Model of CH-47 Lower Planetary Ring-Gear Casing.

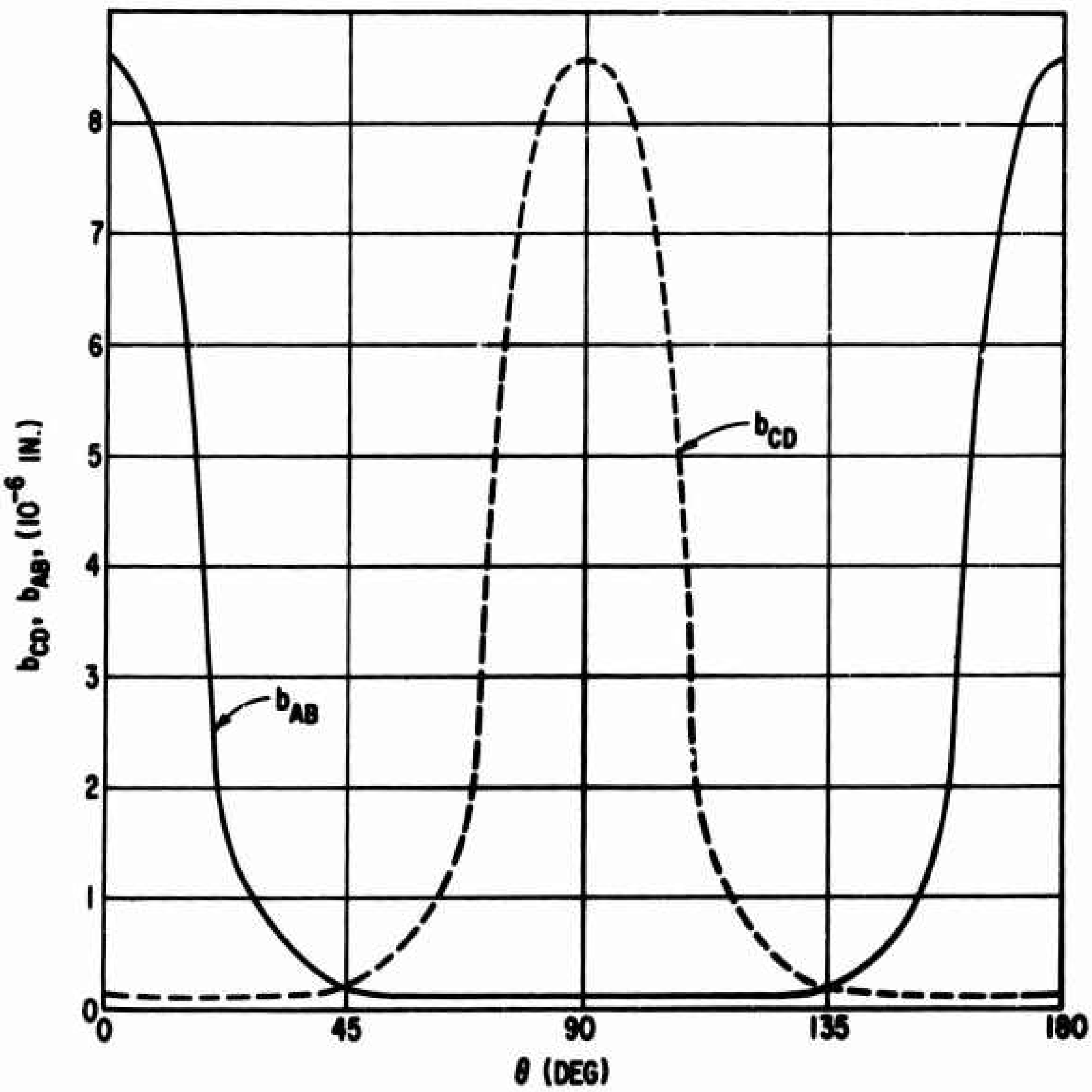

Figure 4. Ring-Gear Casing Response Functions.

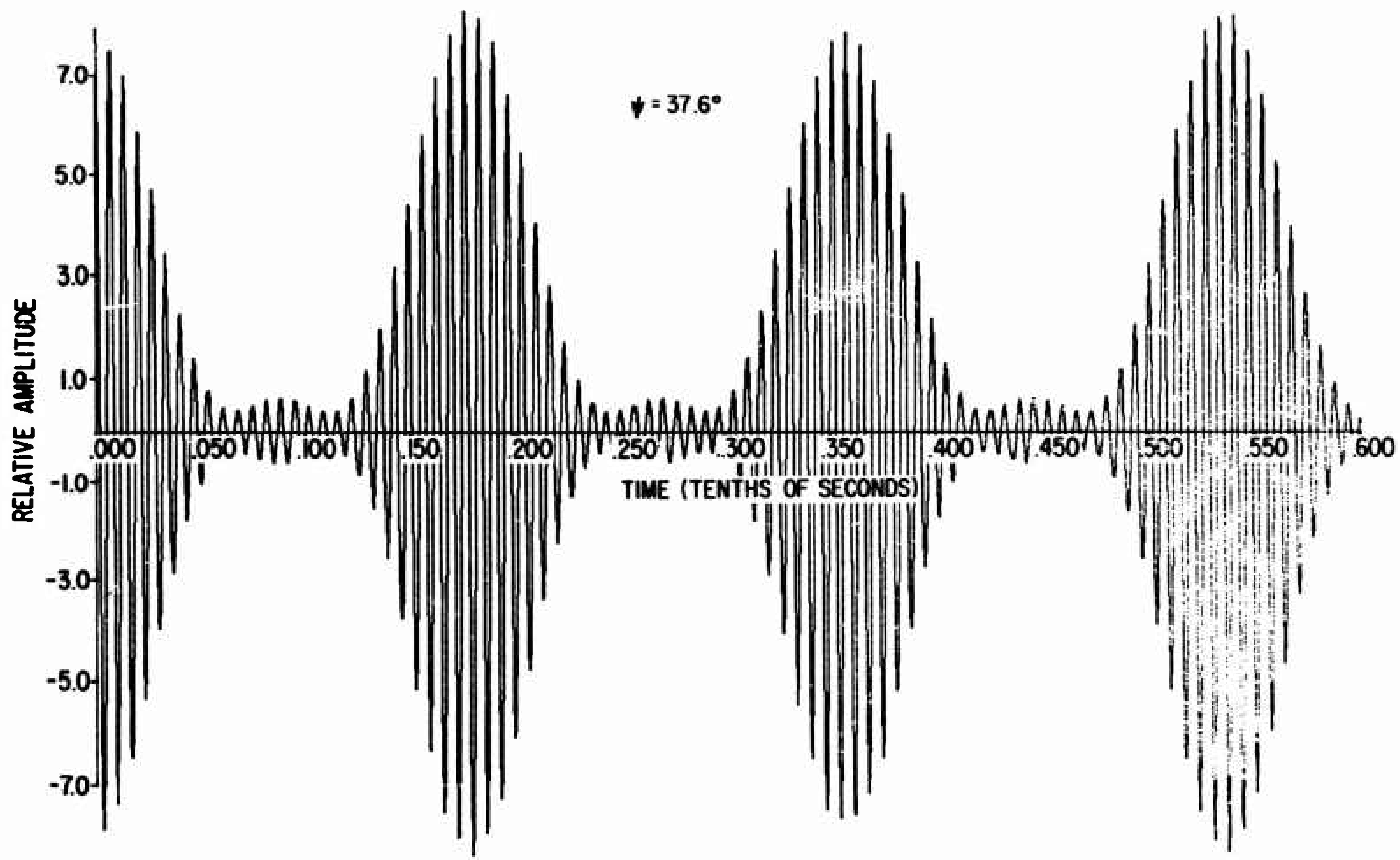

Figure 5. Radial Vibration Amplitude vs. Time at Fixed Location on CH-47 Forward Rotor-Drive Gearbox Ring Gear for $\psi = 37.6°$.

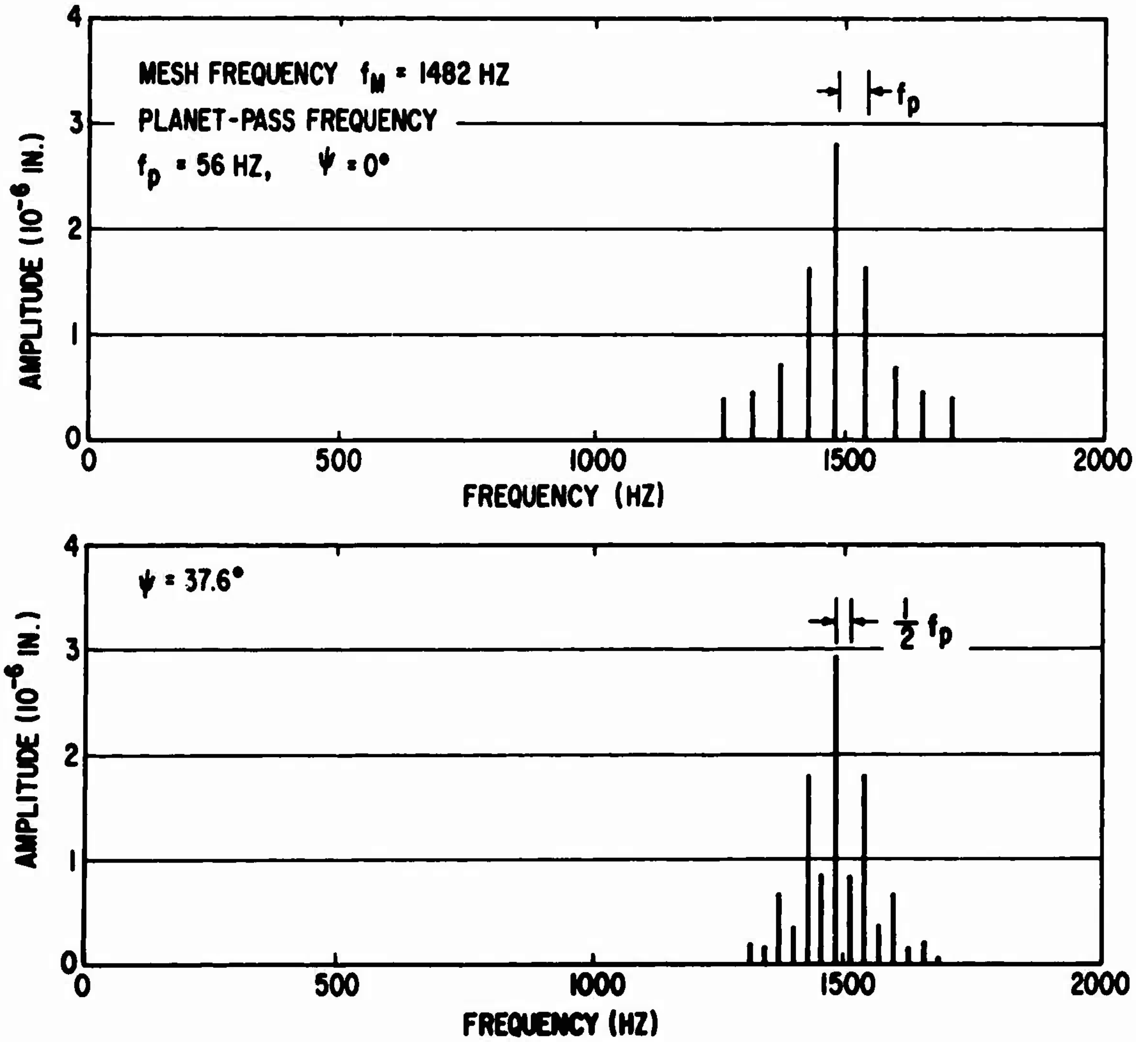

Figure 6. Frequency Spectra for $\psi = 0^\circ$ and 37.6°.

angles ($\Psi = 0^o$, 90^o and 142.4^o) were investigated. The amplitude-time plots of these cases are shown in Figures 7, 8 and 9. In a gross sense, they appear to be similar. However, the frequency spectra for these three cases are quite different. They are shown in the upper diagram of Figure 6 and the upper and lower diagrams of Figure 10 for $\Psi = 0^o$, 90^o and 142.4^o, respectively. It is noted that for $\Psi = 0^o$, sidebands occur only at frequencies of $f_M \pm n f_p$.

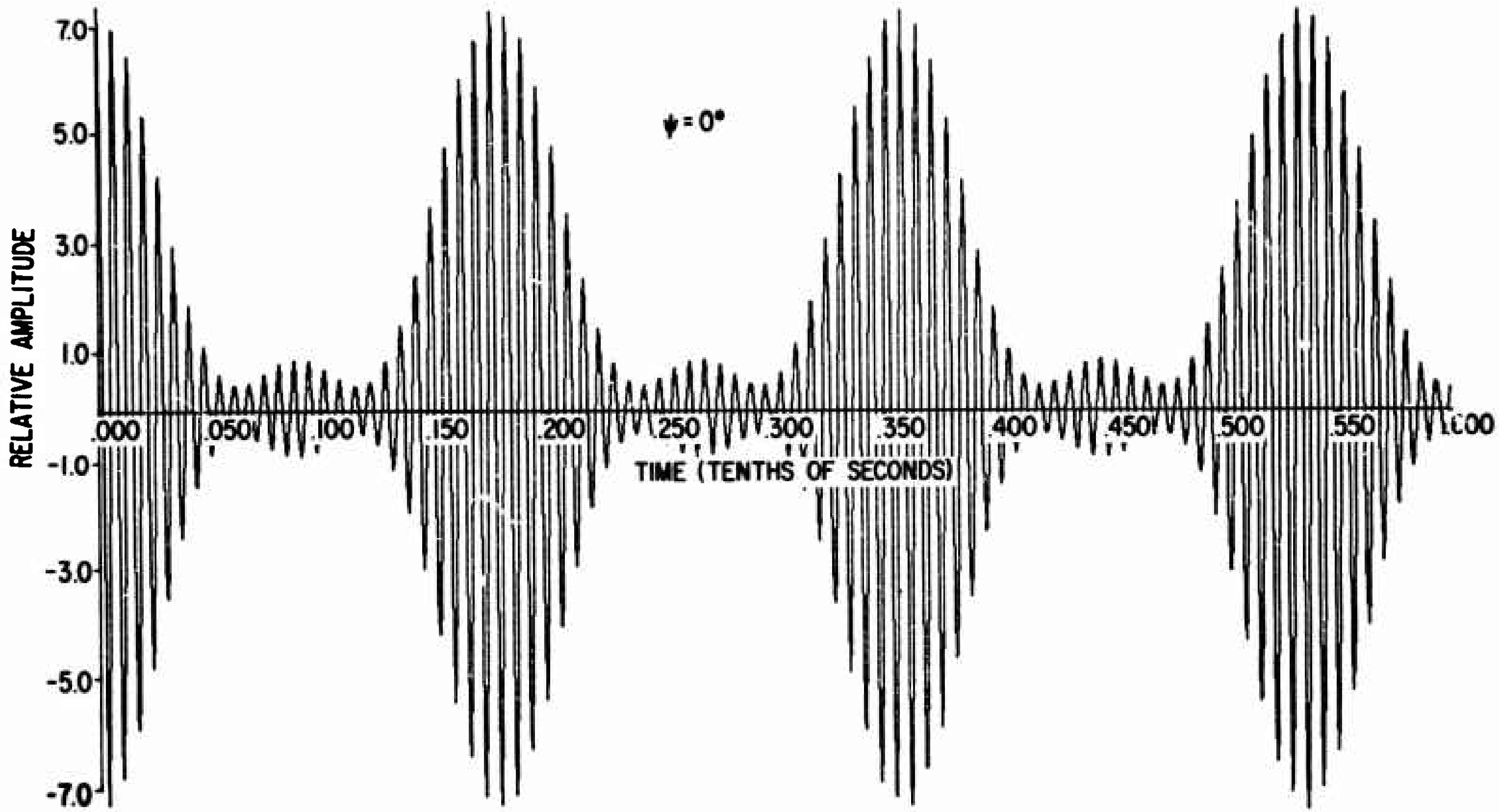

Figure 7. Radial Vibration Amplitude vs. Time at Fixed Location on CH-47 Forward Rotor-Drive Gearbox Ring Gear for $\psi = 0^{o}$.

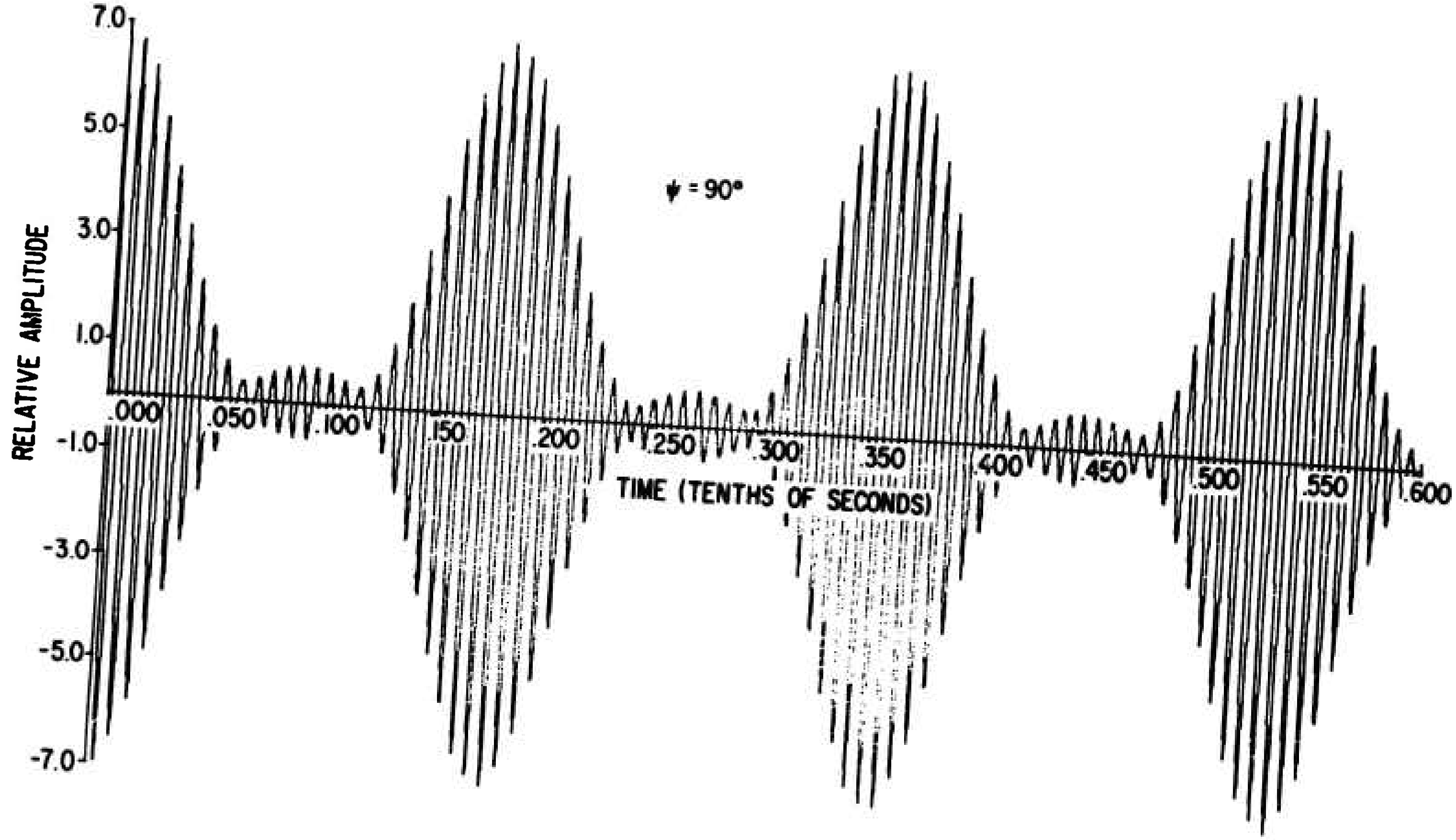

Figure 8. Radial Vibration Amplitude vs. Time at Fixed Location on CH-47 Forward Rotor-Drive Gearbox Ring Gear for $\psi = 90^{o}$.

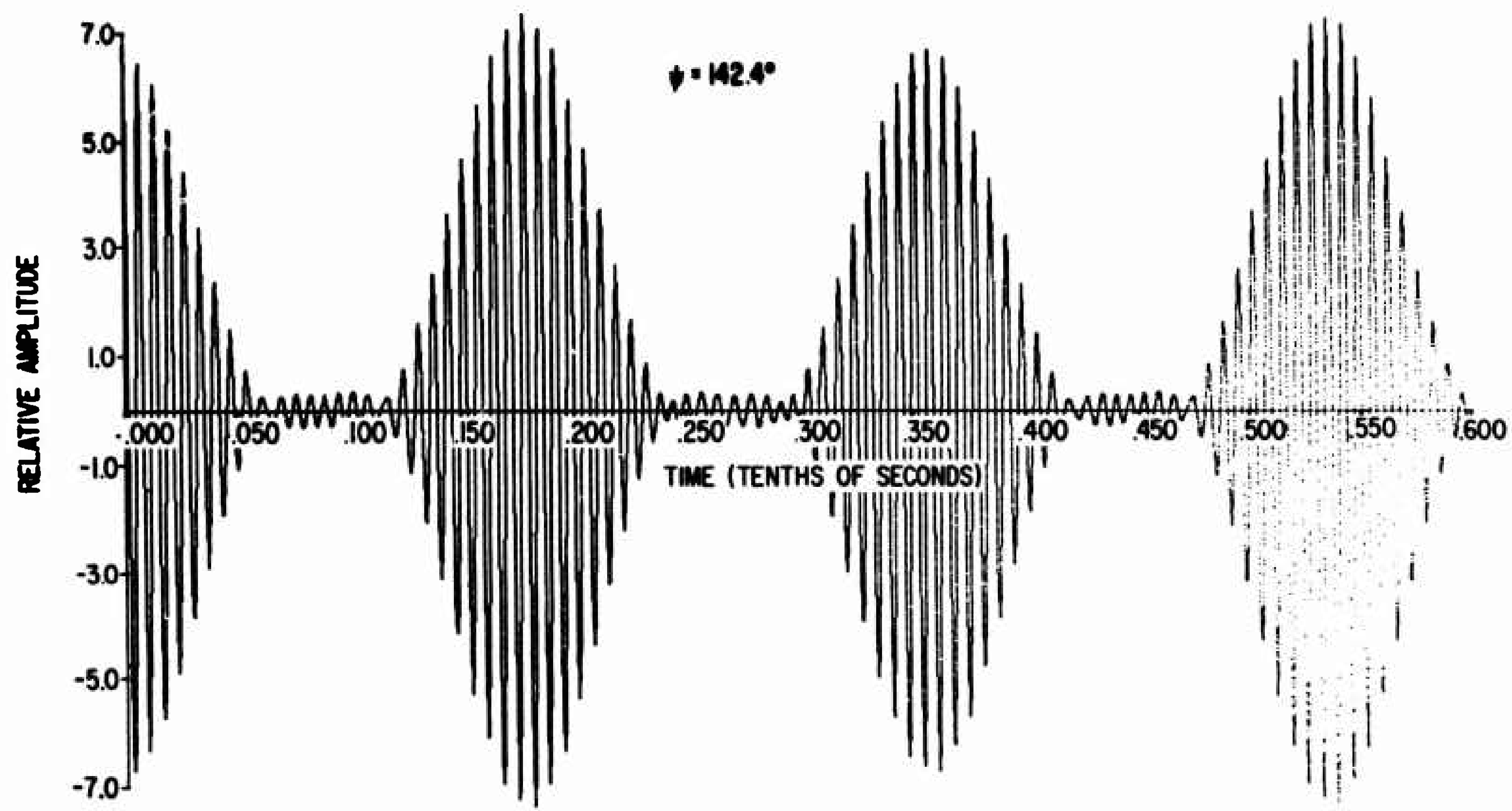

Figure 9. Radial Vibration Amplitude vs. Time at Fixed Location on CH-47 Forward Rotor-Drive Gearbox Ring Gear for $\psi = 142.4^{\circ}$.

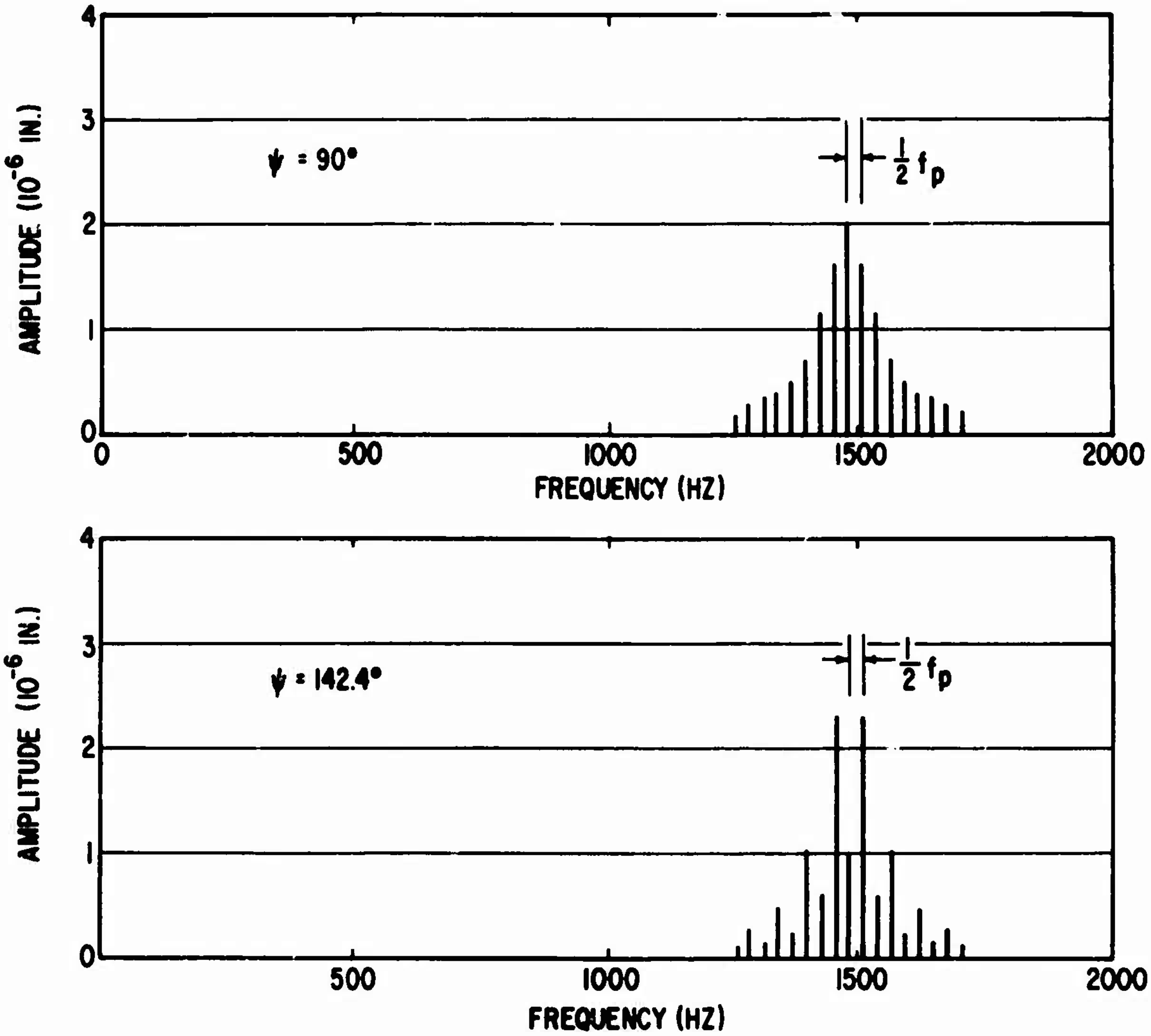

Figure 10. Frequency Spectra for $\psi = 90^{\circ}$ and 142.4°.

ANALYSIS OF GEAR-MESH-INDUCED HIGH-FREQUENCY VIBRATION SPECTRA AND CALCULATIONS

ANALYSIS OF GEAR MESH EXCITATION

The mesh of gears with perfect involute profiles can induce vibration, simply because of the nonuniform deflection resulting from varying tooth compliance along the length of the tooth. The nonuniform deflection or displacement deviation introduces irregular motion superimposed on the uniform rotation of the gears. This irregularity of motion becomes one of the major sources of vibration in the drive system, especially of the vibration associated with noise production. Manufacturing errors in tooth shape or spacing can further increase the magnitude of the motion irregularity and thus the excited vibration amplitude. If all the teeth in each of the meshing gears are identical, and if the mesh is otherwise ideal (i.e., no runout, etc.), then the spectrum of the vibration induced by the gear mesh contains signals at only the mesh frequency and its higher harmonics. The analysis of this gear mesh excitation was performed by Laskin, Orcutt and Shipley [1].

However, if the gear mesh deviates from the ideal (e.g., gear runout, dynamic torque, etc.), or if there is deviation in tooth profiles as the gear mesh continues from one set of mating teeth to the other, the tooth deflection pattern will, in general, vary from tooth pair to tooth pair. The associated vibration will then contain signal components at other than the mesh frequency and its harmonics. These components are the so-called gear mesh excitation sidebands. It is the purpose of this work to study the gear-mesh-induced vibration spectra considering three gear parameters as variables between mesh cycles. These three parameters are:

1. Center-Line Distance

   This variation, in most cases, is due to shaft or gear runout. The center-line distance is treated to be constant within a tooth mesh, but it can vary between mesh cycles. This simplifying approximation is possible because the variation in center-line distance due to shaft or gear runout is slow with respect to tooth mesh frequency.

2. Tooth Load

   This variation may be caused, for instance, by the dynamic effects of other gear meshes in the drive system. The tooth load can also be variable between calculation points within one mesh cycle. This accommodates high-frequency dynamic forces.

3. Tooth Support Compliance

   This is the compliance in addition to the compliance due to tooth bending, shearing, rotation, and contact deformation normally existing during gear mesh. It may be produced by elastic nonuniformity in the gear structure supporting the gear teeth. This compliance can also be variable at all calculation points within one mesh cycle.

Each of these three variations is in general periodic with a definite frequency. For example, the center distance variation caused by shaft run-out has a frequency equal to the rotational speed of the shaft. In each of the cases, there exists a base period for the tooth deflection pattern which is equal to the reciprocal of the largest common factor between the mesh frequency and the frequency (or frequencies) of variation of the gear parameter (or parameters). During one base period, integer multiples of gear mesh cycles and of parameter variation cycles occur. The spectrum of the associated vibration is thus discrete, with the fundamental frequency equal to the reciprocal of the base period. The frequency spectrum is obtained by a Fourier analysis of the tooth deflection profile over one base period.

However, if the variation of the gear parameter is random, the spectrum of the gear-mesh-induced vibration will be continuous. It may be obtained by calculating the power spectral density function of the tooth deflection data over a long period of time. The method of power spectra calculation is included in Appendix I.

Within one mesh cycle, the method of calculating the tooth deflection is directly similar to that in [1]. The limitations and assumptions in the calculation are listed below:

1. Only spur gears are treated, and these are treated only for the two cases of (a) an external gear driving an external gear and (b) an external gear driving an internal gear. Straight bevel gears may be treated in an approximate manner by replacing them with equivalent spur gears by Tregold's Approximation [13].

2. The working portions of the tooth profiles are essentially involute. Design and manufacturing profile deviations are small enough so as not to affect load location, load direction, or tooth stiffness.

3. There is no tip interference, either due to excessive addendum length or due to tooth deflection under load.

4. In any single interval between the pitch points of two successive pairs of teeth, contact and load carrying are limited to the two successive pairs of teeth. In the same interval, there must be at all times at least one pair of teeth in contact and carrying load. This prevents consideration of cases where the contact ratio is less than one or more than two; it may in some unusual designs also eliminate cases where the contact ratio has certain intermediate values.

5. The load is assumed to be transmitted uniformly across the face of the gear except for normal end effects in stress distribution. This excludes any consideration of face crowning, lead modification, lead manufacturing error, gear windup, or nonuniform deflection of gear supports.

6. All variations in tooth deflection as the load point moves along the tooth profile either are confined to elastic effects on the

tooth alone or can be supplied as point-by-point compliances as part of the input data. This means that variations such as might result from the deflection of thin rims are not calculated directly by the analysis.

7. The contact deformation is assumed to be independent of the tooth surface lubricating film.

The above analysis is incorporated in the computer program GGEAR. It is obtained by modifying and extending the program GEARO reported in [1]. The overall structure of the modified program is shown in Figure 11. The modifications consist of the creation of the main program GGEAR and the subroutine SPECT, and some changes in subroutines GEARO, FOUR and PLT to accommodate the extension of computation over multiple mesh cycles. GGEAR accepts those items of gear data that are constant over all mesh cycles. Subroutine GEARO, on the other hand, reads in variable gear data and, together with subroutines AJCDH and CALCJ, calculates the tooth deflection over one mesh cycle. In the computation, the mesh cycle is divided into a number of calculation points as is done in the program GEARO. Tooth deflections at all the calculation points over the prescribed number of mesh cycles are stored and printed out in GGEAR.

With reference to Figure 11, it may be noted that provision is being made for eventual incorporation of other subroutines similar to GEARO for the calculation of excitation levels in high-contact-ratio spur gears, helical gears, and eventually spiral-bevel gears. While such calculation capabilities were not included in the computer program during the present contract, the modified program was prepared on a modular basis for their later inclusion.

According to the user's instruction, either the calculated tangential deflection data can be plotted by subroutine PLT, or it can be analyzed to obtain the Fourier representation of the deflection pattern via the subroutine FOUR, as is now done in program GEARO. The data can also be analyzed by using SPECT to produce the power spectral density function. A description of the computer program is given in Appendix II.

CH-47 SPIRAL BEVEL GEAR MESH CALCULATIONS

The CH-47 forward rotor-drive gearbox spiral bevel gear mesh is analyzed in terms of its equivalent spur gear mesh [2]. The equivalent spur gears will be equivalent to the spiral bevel gears only in the sense that their physical proportions, those likely to influence deflection under load, approximate the mean proportions of the actual spiral bevel gear teeth. The use of the equivalent spur gears is sufficiently adequate for the present purpose of studying the effects of shaft runout and load variation to produce high-frequency-vibration sidebands. The gear mesh parameters and the conversion of the CH-47 spiral bevel gears into equivalent spur gears are summarized in Table I, which has been taken from [2]. The gear mesh tangential load is taken to be 2760 lb, and the gearbox input shaft speed is 7059 rpm. This yields a gear tooth mesh frequency of 3412 Hz. Variations in center distance and in tooth load as the source for generating tooth displacement deviations at sideband frequencies have been studied.

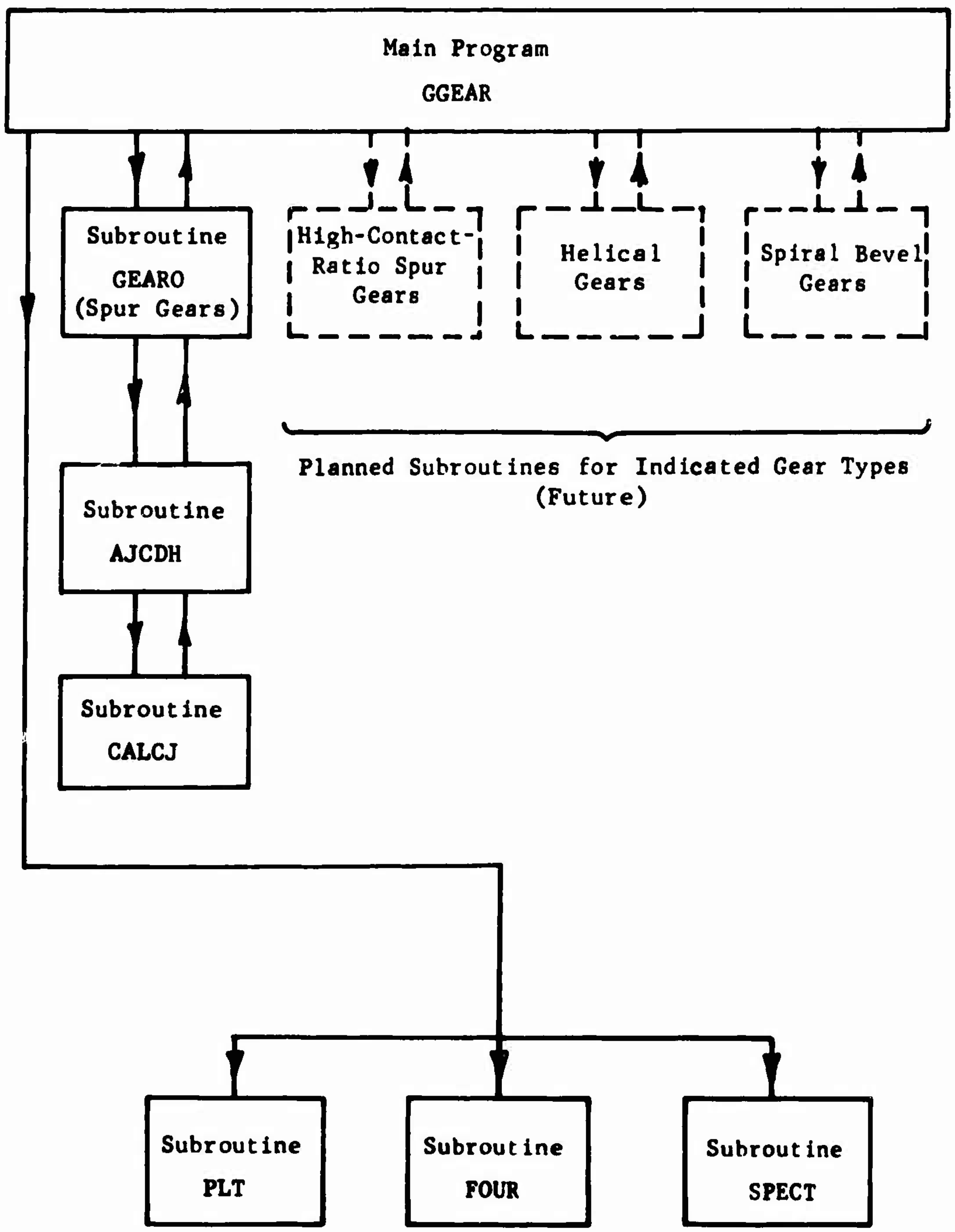

Figure 11. Computer Program Structure.

TABLE I. CONVERSION OF SPIRAL BEVEL GEARS INTO EQUIVALENT SPUR GEARS FOR CH-47 FORWARD ROTOR TRANSMISSION (FROM REFERENCE 2)

SYMBOL	DEFINITION	UNITS	PINION [114D1044(12)] SPIRAL BEVEL	PINION HELICAL	PINION SPUR	GEAR [114D1053(13)] SPIRAL BEVEL	GEAR HELICAL	GEAR SPUR
N	NUMBER OF TEETH OF SPIRAL BEVEL	—	29			51		
γ	PITCH CONE ANGLE OF SPIRAL BEVEL	DEGREES	31° 39'			67° 21'		
	COS γ	—	.85127			.38510		
	SIN γ	—	.52473			.92287		
ϕ	SPIRAL ANGLE OF SPIRAL BEVEL = HELIX ANGLE OF EQUIVALENT HELICAL	DEGREES	25°	25°		25°	25°	
	COS ϕ	—	.90631	.90631		.90631	.90631	
	$COS^2 \phi$	—	.82140	.82140		.82140	.82140	
	$COS^3 \phi$	—	.74444	.74444		.74444	.74444	
N_V	NUMBER OF TEETH OF EQUIVALENT HELICAL = $N/COS\ \gamma$	—		34.0655			132.4331	
N_S	NUMBER OF TEETH OF EQUIVALENT SPUR = $N_V/COS^3\ \phi$	—			45.7623			177.9058
F	FACE WIDTH OF SPIRAL BEVEL	INCHES	2.188			2.188		
F_V	FACE WIDTH OF EQUIVALENT HELICAL = F	INCHES		2.188			2.188	
F_S	FACE WIDTH OF EQUIVALENT SPUR = $F_V/COS\ \phi$	INCHES			2.4142			2.4142
R	PITCH RADIUS OF SPIRAL BEVEL AT LARGE END	INCHES	3.775			6.639		
R_M	MEAN PITCH RADIUS OF SPIRAL BEVEL = $R - (F/2)\ SIN\ \gamma$	INCHES	3.2010			5.6294		
R_V	PITCH RADIUS OF EQUIVALENT HELICAL = $R_M/COS\ \gamma$	INCHES		3.7601			14.6180	
R_S	PITCH RADIUS OF EQUIVALENT SPUR = $R_V/COS^2\ \phi$	INCHES			4.5776			17.7964
α	RATIO OF RADII OF SPIRAL BEVEL = R_M/R	—	.8479			.8479		
a	ADDENDUM OF SPIRAL BEVEL AT LARGE END	INCHES	.297			.146		
a_v	ADDENDUM OF EQUIVALENT HELICAL = $\alpha\ a$	INCHES		.2518			.1237	
a_s	ADDENDUM OF EQUIVALENT SPUR = a_v	INCHES			.2518			.1237
R_{OV}	OUTER RADIUS OF EQUIVALENT HELICAL = $R_V + a_v$	INCHES		4.0119			14.7417	
R_{OS}	OUTER RADIUS OF EQUIVALENT SPUR = $R_S + a_s$	INCHES			4.8294			17.9201
b	DEDENDUM OF SPIRAL BEVEL AT LARGE END	INCHES	.195			.346		
b_v	DEDENDUM OF EQUIVALENT HELICAL = $\alpha\ b$	INCHES		.1653			.2933	
b_s	DEDENDUM OF EQUIVALENT SPUR = b_v	INCHES			.1653			.2933
R_{RV}	ROOT RADIUS OF EQUIVALENT HELICAL = $R_V - b_v$	INCHES		3.5948			14.3247	
R_{RS}	ROOT RADIUS OF EQUIVALENT SPUR = $R_S - b_s$	INCHES			4.4123			17.5031
d	WORKING DEPTH OF SPIRAL BEVEL AT LARGE END	INCHES	.443			.443		
d_M	MEAN WORKING DEPTH OF SPIRAL BEVEL = $\alpha\ d$	INCHES	.3756			.3756		
d_V	WORKING DEPTH OF EQUIVALENT HELICAL = d_M	INCHES		.3756			.3756	
d_S	WORKING DEPTH OF EQUIVALENT SPUR = d_V	INCHES			.3756			.3756
$TIFR_V$	TRUE INVOLUTE FORM RADIUS OF EQUIVALENT HELICAL = $R_{OV} - d_V$	INCHES		3.6363			14.3661	
$TIFR_S$	TRUE INVOLUTE FORM RADIUS OF EQUIVALENT SPUR = $R_{OS} - d_S$	INCHES			4.4538			17.5445
T	CIRCULAR TOOTH THICKNESS OF SPIRAL BEVEL AT LARGE END	INCHES	.506			.312		
T_M	MEAN CIRCULAR TOOTH THICKNESS OF SPIRAL BEVEL = $\alpha\ T\ COS\ \phi$	INCHES	.3888			.2397		
T_V	CIRCULAR TOOTH THICKNESS OF EQUIVALENT HELICAL = T_M			.3888			.2397	
T_S	CIRCULAR TOOTH THICKNESS OF EQUIVALENT SPUR = T_V	INCHES			.3888			.2397
C_V	RADIAL CLEARANCE OF EQUIVALENT HELICAL = $TIFR_V - R_{RV}$	INCHES		.0415			.0414	
C_S	RADIAL CLEARANCE OF EQUIVALENT SPUR = $TIFR_S - R_{RS}$	INCHES			.0415			.0414
r_V	TOOTH FILLET RADIUS OF EQUIVALENT HELICAL = $(.75)C_V$	INCHES		.0311			.0310	
r_S	TOOTH FILLET RADIUS OF EQUIVALENT SPUR = $(.75)C_S$	INCHES			.0311			.0310

1. Center Distance Variation

Center distance variation resulting from a 0.001-in. (peak) input shaft runout is chosen to be the representative case. The runout is assumed to be a sine wave in form. The expression for the center distance is

$$C \text{ (in.)} = 22.3735 + 0.001 \sin \frac{2\pi f_M}{29} t \qquad (21)$$

where the number 22.3735 is the nominal center distance in inches, t the time in seconds, and f_M the mesh frequency in Hz. The input pinion has 29 teeth, and therefore $f_M/29$ is the shaft rotational speed.

Using the computer program, tooth displacement deviation is calculated over 29 mesh cycles covering one period of variation in center distance (one complete shaft rotation). The tooth deviation is periodic with a period equal to one shaft rotation. This periodic tooth deviation pattern is analyzed by using the extended subroutine FOUR to obtain the amplitude-frequency relationship. This relationship is shown in Figure 12. Amplitude is the magnitude of tangential deviation over and above the mean tooth deflection. The frequency is expressed in multiples of mesh frequency f_M. Since the tooth deviation is periodic, the amplitude distribution is discrete and is nonzero only at the multiples of reciprocal of the base period, which is the shaft speed ($f_M/29$). It is seen from Figure 12 that mesh frequency is still the most dominant frequency. However, the sideband amplitudes close to the harmonic frequencies are seen to be comparable to the high harmonic components.

It is expected that a larger shaft runout would produce higher sideband amplitudes. This is indeed shown in Figure 13, which is a frequency-amplitude plot for a 0.002-in. (peak) shaft runout. It is seen that the amplitudes at $f_M/29$ and at sidebands around the higher harmonics are approximately doubled in magnitude.

2. Transmitted Load Variation

A sinusoidal dynamic load of 500 lb at half mesh frequency is assumed to be superimposed on the nominal tooth load of 2760 lb. The total tangential tooth load is therefore

$$W \text{ (lb)} = 2760 + 500 \sin \frac{2\pi f_M}{2} t \qquad (22)$$

The calculated tooth displacement deviation has a periodicity of two mesh cycles. The resulting amplitude-frequency plot of this periodic tooth deviation pattern is shown in Figure 14. It is seen that the first sideband amplitude, which is at $f_M/2$, is larger than all the high harmonic components. Also, all other sideband amplitudes are relatively small. This large first sideband amplitude may be attributed to the large maximum dynamic load (500 lb) relative to the nominal load.

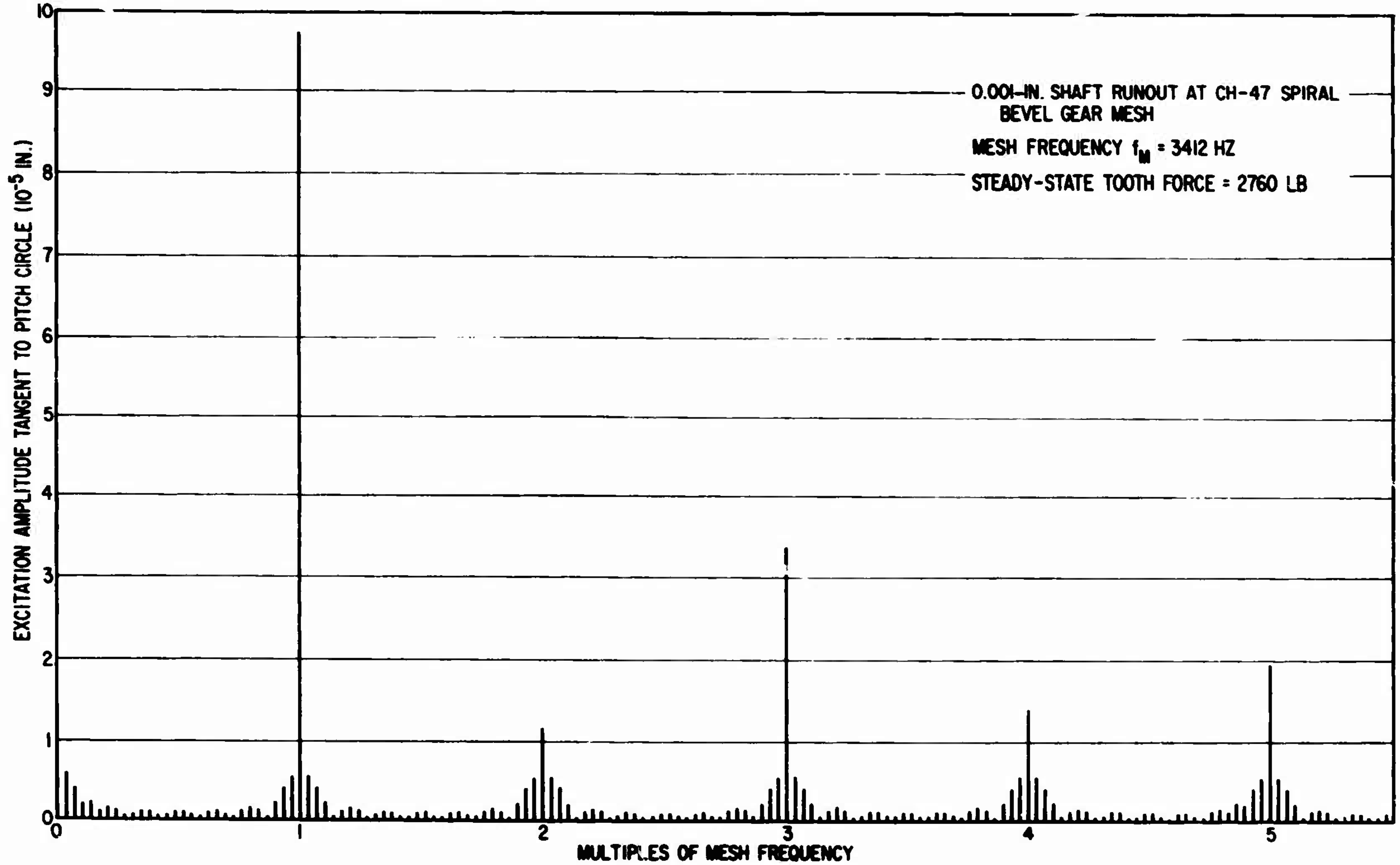

Figure 12. Frequency vs. Excitation Amplitude for Pinion Shaft Runout, CH-47 Spiral Bevel Gear Mesh.

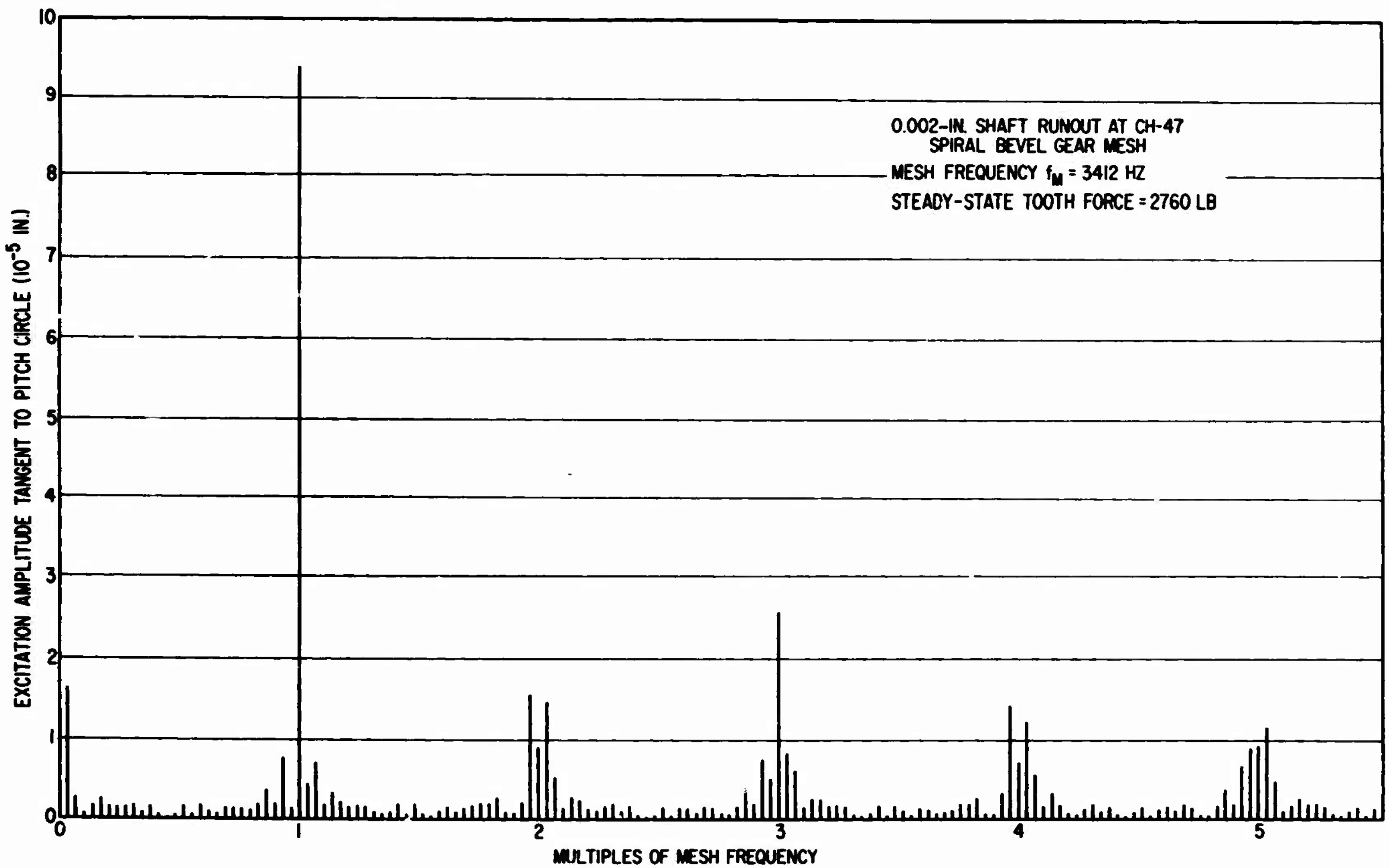

Figure 13. Frequency vs. Excitation Amplitude for Pinion Shaft Runout, CH-47 Spiral Bevel Gear Mesh.

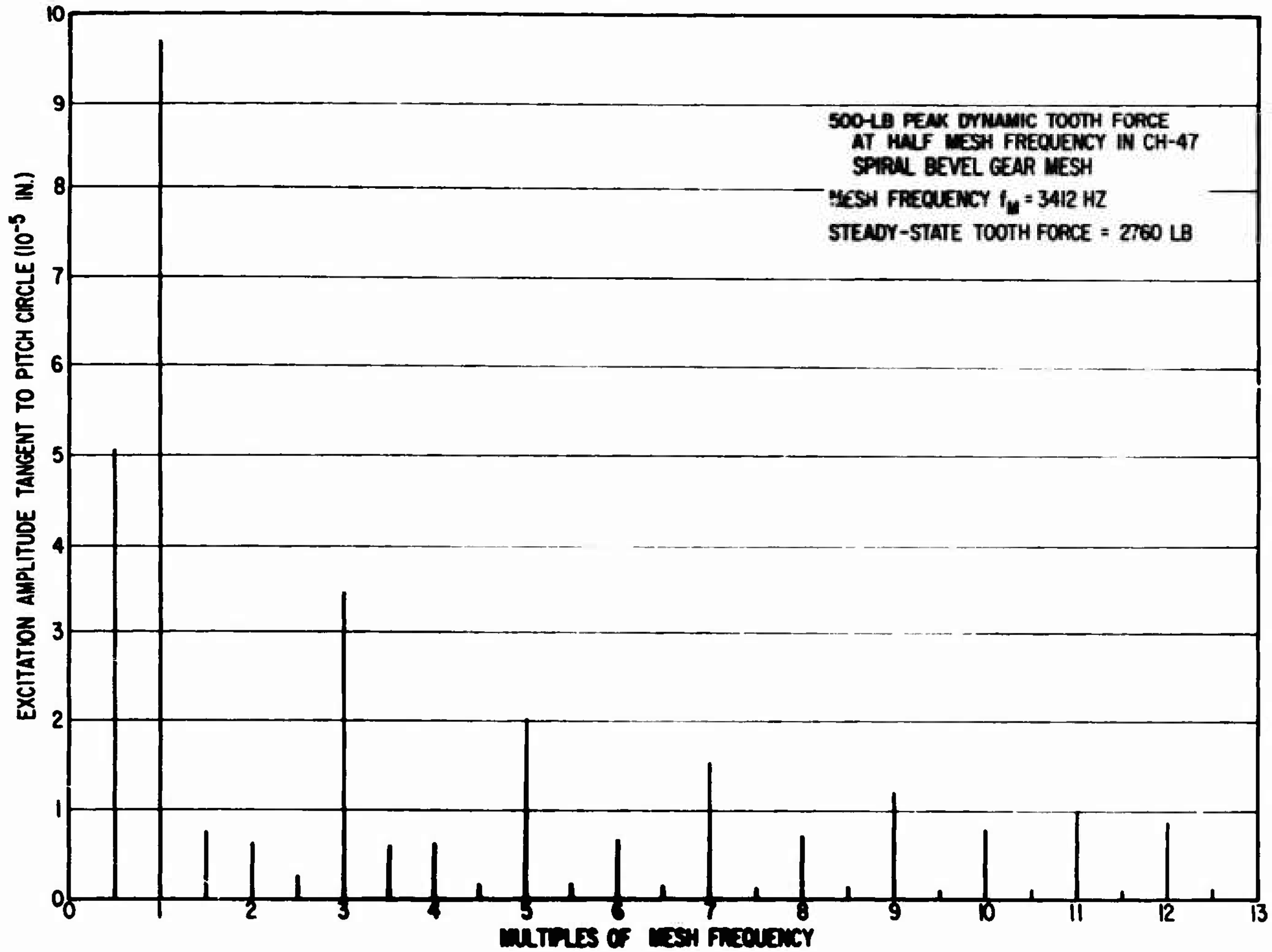

Figure 14. Frequency vs. Excitation Amplitude for Tooth Force Variation, CH-47 Spiral Bevel Gear Mesh.

CH-47 LOWER PLANETARY PLANET-TO-RING GEAR MESH CALCULATIONS

The CH-47 lower planetary planet and ring gear parameters are summarized in Table II. The tangential tooth load at the planet-to-ring gear mesh is taken to be 2103 lb. The planet rotational speed is 2280 rpm. The corresponding mesh frequency is 1482 Hz. Effects of variation in center distances, tooth load, and tooth support compliance to produce vibration sideband frequencies have been investigated.

1. Center Distance Variation

A planet runout of 0.001 in. (peak) in sine wave form is assumed. With a nominal center distance of 6.7 in., the expression for center distance is

$$C \text{ (in.)} = 6.7 + 0.001 \sin \frac{2\pi f_M}{39} t \tag{23}$$

Tooth displacement deviation is calculated using the computer program, over 39 mesh cycles, to cover a full rotation of the planet. The frequency spectrum of the tooth-mesh-induced vibration, obtained by Fourier analyzing the displacement deviation, is plotted in Figure 15. The mesh frequency is still the dominating frequency. The largest sideband amplitudes occur at the sidebands closest to and on each side of the mesh frequency.

TABLE II. CH-47 LOWER PLANETARY PLANET AND RING GEAR PARAMETERS

	Planet	Ring
Number of Teeth	39	106
Face Width	1.55 in.	1.25 in.
Pitch Radius	3.9 in.	10.6 in.
Outer Radius	4.0845 in.	-
Inner Radius	-	10.43 in.
Root Radius	3.69 in.	10.845 in.
Radius to the Beginning of Involute Profile	3.738 in.	10.7935 in.
Circular Tooth Thickness at Pitch Circle	0.3462 in.	0.276 in.
Tooth Fillet Radius	0.075 in.	0.094 in.
Pressure Angle	25 deg	25 deg

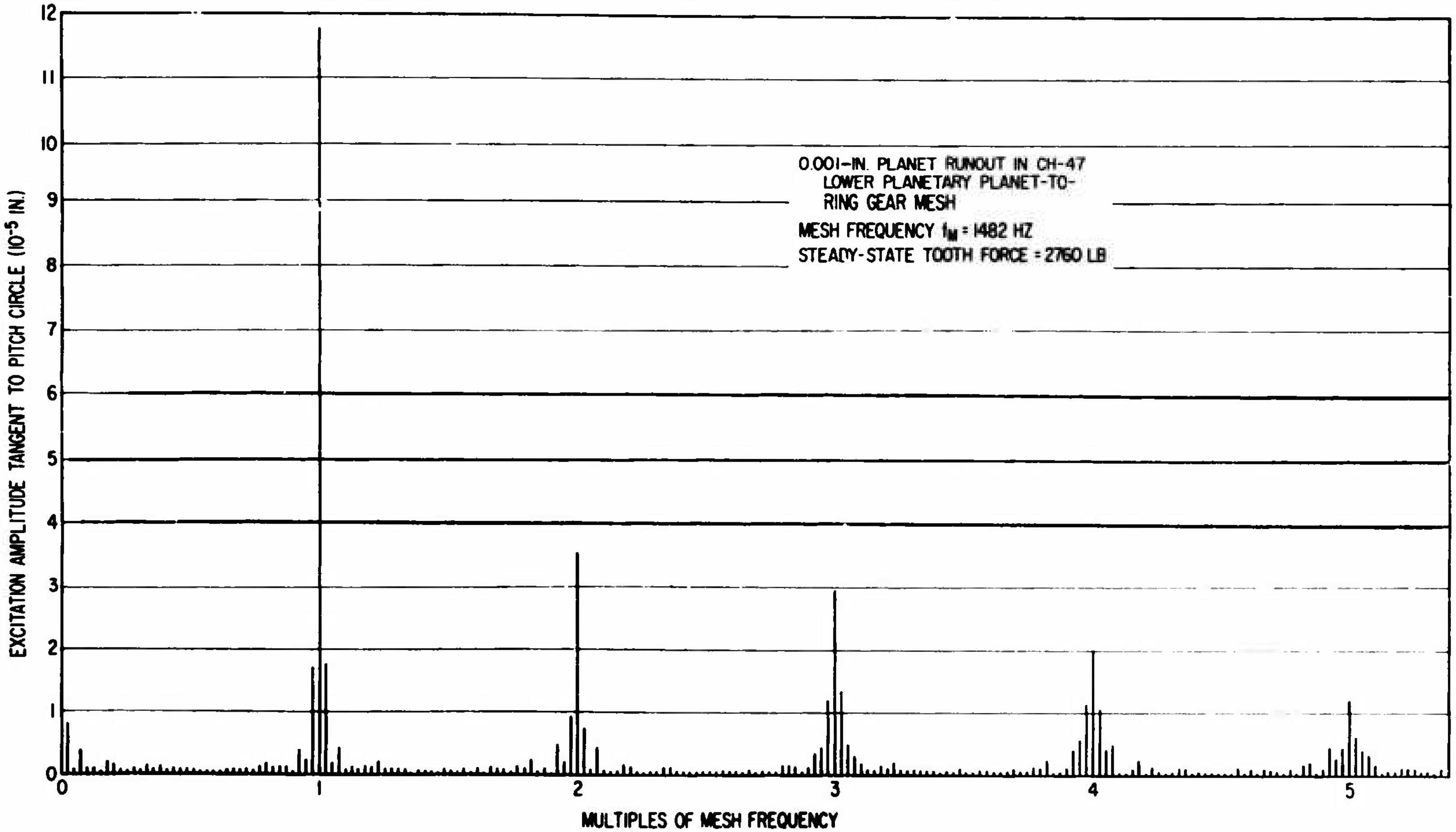

Figure 15. Frequency vs. Excitation Amplitude for Planet Runout, CH-47 Lower Planetary Planet-to-Ring Gear Mesh.

2. Transmitted Load Variation

A dynamic load of 400 lb varying sinusoidally at one-third of the mesh frequency is assumed to be superimposed on the nominal transmitted load of 2103 lb. The total tooth load is therefore

$$W \text{ (lb)} = 2103 + 400 \sin \frac{2\pi f_M}{3} t \qquad (24)$$

The vibration induced by this load variation at gear tooth mesh has a fundamental frequency of $f_M/3$. The frequency spectrum is shown in Figure 16, which is obtained by the computer program calculating the tooth displacement deviation over three mesh cycles. It is seen that the amplitude at $f_M/2$ is higher than those at high harmonics of the mesh frequency.

3. Tooth Support Compliance Variations

Five consecutive ring gear teeth (out of a total of 106 teeth) are assumed to have a finite (tangential) tooth support compliance of 10^{-6} in./lb. This compliance is in addition to the tooth bending, tooth shear, tooth rotation, and contact deformation compliances calculated by the computer program in terms of gear tooth geometry and elastic properties.

The amplitude-frequency plot of the vibration induced by this compliance variation is shown in Figure 17. The information shown in this figure may be interpreted as follows: Assume first that the planets are fixed and the ring gear rotates. The frequency of mesh between a fixed planet and the ring gear is equal to the number of teeth on the ring gear multiplied by the relative rotational speed between them. This speed is actually the orbiting speed of the planet with respect to a fixed body, since the ring gear is stationary. The periodicity of the tooth deflection excitation caused by an assumed local ring gear compliance variation is equal to the time for one full relative rotation of the ring gear with respect to the planet. Since there are 106 teeth on the ring gear, this periodicity is 106 times the tooth mesh time; that is, the reciprocal of the tooth mesh frequency. Therefore, in the amplitude-frequency plot shown in Figure 17, there appear 105 equally-spaced sideband frequencies between two successive harmonics of mesh frequency. Any two neighboring sidebands are separated by the planet orbiting frequency.

It is seen from the figure that the sideband amplitudes are in general quite large and that the amplitudes of the low-frequency sidebands are even larger than the amplitude at the mesh frequency. The compliance due to tooth bending, tooth shear, tooth rotation and contact deformation is about 10^{-7} in./lb calculated by the computer program. The large sideband amplitudes are therefore due to the large tooth support compliance variation relative to the normal compliance existing during tooth mesh.

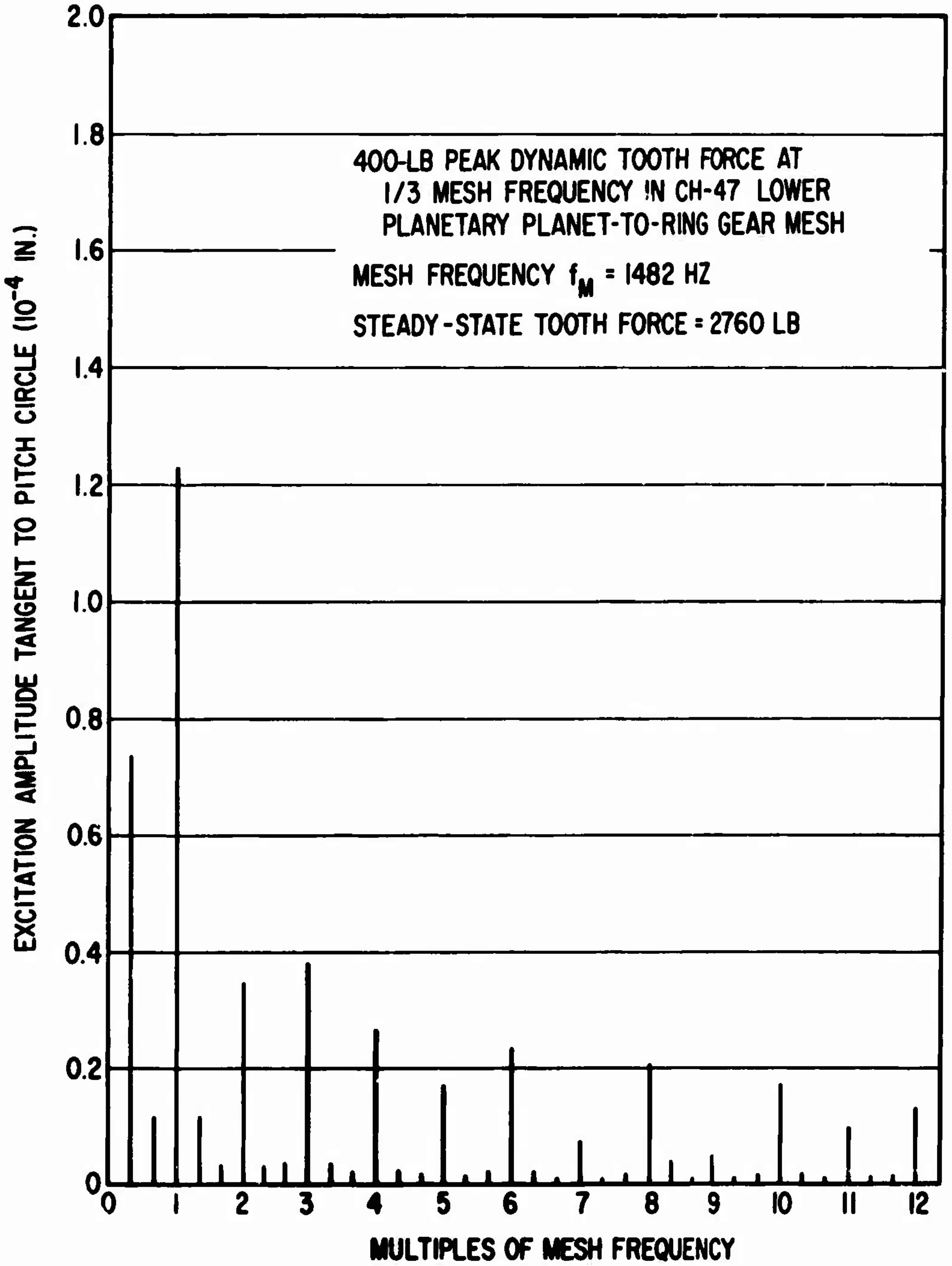

Figure 16. Frequency vs. Excitation Amplitude for Tooth Force Variation, CH-47 Lower Planetary Planet-to-Ring Gear Mesh.

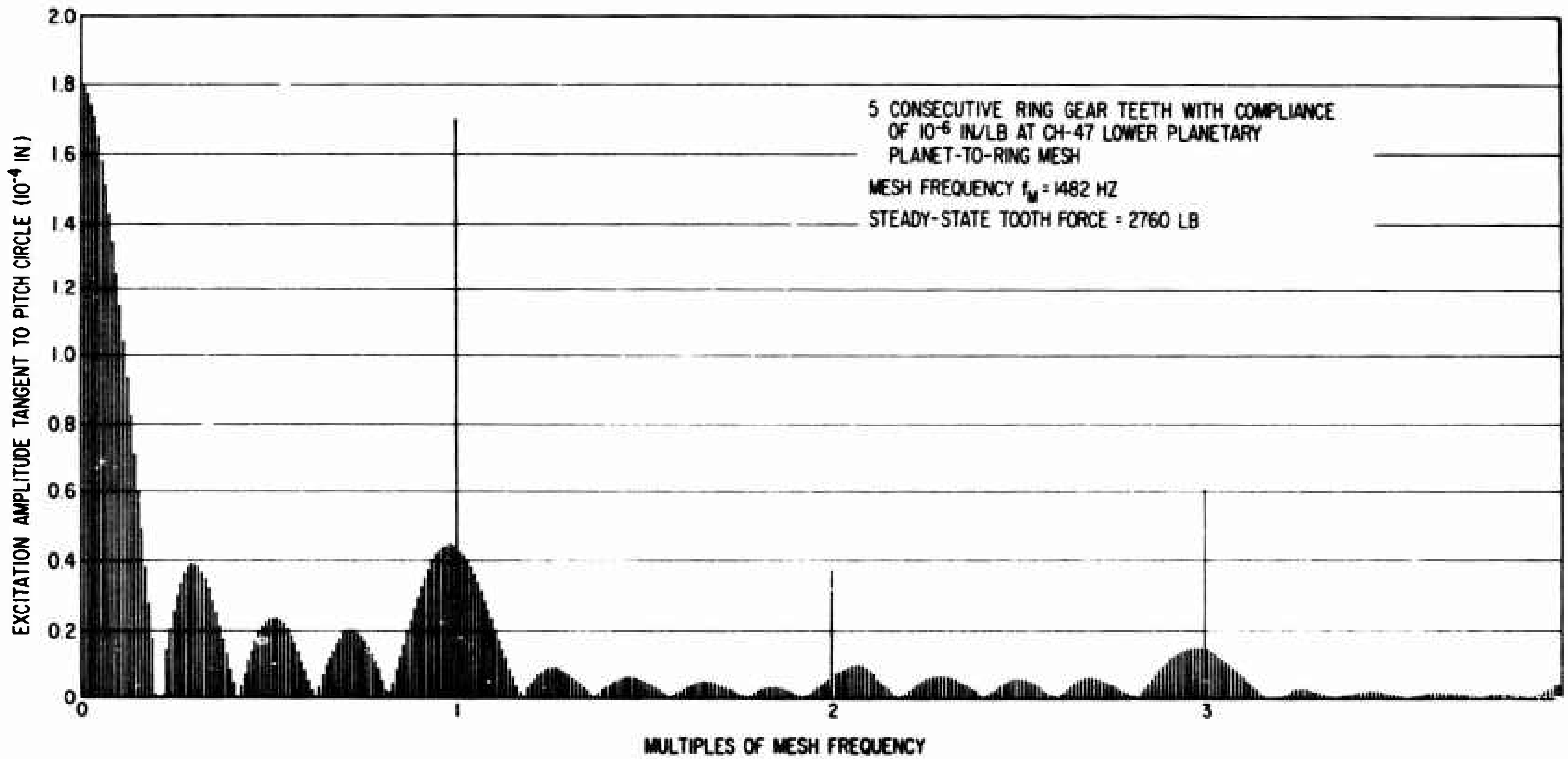

Figure 17. Frequency vs. Excitation Amplitude for Tooth Support Compliance Variation, CH-47 Lower Planetary Planet-to-Ring Gear Mesh.

It is also seen from Figure 17 that sidebands are grouped into a series of bumps, and there are about five bumps between two adjacent harmonic frequencies. This is attributed to the fact that the finite tooth support compliance variation occurs in only five consecutive teeth and that the compliance variation is much larger than the normal tooth mesh compliance. Tooth deflection patterns over one period (106 mesh cycles) may be considered as the sum of two separate deflection profiles. One is the normal tooth mesh deflection profile consisting of 106 identical segments representing deflections for the 106 mesh cycles. The other is the deflection due to the tooth support compliance variation, which is nonzero only in the first five mesh cycles and is much larger in magnitude than the former. The frequency content of the first deflection profile consists of only the mesh frequency and its harmonics, while the frequency spectrum of the latter is roughly periodic with declining amplitude and the period is about one-fifth of the mesh frequency. Therefore, the frequency spectrum of the total tooth deflection pattern appears to be a series of bumps superimposed on the mesh frequency harmonics.

CH-47 SPIRAL BEVEL GEAR SYSTEM RESPONSE CALCULATIONS

In order to demonstrate the manner in which the gear excitation sidebands may be applied in the vibration analysis of geared power trains, and to illustrate the type of response which is produced by gear excitation spectra which include sidebands, a sample calculation has been made using computer program TORRP [2].

In this calculation, the excitation spectrum obtained under the assumption of 0.002-in. runout in the CH-47 spiral bevel mesh was used. Mesh frequency is 3412 Hz, and a steady-state tangential tooth force of 2760 lb was used. The gearbox drive train components were represented dynamically by the torsional response model reported in [2].

Results of the calculations are shown in Table III and Figures 18 and 19. From these results it is apparent that significant torsional response occurs in the gearbox components as a result of the sideband disturbances. It is worth mentioning that essentially zero response occurs at frequencies between the peaks shown because there are no sources of excitation at these frequencies.

TABLE III. CH-47 SPIRAL BEVEL MESH EXCITATION AMPLITUDES AND CORRESPONDING PREDICTED PEAK DYNAMIC TOOTH FORCES AT INDICATED FREQUENCIES

Frequency (Hz)	Tangential Excitation Amplitude (10^{-6} in.)	Peak Dynamic Tooth Force (lb)	
		Spiral Bevel Mesh	Ring-Planet Mesh
117	16.35	0.71	0.21
2941	3.65	7.37	48.46
3059	1.82	196.46	165.61
3177	7.44	282.61	132.62
3294	1.11	26.01	9.78
3412	93.88	1672.19	606.54
3530	4.27	60.80	25.49
3647	6.99	73.38	48.42
3765	1.66	1.99	21.81
3883	3.18	119.34	61.66
6589	1.97	32.84	0.15
6707	15.52	230.07	0.94
6824	8.87	122.31	0.46
7059	4.02	50.49	0.16
10,001	7.33	71.74	0.08
10,118	4.99	48.67	0.05
10,236	25.53	247.61	0.26
10,354	8.22	79.43	0.08
10,471	6.04	58.16	0.06

TABLE III - Continued			
Frequency (Hz)	Tangential Excitation Amplitude (10^{-6} in.)	Peak Dynamic Tooth Force (lb)	
		Spiral Bevel Mesh	Ring-Planet Mesh
13,413	3.11	27.98	0.09
13,530	14.15	121.36	0.61
13,648	7.00	51.97	0.58
13,765	12.23	1044.30	33.84
13,883	5.51	64.10	0.40
16,825	6.66	61.93	0.01
16,942	8.95	83.11	0.01
17,060	9.17	85.10	0.01
17,178	11.64	107.88	0.01
17,295	4.67	43.25	0.005

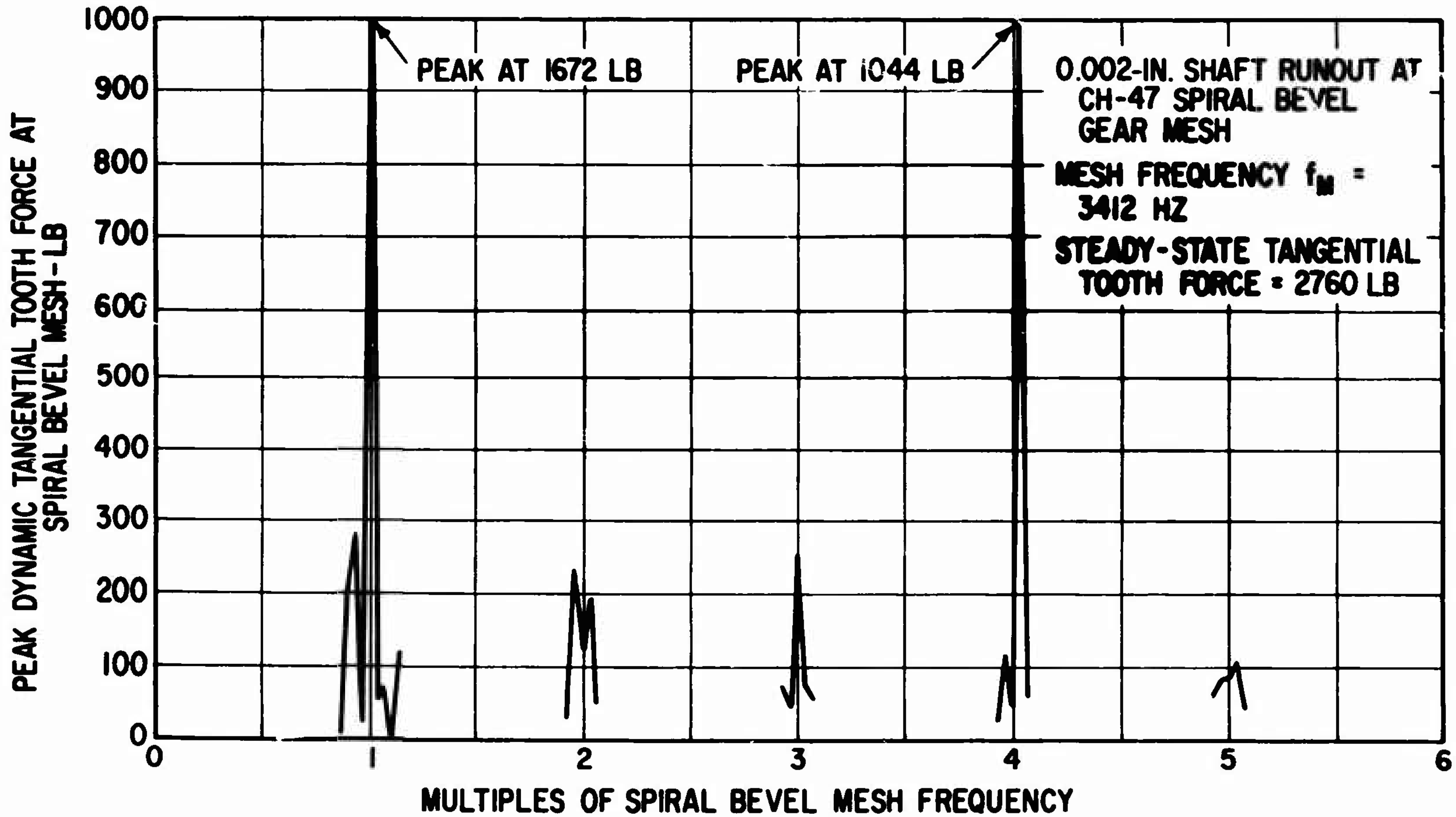

Figure 18. Calculated Dynamic Tooth Force at CH-47 Spiral Bevel Gear Mesh.

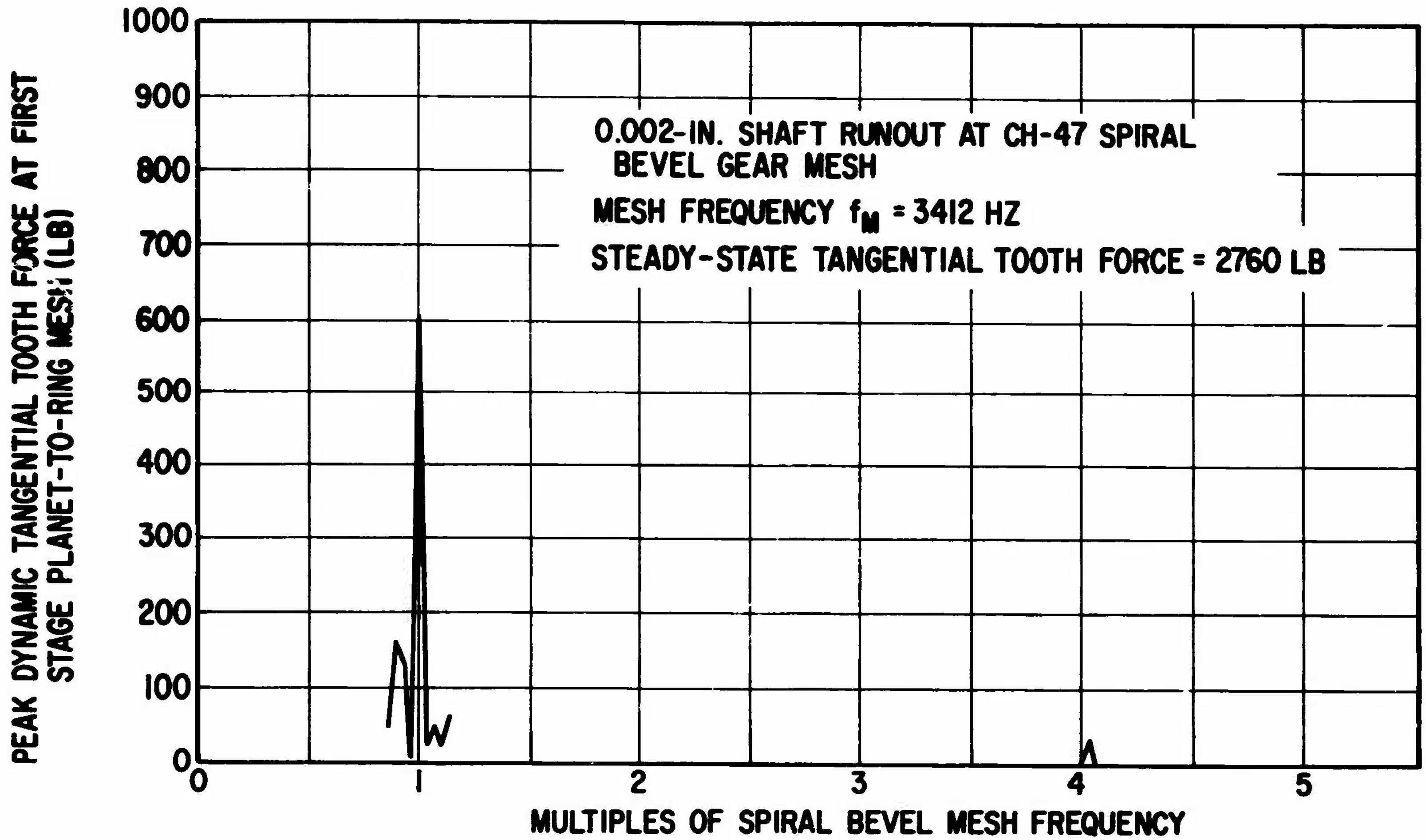

Figure 19. Calculated Dynamic Tooth Force at CH-47 Planet-Ring Gear Mesh.

DISCUSSION OF RESULTS

DISCUSSION OF TASK I RESULTS

The planet-pass induced vibration given by Equation (17) is the amplitude-time history of radial displacement at a fixed point on the ring gear casing. The zero time is arbitrarily chosen to be the moment when planet A (see Figure 2) is at the observation point. As time progresses, planets D, B and C pass the observation point in sequence. This sequence repeats with a frequency equal to the planet orbiting speed ω_b.

Since ring gear radial vibration results from the planet-ring gear mesh dynamic tooth force, the vibration amplitude is large when the planet is close to the observation point and smaller when the planet is more distant. This is seen from the calculated results in Figures 5, 7, 8 and 9, which are for phase angles $\psi = 37.6^\circ$, 0°, 90° and 142.4° (between opposite pairs of planets), respectively. The four major large-vibration-amplitude areas in each of the figures correspond to the passage of the four planets past the fixed observation point.

In general, it appears that the shape and magnitude of the vibration data in Figures 5 through 9 are quite similar, and that only the amplitude between planet passes varies appreciably with the phase angle ψ. This is because the two components of the total response function, b_{AB} and b_{CD}, are quite localized (i.e., peaked at 0° and 90°, respectively). Also, they are identical in shape due to the axisymmetry of the ring gear casing, but with 90° phase difference (see Figure 4). This 90° phase difference corresponds to the time spacing between the passes of adjacent planets. Using the first two bumps as examples, the vibration amplitude around the passes of planets A and D (around $\theta = 0^\circ$ and 90°) are dominantly determined by b_{AB} and b_{CD}, respectively, without much interference between them. Only between planet passes (around $\theta = 45^\circ$) does appreciable interference exist, and therefore the local amplitude depends on the temporal phase difference ψ between the two response functions (see Equations (6) and (7)).

The vibration of the ring gear casing is induced by the passing of the planet gears and originates in the dynamic tooth forces which exist in the planet-ring gear tooth meshes. The vibration occurs, therefore, at the gear tooth mesh frequency, f_M, modulated by the planet-pass frequency. This is shown in the frequency spectrum plots of Figures 6 and 10. It is seen that the mesh frequency is the center frequency and that around it, there are a number of sidebands which are found at mesh frequency plus or minus (in general) integer multiples of half of the planet-pass frequency f_p. In the special case of $\psi = 0$, four equally spaced planets (small positional offset δ has been neglected) pass the observation point with orbiting speed ω_b. Dynamically, this is equivalent to one planet passing this point with planet-pass frequency f_p (where $f_p = 4\,\omega_b$). Therefore, sidebands occur only at $f_M \pm n\, f_p$, where n is an integer. In the more general case where $\psi \neq 0$, there is some phase difference between the planet pairs (A,B) and (C,D). Each pair passes the observation point with a frequency of $f_p/2$. Therefore, sidebands in general appear at

$$f_M \pm n \frac{f_p}{2} .$$

Comparison of the four spectrum diagrams shown in Figures 6 and 10 reveals that the effect of the phase angle ψ is to increase the sideband amplitude at mesh frequency plus and minus integer multiples of $f_p/2$. For $\psi = 0$, the amplitudes at these sidebands are zero, while for $\psi = 142.4^o$, the corresponding amplitudes are even greater than those at the neighboring frequencies of $f_M \pm n\ f_p$.

Under some circumstances, it may be desirable to control the vibration amplitudes at certain sidebands. For the CH-47 lower planetary gear system, the phase angle ψ is a major controlling parameter of sideband amplitudes for the planet-pass induced vibration. The angle in turn is determined by other gear parameters including the numbers of teeth of component gears. For example, Equation (4) indicates that the greater the number of teeth on the sun gear, the larger the phase angle. However, other gear performance characteristics such as speed ratio, load distribution, etc., must be considered when gear parameters are altered to control the value of ψ.

Finally, it should be noted that the analysis used herein assumes that the normal components of the planet gear dynamic tooth forces vary sinusoidally with time. This variation occurs about the nominal steady-state normal tooth force component which accompanies the transfer of torque. Passage of this nominal steady-state force itself causes quasi-static ring gear deflections, which are ignored in the vibration calculations.

DISCUSSION OF TASK II RESULTS

Vibration can be excited by nonuniform tooth deflection and tooth profile characteristics during the mesh of even precisely machined gears. If the center distance and nominal tooth load are constant and all other gear parameters are the same from one pair of teeth to the next, the nonuniform tooth deflection pattern in one mesh cycle will repeat in all successive cycles. The frequency content of this tooth-mesh-induced vibration will consist, therefore, of only the mesh frequency and its harmonics. However, if there is any variation in center distance or tooth load, or any change of any other gear parameters from mesh to mesh, other vibration frequencies (the so-called sidebands) are introduced. The results of this investigation have clearly shown this point.

From the frequency spectra shown in Figures 12, 13, and 15, it is seen that major sidebands due to variation in center distance occur around the mesh frequency and its harmonics. In all cases the mesh frequency is still the most dominating frequency. A comparison of Figures 12 and 13 reveals that the sideband amplitudes depend quite strongly on the magnitude of the center distance variation. The general shape and magnitude of the harmonic components in Figure 13 (0.002-in. runout) are similar to those shown in Figure 12 (0.001-in. runout). However, the amplitudes at major sidebands in Figure 13 are about twice those at corresponding sidebands shown in Figure 12. Furthermore, in the 0.002-in. runout case, the sideband amplitudes around the fourth and fifth harmonics are even larger than the harmonic amplitudes.

Actual vibration frequency spectrum measurements [8] taken from an accelerometer mounted on the CH-47 rotor-drive gearbox bear some similarity to those in Figures 12, 13, and 15. Output from this accelerometer, located on the outside of the gearbox near the spiral bevel gear shaft support bearings, is reproduced in Figure 20. It should be noted that the noise signals shown in Figure 20 are generated not only by the spiral bevel gear mesh but also by a number of other possible vibration sources, such as gear runout, planet-pass, etc., occurring in the drive system. The signal is strongest at the spiral bevel mesh frequency because the accelerometer is located near the spiral bevel gears' shaft support bearings. The sideband with large amplitude near the spiral bevel gear mesh fundamental is separated by 118 Hz from the mesh frequency. This difference is the rotational speed of the input pinion. Therefore, this sideband is clearly due to input shaft runout, and it is equivalent to the relatively large-amplitude sidebands around the mesh frequency shown in Figures 12 and 13.

The sideband amplitudes produced by tooth load variations as shown in Figures 14 and 16 are quite large in comparison with the harmonic components. In both cases the amplitude of the first sideband is greater than the amplitudes at high harmonics of the mesh frequency. These large sideband amplitudes may be attributed to the large load variation relative to the nominal tooth load (500 lb vs. 2760 lb for spiral bevel gear mesh and 400 lb vs. 2103 lb for lower planetary planet-to-ring gear mesh).

In the example of tooth support compliance variation, five consecutive teeth were assumed to have a finite compliance of 10^{-6} in./lb in the tangential direction. This represents a case in which the lower planetary ring gear casing has a relatively weak local elastic stiffness. This finite support compliance produces tangential tooth displacement in addition to that due to normal tooth bending, shear, rotation and contact deformation during mesh. Figure 17 shows that the sideband amplitudes resulting from this compliance consist of a number of bumps superimposed on the harmonic components. The amplitudes at small sideband frequencies are large, and those at the first few sidebands are even greater than the amplitude at the gear mesh frequency. This is because the nominal compliance with respect to tooth deflection during gear mesh is only on the order of 10^{-7} in./lb, which is one order of magnitude smaller than the assumed local tooth support compliance.

In all of the cases studied in this investigation, the frequency spectrum is discrete (i.e., the amplitudes are nonzero only at discrete frequencies), because the frequency of variation of the gear

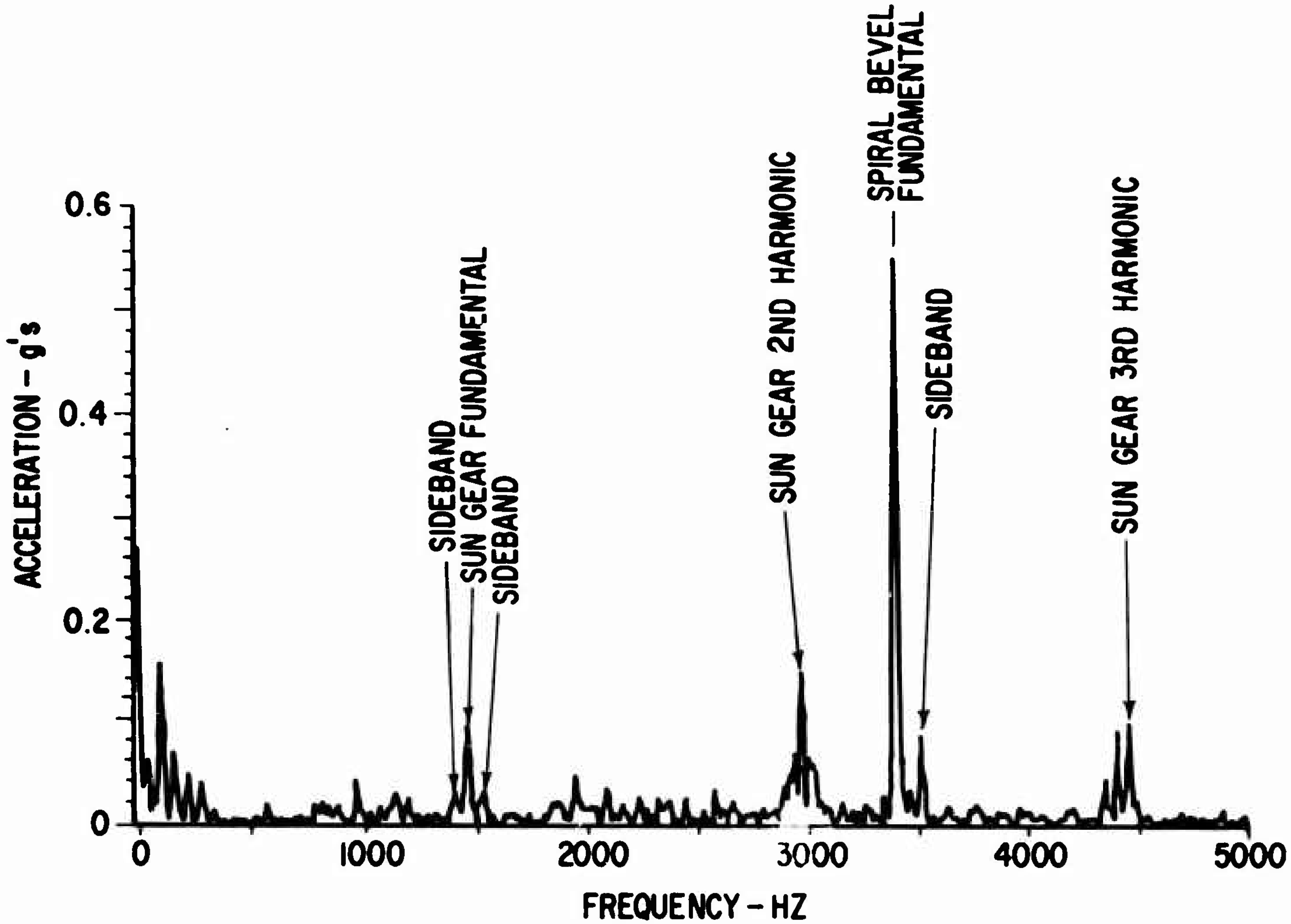

Figure 20. Vibration Spectrum Measured Near the Spiral Bevel Gears (From Reference 8).

parameter selected for study is in all cases a rational fraction of the gear mesh frequency. There thus always exists a base period over which the tooth displacement pattern repeats itself. This base period is an integer multiple of the gear mesh time, which is the reciprocal of the mesh frequency. Therefore, the vibration frequencies are integer multiples of the reciprocal of the base period, and the frequency spectrum is thus discrete. The frequency spectrum is obtained by performing a Fourier analysis of the periodic tooth deflection pattern.

If the variation of the gear parameter is random, or if its frequency is an irrational fraction of the mesh frequency, the corresponding frequency spectrum of the gear-mesh-induced vibration will be continuous. The subroutine SPECT may be used to compute the power spectral density function based on the tooth deflection data over a large number of mesh cycles in such cases.

CONCLUSIONS

The following conclusions are drawn as a result of the studies reported herein:

With respect to planet-pass vibration sidebands:

1. Methods have been developed for predicting geometrically-induced planet-pass vibration sidebands which accompany normal planetary gear reduction operation.

2. Planet-pass vibration sideband amplitudes may exceed that of the base signal, and plans for dealing with them must be part of any vibration and noise reduction program.

3. Planet-pass vibration sideband frequencies exist both below and above the base signal at integer multiples of one-half planet-pass frequency in four-planet systems with opposite pairs of planets in phase.

4. Planet-pass vibration sideband spectra are affected by the phase relationships of the planets, and spectra for several such relationships have been determined for the CH-47 forward rotor drive gearbox first-stage planetary reduction.

With respect to vibration sidebands in single gear meshes:

1. Methods have been developed for predicting vibration sidebands which are produced by gear runout, dynamic variations in tooth transmitted force, and tooth support discontinuities.

2. Shaft runout vibration sideband amplitudes may exist with significant amplitudes. They must therefore be considered in vibration and noise reduction efforts. Conversely, such sidebands if detectable could be used for the diagnosis of improperly assembled shafts and bearings.

3. Dynamic transmitted tooth force variations can produce vibration sidebands with significant amplitudes. While the presence of such signals is important from the vibration and noise reduction standpoint, the most important aspects of this type of sideband are as follows:

   a) This type of disturbance implies the presence of additional dynamic loads on gear teeth and bearings, with resulting degradation of component lifetimes. The importance of this type of dynamic force on gear and bearing life has yet to be assessed.

   b) A major source of vibration signals within operating gearboxes has been explained, thereby reducing the number of unknown signals which must be explained in any diagnostic exercise. Likewise, the dynamic interactions between gear meshes in multiple-mesh gear trains have been explained.

4. Vibration sidebands of a very distinctive character are predicted herein to be produced by gear meshes with tooth support discontinuities, such as cracks. Consequently, a very important diagnostic method has been identified for identifying gear structural integrity problems which may be introduced during manufacture or which may appear in service.

In summary, methods have been devised both for designing low-vibration and noise gear reductions and for identifying the existence of several types of gear problems. It is felt that the diagnostic potential of the vibration analysis methods described herein is of considerable importance.

RECOMMENDATIONS

The results reported herein strengthen considerably an already valuable body of technology which relates gear train component condition to measurable symptoms. The most important aspect of this technology is that much of it appears as computer-implemented analytical procedures which can be utilized by the gearbox designer.

Recommendations for future efforts in this important area fall into three specific areas:

1. It is recommended that the analytical procedures next be extended to include high-contact-ratio gearing and coupled response of gear train components.

2. It is recommended that the high-frequency vibration analysis tools be utilized in their present form, where applicable, in the design of future gearboxes; further, that the results of this usage be documented in specific instances, particularly where comparative testing accompanies this usage, for feedback to this technology program.

3. It is recommended that the use of high-frequency gearbox vibration technology be included as an integral part of future efforts directed at drive train condition monitoring and diagnosis, and at component life and/or failure prognosis.

LITERATURE CITED

1. Laskin, I., Orcutt, F. K., and Shipley, E. E., ANALYSIS OF NOISE GENERATED BY UH-1 HELICOPTER TRANSMISSION, Mechanical Technology Incorporated; USAAVLABS Technical Report 68-41, U.S. Army Aviation Materiel Laboratories, Fort Eustis, Virginia, June 1968, AD 675 457.

2. Badgley, R. H., and Laskin, I., PROGRAM FOR HELICOPTER GEARBOX NOISE PREDICTION AND REDUCTION, Mechanical Technology Incorporated; USAAVLABS Technical Report 70-12, U.S. Army Aviation Materiel Laboratories, Fort Eustis, Virginia, March 1970, AD 869 822.

3. Badgley, R. H., MECHANICAL ASPECTS OF GEAR-INDUCED NOISE IN COMPLETE POWER TRAIN SYSTEMS, ASME Paper No. 70-WA/DGP-1, presented at the ASME Winter Annual Meeting, New York, December 1970.

4. Badgley, R. H., and Chiang, T., INVESTIGATION OF GEARBOX DESIGN MODIFICATIONS FOR REDUCING HELICOPTER GEARBOX NOISE, Mechanical Technology Incorporated; USAAMRDL Technical Report 72-6, Eustis Directorate, U.S. Army Air Mobility Res & Dev Lab, Ft. Eustis, Va, March 1972, AD 742 735.

5. Badgley, R.H., GEARBOX DYNAMICS — THE KEY TO UNDERSTANDING AND REDUCING ACOUSTIC-FREQUENCY ENERGY IN GEARED POWER TRAINS, presented at the Meeting of the Aerospace Gearing Committee of the American Gear Manufacturers Association, Cleveland, Ohio, January 17-18, 1972.

6. Chiang, T., and Badgley, R.H., REDUCTION OF VIBRATION AND NOISE GENERATED BY PLANETARY RING GEARS IN HELICOPTER AIRCRAFT TRANSMISSIONS, ASME Paper No. 72-PTG-11, presented at ASME Mechanisms Conference & International Symposium on Gearing and Transmissions, San Francisco, California, October 8-12, 1972.

7. Badgley, R.H., REDUCTION OF NOISE AND ACOUSTIC-FREQUENCY VIBRATIONS IN AIRCRAFT TRANSMISSIONS, AHS Paper No. 661, presented at the 28th Annual National Forum of the American Helicopter Society, Washington, D C., May 1972.

8. Sternfeld, H., Schairer, J., and Spencer, R., AN INVESTIGATION OF HELICOPTER TRANSMISSION NOISE REDUCTION BY VIBRATION ABSORBERS AND DAMPING, Boeing Vertol Company; USAAMRDL Technical Report 72-34, Eustis Directorate, U.S. Army Air Mobility Research and Development Laboratory, Ft. Eustis, Virginia, August 1972, AD 752 579.

9. Hartman, R. M., and Badgley, R. H., MODEL 301 H1H/ATC TRANSMISSION NOISE REDUCTION PROGRAM-TEST RESULT REPORT, The Boeing Vertol Company, USAAMRDL Technical Report (Not Yet Issued), U.S. Army Air Mobility Research and Development Laboratory, Fort Eustis, Virginia.

10. Badgley, R. H., and Hartman, R. M., GEARBOX NOISE REDUCTION: PREDICTION AND MEASUREMENT OF MESH-FREQUENCY VIBRATIONS WITHIN AN OPERATING HELICOPTER ROTOR-DRIVE GEARBOX, ASME Paper No. 73-DET-31, presented at the ASME Design Engineering Technical Conference, Cincinnati, Ohio, September 9-12, 1973.

11. Hartman, R. M., A DYNAMICS APPROACH TO HELICOPTER TRANSMISSION NOISE REDUCTION AND IMPROVED RELIABILITY, presented at the 29th Annual National Forum of the American Helicopter Society, Washington, D.C., May 1973.

12. Bendet, S. J., and Piersol, A. G., MEASUREMENT AND ANALYSIS OF RANDOM DATA, John Wiley & Sons, 1966.

13. Buckingham, Earle, ANALYTICAL MECHANICS OF GEARS, Dover Publications, Inc., New York, 1963, p 324.

APPENDIX I
CALCULATION OF POWER SPECTRAL DENSITY FUNCTION

The method of calculation presented herein follows that given in [12]. Let n be the number of calculation points in one tooth mesh cycle. The time interval between data points is

$$\Delta t = \frac{1}{n\, f_M} \qquad (25)$$

where f_M is the mesh frequency. The cutoff frequency is defined as

$$f_c = \frac{n\, f_M}{2} \qquad (26)$$

The total time of record is defined as

$$T_r = n_M \cdot n \cdot \Delta t$$

$$= \frac{n_M}{f_M} \qquad (27)$$

where n_M is the number of mesh cycles over which tooth deflection data is recorded.

The autocorrelation function is, by definition,

$$R(\tau) = \lim_{T \to \infty} \frac{1}{T} \int_0^T x\,(t)\; x\,(t+\tau)\; dt \qquad (28)$$

where x is the tooth deflection and t is the time. The power spectral density function is related to $R(\tau)$ by

$$G\,(f) = 4 \int_0^\infty R(\tau) \cos 2\pi\, f\tau\; d\tau \qquad (29)$$

where f is frequency.

Tooth deflection x is known numerically at discrete points separated by Δt. Let

$$x_i = x(i\, \Delta t) \qquad i = 1, 2, \ldots, nn_M \qquad (30)$$

The autocorrelation function at displacement r Δt may be estimated by

$$\tilde{R}_r\ (r\ \Delta t) = \frac{1}{nn_M - r} \sum_{i=1}^{nn_M - r} x_i\, x_{i+r} \tag{31}$$

$$r = 0,\ 1,\ 2,\ \ldots,\ m$$

where r is the lag number and m the maximum lag number. This maximum lag number determines the maximum displacement and the equivalent resolution bandwidth for power spectral calculation as follows:

$$\tau_{max} = m\ \Delta t = \frac{m}{n\ f_M} \tag{32}$$

$$B_e = \frac{1}{\tau_{max}} = \frac{n\ f_M}{m} \tag{33}$$

It is desirable to keep τ_{max} less than one-tenth of the time of record T_r. This will avoid certain instabilities that can occur in autocorrelation function estimates. In the calculation, τ_{max} is set to be about 1/20 of T_r.

m is then determined by

$$m \leq \frac{n\ n_M}{20} \tag{34}$$

In other words, m is set equal to the integer part of the right-hand side.

The numerical approximation of Equation (29) is

$$\tilde{G}\ (f) = 2\ \Delta t \left[\tilde{R}_o + 2 \sum_{r=1}^{m-1} \tilde{R}_r \cos\left(\frac{\pi r\ f}{f_c}\right) + \tilde{R}_m \cos\left(\frac{\pi m\ f}{f_c}\right)\right] \tag{35}$$

The numerical estimate of the power spectral function should be calculated only at the m+1 special discrete frequencies where

$$f = \frac{k\ f_c}{m} \qquad k = 0,\ 1,\ 2,\ \ldots\ m \tag{36}$$

This will provide m/2 independent spectral estimates since the bandwidth B_e is $\frac{2\ f_c}{m}$. At these discrete frequencies,

$$\tilde{G}_k = \frac{2}{n\ f_M} \left[\tilde{R}_o + 2 \sum_{r=1}^{m-1} \tilde{R}_r \cos\left(\frac{\pi r\ k}{m}\right) + (-1)^k\ \tilde{R}_m\right] \tag{37}$$

The index k is called the harmonic number. $\tilde{G}_k$ is the "raw" estimate of the power spectral density function at harmonic k. The "smooth" estimate G_k at harmonic k is

$$G_o = 0.5\,\tilde{G}_o + 0.5\,\tilde{G}_1$$

$$G_k = 0.25\,\tilde{G}_{k-1} + 0.5\,\tilde{G}_k + 0.25\,\tilde{G}_{k+1} \qquad k = 1, 2, \ldots m-1 \qquad (38)$$

$$G_m = 0.5\,\tilde{G}_{m-1} + 0.5\,\tilde{G}_m$$

The ratio of the frequency at harmonic k to mesh frequency is

$$\frac{f_k}{f_M} = \frac{kn}{2m} \qquad (39)$$

where m is given by Equation (34). The frequency interval is approximately

$$\Delta f_k \sim \frac{10\ f_M}{n_M} \qquad (40)$$

The above method of calculation has been programmed in subroutine SPECT. This subroutine has been tested successfully by using a simple sine function over a hundred cycles of time. A sharp peak was clearly seen at the single frequency of the sine function. In the application to the gear mesh induced vibration, Equation (40) indicates that n_M should be set equal to about a hundred times the minimum number of cycles to complete a base period of tooth deflection variation. Therefore, for periodic tooth deflection variation, Fourier analysis (subroutine FOUR) is more economical to use to extract the frequency content of the induced vibration, since it requires the tooth deflection data over only the minimum number of mesh cycles to cover one base period. However, for random variation of gear parameters, only subroutine SPECT can be used to obtain the frequency spectrum of the induced vibration.

APPENDIX II

COMPUTER PROGRAM FOR PREDICTION OF GEAR MESH EXCITATION SPECTRA

Input Variables, Format, and Instructions

Card 1 Title, columns 2 through 72.

Card 2 Control numbers. Format (7I5)

a. NMC Number of mesh cycles.

Place the last digit of this number in column 5.

b. INT Identification as to whether this control card represents the last complete set of input data being submitted.
If more sets of input data follow, use 0.
If this is the last set, use 1.

Place this digit in column 10.

c. MN Classification of the types of spur gears to be considered.
If both the driving and the driven gears are external gears, use 1.
If the driving gear is an external gear and if the driven gear is an internal (ring) gear, use 0.
(The program will not run properly if the internal gear is submitted as the driving gear.)

Place this digit in column 15.

d. MMM Number of initial terms of the Fourier analysis for which coefficients will be printed, beyond the coefficient for the constant term. This number cannot exceed (FI x NMC + NMC/2), where FI is the input variable submitted on card 4.

Place the last digit of this number in column 20.

e. IPLT Instruction as to whether the calculated tooth meshing error is to be plotted.
If tooth meshing error is to be plotted, use 1.
If plotting is to be bypassed, use 0.

Place this digit in column 25.

f. IFOUR Instruction as to whether Fourier analysis of the tooth meshing error is to be performed.
If it is to be performed, use 1.
If it is to be bypassed, use 0.

Place this digit in column 30.

g. ISPECT Instruction as to whether power spectral density function for the tooth meshing error is to be calculated.
If it is to be calculated, use 1.
If it is to be bypassed, use 0.

Card 3 Gear design data. Format (6E 13.5)

a. FN1 Number of teeth in the driving gear.

Use columns 1 through 13. (Do not omit decimal point.)

b. FN2 Number of teeth in the driven gear.

Use columns 14 through 26. (Do not omit decimal point.)

c. RB1 Base circle radius of driving gear, in.

Use columns 27 through 39.

d. RØ1 Radius to the outside diameter of the driving gear, in. This should be reduced by any radial loss in working surface at the tip of the teeth, as from tip rounding or chamfering.

Use columns 40 through 52.

e. RØ2 or RI2 Radius to the outside diameter of the driven gear, if external, and to the inside diameter, if internal, in. This should be corrected for any radial loss in working surface at the tip of the teeth, as from tip rounding or chamfering. In the case of an internal gear, this radius must be equal to or greater than the base circle radius. No check for this is provided.

Use columns 53 through 65.

Card 4 Gear design data, continued. Format (6E 13.5)

a. RT1 Radius to the beginning (near the base of the tooth) of the involute profile on the driving gear, in.

This is used in the program only in a design check as to whether adequate length of involute has been provided for contact on the teeth of the mating gear up to its tip. If this radius is not specified in the gear design data, this check may be bypassed by substituting the root circle radius.

Use columns 1 through 13.

b. RT2 Radius to the beginning (near the base of the tooth) of the involute profile on the driven gear, in. See above for substitute when not specified.

Use columns 14 through 26.

c. RM1 Radius to the root circle of the driving gear, in. If the radius submitted is smaller than the computed base circle radius, this is noted in the output, and the input value of root radius is used at some points in the program. If the root radius is sufficiently smaller than the base circle radius so that the root fillet center lies inside the base circle, the tooth outline between the base circle and the fillet is assumed to be a radial line by the program.

Use columns 27 through 39.

d. RM2 Radius to the root circle of the driven gear, in. For the case of an external gear, the same comments as above apply.

Use columns 40 through 52.

e. FI Number which indirectly establishes the number of calculation points. The number of these points will equal one plus twice the value of FI. The calculation points may be viewed as selected contact points on the true involute profile, extended where necessary. These contact points with the mating involute are associated with specific angular positions taken by the gear as it is rotated, where the angular positions correspond to uniform subdivisions of the tooth spacing angle. A greater number of these points will give more closely spaced point-by-point output data. A greater number will also give more accurate calculations of tooth deflections and Fourier coefficients. A value of FI equal to 12 giving 25 calculation points has been found to be convenient.

Use columns 52 through 65. (Do not omit decimal point.)

f. T1 Circular tooth thickness at the pitch circle of the driving gear, in. The radius of the pitch circle is as defined in card 3. If not specified in the gear design data, it may be estimated as one-half of the difference between the actual circular pitch and the working backlash.

Use columns 66 through 78.

Card 5 Gear design data, continued. Format (5E 13.5)

a. T2 Circular tooth thickness at the pitch circle of the driven gear, in. The comments for T1 also apply here.

Use columns 1 through 13.

b. F1 Effective tooth face width of the driving gear, in. Where the face widths of the two gears are similar, use the actual face width without any reduction for normal end chamfering or rounding. Where one tooth is much wider, use as its effective face width an amount suitably larger than the narrower width to allow for the limited additional support that the greater width provides.

Use columns 14 through 26.

c. F2 Effective tooth face width of the driven gear, in. The comments for F1 also apply here.

Use columns 27 through 39.

d. RF1 Fillet radius on the driving gear, in.

Use columns 40 through 52.

e. RF2 Fillet radius on the driven gear, in.

Use columns 53 through 65.

Card 6 Gear material properties. Format (6E 13.5)

a. YE1 Young's modulus (in bending) for the material of the driving gear, $lb/in.^2$

Use columns 1 through 13.

b. YE2 Young's modulus (in bending) for the material of the driven gear, $lb/in.^2$

Use columns 14 through 26.

c. GE1 Shear modulus for the material of the driving gear, $lb/in.^2$

Use columns 27 through 39.

d. GE2 Shear modulus for the material of the driven gear, $lb/in.^2$

Use columns 40 through 52.

e. PØS1 Poisson's ratio for the material of the driving gear. Since this ratio is used only in the allowance for the "wide beam effect," it should be reduced for the cases where tooth face width is not much greater than tooth thickness, with a limiting value of zero when the teeth have a width smaller than the thickness.

Use columns 53 through 65.

f. PØS2 Poisson's ratio for the material of the driven gear. Comments for PØS1 also apply here.

Use columns 66 through 78.

There are NMC sets of the following Card 7 and Card 8. Each set supplies center distance, tooth spacing errors, tooth profile errors, tooth support compliances and tangential load for one mesh cycle.

Card 7 Center distance and tooth spacing error data. Format (3E 13.5)

a. CL Center distance, in.
This must be the actual center distance, including any substantial spreading under load.

Use columns 1 through 13.

b. VPT1 Tooth spacing error on the driving gear, in. This error is based on the distance between the pitch points of successive teeth, but the error is adjusted to apply to the direction of the line of action. This adjustment is accomplished by multiplying the pitch line error by the cosine of the pressure angle. The error is positive if the measured spacing is smaller than the desired spacing.

Use columns 14 through 26.

c. VPT2 Tooth spacing error on the driven gear, in. The comments under VPT1 also apply here.

Use columns 27 through 39.

Cards 8-1 to 8-2N Point-by-point data. Format (5E 13.5)

Total number of cards equal to twice the number of calculation points (N_J) between pitch points of adjacent teeth, or the same as two plus four times the value of F1 (see card 4). This specifies that cards must be introduced even if it is known that there is no contact at the particular calculation point or even if the tooth profile does not actually extend to the calculation point. As explained below, a blank card may be used for these points.

For the driving gear, the first card is for the calculation point located (N_J-1) points preceding the pitch point (or inside the pitch circle); the (N_J)th card is for the pitch point; the last or ($2N_J$)th card is for the calculation point located (N_J) points after the pitch point (or outside the pitch circle). The last point may also be described as the point of contact on one meshing tooth when the pitch point is the point of contact on the next meshing tooth.

For the driven gear which is an external gear, the first card is for the calculation point located (N_J) points before the pitch point (or inside the pitch circle); the (N_J+1)th card is for the pitch point; the last or ($2N_J$)th card is for the calculation point located (N_J-1) points after the pitch point (or outside the pitch circle). The point for the first card may also be described as the point of contact on one meshing tooth when the pitch point is the point of contact on the previous meshing tooth.

For the driven gear which is an internal gear, the first card is for the calculation point located (N_J) points following the pitch point (or outside the pitch circle); the (N_J+1)th card is for the pitch point; the last or ($2N_J$)th card is for the calculation point located (N_J-1) points before the pitch point (or inside the pitch circle). The point for the first card may also be described as the point of contact on the meshing tooth when the pitch point is the point of contact on the next meshing tooth.

a. ZJ1 Deviation of the point on the actual tooth profile on the driving gear from the true involute (as defined by the gear design data), in. This true involute is positioned relative to the actual profile so that its deviation at the pitch point is zero. Where the deviation represents material added to the true involute, it is positive; where it represents material subtracted, it is negative. The deviation is measured normal to the involute profile. If the profile does not extend to the particular calculation point or if it is known that the mating gear will not contact at this point, the deviation may be noted as zero.

Use columns 1 through 13.

b. UJ1 Tooth support compliance, or any compliance supplementary to the tooth compliance included in the analysis, on the driving gear, in./lb. This compliance is the deflection under unit load at the calculation point on the profile in the direction of the load (or normal to the profile). A uniform compliance for all calculation points, such as would result from a uniform gear shaft compliance, would not affect the final results as far as motion irregularities or load transfer is concerned; it would only increase the mean deviation in transmitted motion.

Use columns 14 through 26.

c. ZJ2 Deviation of the point on the actual tooth profile on the driven gear from the true involute, in. The comments under ZJ1 also apply here.

Use columns 27 through 39.

d. UJ2 Tooth support compliance, etc., on the driven gear, in./lb. The comments under UJ1 also apply here.

Use columns 40 through 52.

e. WT Total load, tangent to the pitch circle, transmitted by the gear teeth, lb.

In the first N card 8s, WT should be left blank. WT in the second N card 8s represents the loads at the N calculation points in one gear mesh.

Use columns 53 through 65.

Card 9 Gear Speed. Format (I5,E 13.5)

a. NWS Identification as to whether the input speed is the speed of driving or driven gear.
If driving gear speed is inputted, use 1.
If driven gear speed is inputted, use 2.

Place this digit in column 5.

b. WS Driving or driven gear speed, rpm.

Use columns 6 through 18.

Output Variables and Explanations

1. Title

2. Control numbers — NMC, INT, NMZ, MMM, as in input card 2.

3. Design — FI(=I), FN1(=N1), RB1, RO1, TR1, RM1
BLANK, FN2(=N2), BLANK, RO2 or RI2, RT2, RM2
T1, F1, RF1, YE1, GE1, PØS1
T2, F2, RF2, YE2, GE2, PØS2
all as in input cards 3 through 6.

Items 4-11 are printed for every mesh cycle, totally NMC cycles.

4. Mesh cycle identification and center distance.

5. Input listing of profile error and supplementary compliance — ZJ1, UJ1, ZJ2, UJ2 as in input card 8.

6. Pressure angle, degrees.

7. Incidental data — RP1, RB1, BA1, BR1, AT1
RP2, RB2, BA2, BR2, AT2

where:

RPL	pitch circle radius of driving gear, in.
RP2	pitch circle radius of driven gear, in.
RB1	base circle radius of driving gear, in.
RB2	base circle radius of driven gear, in.
BA1	arc of approach of driving gear, rad.
BA2	arc of approach of driven gear, rad (negative on internal gears).
BR1	arc of recess of driven gear, rad.
BR2	arc of recess of driving gear, rad (negative on internal gears).
AT1	angle of rotation of driving gear from the position at which the line of action intersects the involute at the start of the involute profile to the position at which the line of action intersects the involute at the pitch point, rad.
AT2	similar angle of rotation of driven gear, rad.

Check statement when part of the profile extends within the base circle.

Program will continue in any case, and, where necessary, the root radius will be set equal to the base circle radius. However, in calculating the tooth profile and the tooth deflections, the original root circle radius will be used with the specified fillet radius. If the root circle lies inside the base circle by more than this fillet radius, a radial line is assumed to connect fillet and involute.

8. Driving gear data — J1, CJ1, AJ1, QJ1ABC, XJ1, YJ1, XME1(=X), YME1(=Y), J1, QJ1A, QJ1B, QJ1C

where: J1 identification number for calculation points (see under F1 of card 4 in the input data). Listed for values of (-2I) to (2I+1).

CJ1 condition of engagement if equal to one and no engagement if equal to zero.

AJ1 angle of rotation from the position of contact at the pitch point to the position of contact at the calculation point - negative for points inside the pitch circle, rad.

XJ1 and YJ1 coordinates of the calculation point on the involute profile with the origin at the gear center and with the X-axis as the centerline of the tooth, given only for the points at which contact will take place with the mating gear, in.

XME1 and YME1 coordinates of the point on the root circle midway between the tangent point of the fillet radius and the involute profile extended (and radial inside the base circle), in. This point is considered to be the end of the effective base of the tooth for deflection purposes.

QJ1A elastic compliance of the gear tooth acting as a cantilever beam in bending only, normal to the profile at the calculation point, in./lb.

QJ1B elastic compliance of the gear tooth as a cantilever beam in shear only; otherwise as above.

QJ1C elastic compliance of the gear tooth as a rigid member rotating in its supporting structure; otherwise as above.

QJ1ABC combined compliance of the three above, in./lb.

9. Driven gear data — J2, BLANK, AJ2, QJ2ABC, XJ2, YJ2, XME2, YME2, J2, QJ2A, QJ2B, QJ2C

where: J2 identification number for the calculation points. For external gears, J2 is listed for values of (-2I-1) to (2I). For this case, contact takes place between points of the two gears for which J1 = -J2. For internal gears, J2 is listed for values of (2I+1) to (-2I). For this case, contact takes place between points of the two gears for which J1 = J2.

All other variables are similar to their counterparts for the driving gear.

10. Input tooth spacing error data — VPT1, VPT2 as in input card 7.

11. Tooth meshing errors, loads and contact compliance — JC1, AJC1, EJT, WTC, WTD, WN, WT, QJD

where:

JC1 identification number for the calculation point on the first tooth of the driving gear, starting with the first point after the pitch point and ending with the point corresponding to the pitch point of the next tooth.

AJC1 angle of rotation of the driving gear from the position with contact at the pitch point of the first mesh cycle to the position with contact at the calculation point, rad. The last angle in the first mesh cycle is the tooth spacing angle.

EJT tooth meshing error or deviation from pure conjugate action, as a pitch-line linear measurement of the motion of the driven gear leading the driving gear, in. A negative value indicates that the driven gear is lagging the driving gear, as might be caused by deflection of the teeth.

WTC tangential load carried by the first pair of teeth, lb.

WTD tangential load carried by the second pair of teeth, lb.

WN total normal load transmitted by the teeth, lb.

WT input tangential tooth load, lb.

QJD contact or Hertzian compliance combined for both teeth at the contact point, in./lb.

12. List of tooth meshing error over NMC mesh cycles — JC1, AJC1, EJT

where:

JC1 identification number for the calculation point. The last value should be equal to (NMCxN).

AJC1 same as AJC1 in item 11.

EJT same as EJT in item 11.

13. Plot of tooth meshing error.
Appears only if IPLT in input card 2 is set to be 1.

14. Fourier coefficients – I, A, B, C, KM

where:

I — order of the harmonic to which the coefficients apply. The zero order refers to the constant component.

A — the Fourier coefficient of the consine or real component for that harmonic of the meshing error, in. The value for I = 0 is twice the constant component or mean value of the meshing error.

B — the Fourier coefficient of the sine or imaginary component for that harmonic of the meshing error, in.

C — square root of $(A^2 + B^2)$. Appears only if IFOUR in input card 2 is set to be 1.

KM — ratio of frequency to tooth mesh frequency.

The following output is concerned with the power spectral density function of the tooth meshing error. Appears only if ISPECT in input card 2 is set to be 1.

15. Mesh frequency, cps

16. Incidental data – FC, FO, BE, H, TR, TMAX, SM

where:

FC — cutoff frequency, cps.

FO — fundamental frequency, cps.

BE — equivalent resolution bandwidth, cps.

H — sampling interval, cps.

TR — total record time, sec.

TMAX — maximum displacement, sec.

SM — maximum lag number.

17. Power spectral density function – K, FR, GK, GKK, KM

where: K — harmonic number, from 0 to SM.

FR frequency, cps.

GK "raw" power spectral density function, in.^{2}

GKK "smooth" power spectral density function, in.^{2}

KM ratio of frequency to tooth mesh frequency.

RUN VERSION 2.3 --PSR LEVEL 332--

```
                 PROGRAM GGEAR(INPUT,OUTPUT,TAPE5=INPUT,TAPE6=OUTPUT,TAPE22)          GGEAR      2
000003           COMMON/YY/UJC1(25),UJD1(25),UJ2(25),UJC2(25),UJD2(25),ZJ1(50)         CZIG       1
                1,ZJC1(25),ZJD1(25),ZJ2(50),ZJC2(25),ZJD2(25),QJ1(50),QJC1(25),QJD1   GGEAR      4
                2(25),QJ2(50),QJC2(25),                FJ1(50),UJ1(50),       CJC1(2  GGEAR      5
                35),CJD1(25),         AJ1(50),AJ2(50),QJC(50),QJD(50),ZJC(50),ZJD(50  GGEAR      6
                4),VJ(50),EJ1(56),FJ2(50),AJC1(25),AJC2(25),FJC1(27),QJD2(25),ZM2(    GGEAR      7
                550),UM2(50),WTC(27)                                                  GGEAR      8
000003           COMMON PJ(50),CJ(50),QJ(50),AJ(50),XJ(50),YJ(50),                    GGEAR      9
                1A(1500),B(1500),G(3000)                                              MAY11      1
000003           COMMON DD,BR,BA,FJ,CC,YM,NN,N,FNJ,EP,TAN,RB,GM,F,XM,MN,II,M          ALG        1
000003           COMMON QA(50),QB(50),QC(50),QA1(50),QB1(50),QC1(50),QA2(50),QB2(50   GGEAR     12
                1),QC2(50)  ,IH,IP                                                    GGEAR     13
000003           COMMON WT(50),HEAD1(6),HEAD2(6)                                      GGEAR     14
000003           COMMON/GU/NMC,INT,MMM,IPLT,FN1,FN2,RB1,RO1,RO2,RT1,RT2,RM1,RM2,FI,   ALG        2
                1T1,T2,F1,F2,RF1,RF2,YE1,YE2,GE1,GE2,POS1,POS2,ANG                    ALG        3
000003           DIMENSION GGG(3000),WTCC(3000),FJCC1(3000),AANG(3000)                MAY11      2
000003           NR=5                                                                 GGEAR     18
000004           NW=6                                                                 GGEAR     19
000005       198 READ(NR,100) (HEAD1(I),I=1,4),(HEAD2(I),I=1,4)                       GGEAR     20
000025           READ(NR,117) NMC,INT,MN,MMM,IPLT,IFOUR,ISPECT                        MAY9       1
000047           READ(NR,112)FN1,FN2,RB1,RO1,RO2                                      GGEAR     22
000065           READ(NR,112)RT1,RT2,RM1,RM2,FI,T1                                    GGEAR     23
000105           READ(NR,112)T2,F1,F2,RF1,RF2                                         GGEAR     24
000123           READ(NR,112)YE1,YE2,GE1,GE2,POS1,POS2                                GGEAR     25
000143           WRITE(NW,100) (HEAD1(I),I=1,4),(HEAD2(I),I=1,4)                      GGEAR     26
000163           WRITE(NW,101)                                                        GGEAR     27
000167           WRITE(NW,108)                                                        GGEAR     28
000173           WRITE(NW,109) NMC,INT,MN,MMM                                         GGEAR     29
000207           WRITE(NW,104)                                                        GGEAR     30
000213           WRITE(NW,102) FI,FN1,RB1,RO1,RT1,RM1                                 GGEAR     31
000233           IF(MN) 511,510,511                                                   GGEAR     32
000234       510 WRITE(NW,103)                                                        GGEAR     33
000240           GO TO 512                                                            GGEAR     34
000241       511 WRITE(NW,160)                                                        GGEAR     35
000245       512 WRITE(NW,158)THETP,FN2,RO2,RT2,RM2                                   GGEAR     36
000263           WRITE(NW,105)                                                        GGEAR     37
000267           WRITE(NW,102)T1,F1,RF1,YE1,GE1,POS1                                  GGEAR     38
000307           WRITE(NW,107)                                                        GGEAR     39
000313           WRITE(NW,102)T2,F2,RF2,YE2,GE2,POS2                                  GGEAR     40
000333           WRITE(NW,164)                                                        GGEAR     41
000337           ANG=0.                                                               GGEAR     42
000340           IMC=1.                                                               GGEAR     43
000342           N=2.*FI+1.                                                           GGEAR     44
000345           NN=N+N                                                               GGEAR     45
000346           IF(MN.EQ.0) T2=-T2                                                   JUNE14     1
000351       150 WRITE(NW,1500)                                                       MAY3       2
000355           READ(NR,112)CL,VPT1,VPT2                                             ATTI       1
000367           WRITE(NW,1000) IMC,CL                                                GGEAR     47
000377           WRITE(NW,110)                                                        FINAL      1
000403           L=NN                                                                 CZIG       2
000405           DO 209 I=1,NN                                                        GGEAR     48
000406           READ(NR,112)ZJ1(I),UJ1(I),ZJ2(I),UJ2(I),WT(I)                        GGEAR     49
000423           WRITE(NW,102)ZJ1(I),UJ1(I),ZJ2(I),UJ2(I)                             GGEAR     50
000437           ZM2(L)=ZJ2(I)                                                        GGEAR     51
```

```
000442         UM2(L)=UJ2(I)                                            GGEAR     52
000444         IF(L-1) 209,209,225                                      GGEAR     53
000446     225 L=L-1                                                    GGEAR     54
000450     209 CONTINUE                                                 GGEAR     55
000453         CALL GEARO(CL,VPT1,VPT2)                                 GGEAR     56
000455         NNN=IMC*N                                                GGEAR     57
000460         DO 200 I=1,N                                             GGEAR     58
000461         JJ=NNN+I-N                                               GU         1
000463         AANG(JJ)=AJC1(I)                                         MAY3       3
000466         GGG(JJ)=EJ1(I)                                           GGEAR     60
000470         G(JJ)=GGG(JJ)                                            GGEAR     61
000472         WTCC(JJ)=WTC(I)                                          GGEAR     62
000474     200 FJCC1(JJ)=JJ                                             MAY2       1
000500         IMC=IMC+1                                                GGEAR     64
000501         IF(IMC.LE.NMC) GO TO 150                                 GGEAR     65
000503         WRITE(NW,1500)                                           MAY3       4
000507         WRITE(NW,2000)                                           MAY3       5
000513         DO 2500 I=1,NNN                                          MAY3       6
000515    2500 WRITE(NW,102)FJCC1(I),AANG(I),GGG(I)                     MAY3       7
000531         IF(IPLT.EQ.1) CALL PLT(FJCC1,GGG,WTCC,NNN)               GGEAR     66
000536         M=FI                                                     GU         3
000540         IF(IFOUR.NE.1) GO TO 3000                                MAY9       2
000542         WRITE(NW,128)                                            ALG        4
000546         CALL FOUR                                                GGEAR     67
000547         LL=MMM+1                                                 GGEAR     68
000551         DO 250 I=1,LL                                            GGEAR     69
000553         LP=I-1                                                   GGEAR     70
000554         SMK=1.*LP/NMC                                            JUNE7      1
000560         RESLT=SQRT(A(I)**2+B(I)**2)                              GGEAR     71
000566     250 WRITE(NW,129)LP,A(I),B(I),RESLT,SMK                      JUNE7      2
000606    3000 IF(ISPECT.NE.1) GO TO 3500                               MAY9       3
000610         CALL SPECT                                               MAY9       4
000611    3500 CONTINUE                                                 MAY9       5
000611         IF(INT)300,198,300                                       GGEAR     73
000612     300 CALL EXIT                                                GGEAR     74
000613     100 FORMAT(8A10)                                             GGEAR     75
000613     101 FORMAT(72H0  PN0335=COMPUTATIONS OF GEAR TOOTH MESHING ERRORS    GGEAR     76
              1  3-22-1966      )                                      GGEAR     77
000613     102 FORMAT(7E13.5)                                           MAY9       6
000613     103 FORMAT(12H0  PRE.ANGLE7X2HN224X3HRI210X3HRT210X3HRM2)   GGEAR     79
000613     104 FORMAT(/7X1HI11X2HN111X3HRB110X3HRO110X3HRT110X3HRM1)   GGEAR     00
000613     105 FORMAT(/6X2HT111X2HF111X3HRF15X12HYOUNGS MOD-12X$1HSHEAR MOD-12X11 GGEAR     81
              1HPOS.RATIO-1)                                           GGEAR     82
000613     107 FORMAT(/6X2HT211X2HF211X3HRF25X12HYOUNGS MOD-22X11HSHEAR MOD-22X11 GGEAR     83
              1HPOS.RATIO-2)                                           GGEAR     84
000613     108 FORMAT(50H0 MESH CYCLES   INPUT,    DIFF.GEAR N.OF HARMONIC)     GGEAR     85
000613     109 FORMAT(4XI4,4(8XI4))                                     GGEAR     86
000613     110 FORMAT(60H0INPUT LISTING OF PROFILE ERROR AND SUPPLEMENTARY COMPLI FINAL      2
              1ANCE/6X2HZ111X2HU111X2HZ211X2HU2)                       FINAL      3
000613     112 FORMAT(6E13.5)                                           GGEAR     87
000613     117 FORMAT(8I5)                                              MAY9       7
000613     128 FORMAT(43H0CALCULATED FOURIER COEFFICIENTS FOR ERRORS//7H      19X ALG        5
              15HA(I) 13X4HB(I)14X1HC14X2HKM)                          JUNE7      3
000613     129 FORMAT(I7,3(4X  E14.7),F14.7)                            JUNE7      4
000613     158 FORMAT(2E13.5,13X,3E13.5)                                GGEAR     90

000613     160 FORMAT(12H0          7X2HN224X3HRO210X3HRT210X3HRM2)     GGEAR     91
000613     164 FORMAT(//16H CALCULATED DATA)                            GGEAR     92
000613    1000 FORMAT(16H MESH CYCLE NO.=,I3,20H,   CENTER DISTANCE=,E13.6)  MAY14      1
000613    1500 FORMAT(/6X 20(H*3X)/)                                    MAY3       8
000613    2000 FORMAT(5X 3HJC19X4HAJC16X11HTANG. ERROR)                 MAY3       9
000613         STOP                                                     GGEAR     94
000615         END                                                      GGEAR     95
```

RUN VERSION 2.3 --PSR LEVEL 332--

```
                SUBROUTINE GEARO(CL,VPT1,VPT2)                                   JUN13     1
000006          COMMON/YY/UJC1(25),UJD1(25),UJ2(25),UJC2(25),UJD2(25),ZJ1(50)    CZIG      3
               1,ZJC1(25),ZJD1(25),ZJ2(50),ZJC2(25),ZJD2(25),QJ1(50),QJC1(25),QJD1 GEARO     4
               2(25),QJ2(50),QJC2(25),           FJ1(50),UJ1(50),        CJC1(2 GEARO     5
               35),CJD1(25),        AJ1(50),AJ2(50),QJC(50),QJD(50),ZJC(50),ZJD(50 GEARO     6
               4),VJ(50),EJ1(56),FJ2(50),AJC1(25),AJC2(25),FJC1(27),QJD2(25),ZM2( GEARO     7
               550),UM2(50),WTC(27)                                             GEARO     8
000006          COMMON PJ(50),CJ(50),QJ(50),AJ(50),XJ(50),YJ(50),               GEARO     9
               1A(1500),B(1500),G(3000)                                         MAY11     3
000006          COMMON DD,BR,BA,FJ,CC,YM,NN,N,FNJ,EP,TAN,RB,GM,F,XM,MN,II,M     ALG       7
000006          COMMON QA(50),QB(50),QC(50),QA1(50),QB1(50),QC1(50),QA2(50),QB2(50 GEARO    12
               1),QC2(50) ,IH,IP                                                GEARO    13
000006          COMMON WT(50),HEAD1(6),HEAD2(6)                                 GEARO    14
000006          COMMON/GU/NMC,INT,MMM,IPLT,FN1,FN2,RB1,RO1,RO2,RT1,RT2,RM1,RM2,FI, ALG       8
               1T1,T2,F1,F2,RF1,RF2,YE1,YE2,GE1,GE2,POS1,POS2,ANG               ALG       9
         C SPECIFY AND INITIALIZE   READING AND WRITING UNITS FOR IBM 1800      GEARO    17
000006          NR=5                                                            GEARO    18
000006          NW=6                                                            GEARO    19
000010      198 CONTINUE                                                        GEARO    20
000010          RP1=CL*FN1/(FN1+FN2)                                            APR30     1
000013          IF(MN.EQ.0)RP1=CL*FN1/(FN2-FN1)                                 JUNE7     5
000017          CTT=RB1/RP1                                                     GEARO    22
000021          TTT=SQRT(1.-CTT**2)/CTT                                         GEARO    23
000026          THETP=ATAN(TTT)                                                 JUNE5     1
000030          THETPP=THETP*180./3.1415927                                     JUNE5     2
000033          WRITE(NW,112)                                                   YUNG      1
000036          WRITE(NW,102) THETPP                                            JUNE5     3
000044          IF(F1-F2) 320,320,321                                           GEARO    25
000051      321 FF2=F2                                                          GEARO    26
000053          GO TO 322                                                       GEARO    27
000053      320 FF2=F1                                                          GEARO    28
000055      322 FF2=FF2**0.8                                                    GEARO    29
000061      304 DD1=-T1/2.0/RP1+THETP                                           GEARO    33
000065          F12=FN1/FN2                                                     GEARO    34
000067          RP2=RP1/F12                                                     GEARO    35
000070          DD2=-T2/2.0/RP2+THETP                                           GEARO    36
000074          FNJ=2.0*FI+1.0                                                  GEARO    37
000077          N=FNJ                                                           GEARO    38
000101          NN=N+N                                                          GEARO    39
000102          CS=CTT                                                          JUNE6     1
000104          TAN=TTT                                                         JUNE5     4
000105          EP1=1.0-POS1*POS1                                               GEARO    43
000107          EP1=YE1/EP1                                                     GEARO    44
000111          EP2=1.0-POS2*POS2                                               GEARO    45
000114          EP2=YE2/EP2                                                     GEARO    46
000115          EP12=(1.0/EP1+1.0/EP2)*0.5                                      GEARO    47
000121          EP12=EP12**0.9                                                  GEARO    48
000125          RB2=RB1/F12                                                     JUNE5     5
000127          C1=RO1/RB1                                                      GEARO    51
000130          C2=RO2/RB2                                                      GEARO    52
000132          BR2=(SQRT (C2*C2-1.0)-TAN)                                      GEARO    53
000140          BR1=(SQRT (C1*C1-1.0)-TAN)                                      GEARO    54
000146          C3=TAN/F12                                                      GEARO    55
000147          IF(BR1-C3) 403,403,404                                          GEARO    56
```

```
000154      404 BR1=C3                                                  GEARO      57
000156          WRITE(NW,126)BR1                                        GEARO      58
000163      403 BA1=BR2/F12                                             GEARO      59
000165          BA2=BR1*F12                                             GEARO      60
000166          IF(MN) 440,450,440                                      GEARO      61
000172      450 BA1=-BA1                                                GEARO      62
000173          BA2=-BA2                                                GEARO      63
000175      440 IF(BA1-TAN) 401,401,402                                 GEARO      64
000200      402 BA1=TAN                                                 GEARO      65
000202          WRITE(NW,125)BA1                                        GEARO      66
000207      401 C1=6.2831845/FN1                                        GEARO      67
000211          IF(BA1-C1) 213,213,611                                  GEARO      68
000216      611 WRITE(NW,174)                                           GEARO      69
000222      213 IF(BR1-C1) 215,612,612                                  GEARO      70
000227      612 WRITE(NW,175)                                           GEARO      71
000233      215 C1=RT1/RB1                                              GEARO      72
000235          C2=RT2/RB2                                              GEARO      73
000237          C1 =SQRT (C1*C1-1.0)-TAN                                GEARO      74
000245          AT1=ABS (C1)                                            GEARO      75
000246          C2 =SQRT (C2*C2-1.0)-TAN                                GEARO      76
000255          AT2=ABS (C2)                                            GEARO      77
000257          WRITE(NW,122)                                           GEARO      78
000262          WRITE(NW,102)RP1,RB1,BA1,BR1,AT1                        FINAL       6
000300          WRITE(NW,162)                                           GEARO      80
000304          WRITE(NW,102)RP2,RB2,BA2,BR2,AT2                        GEARO      81
000322          NMZ=1                                                   JUN13       2
000323          NUZ=1                                                   JUN13       3
000324          IF(AT1-BA1) 311,216,216                                 GEARO      84
000331      311 WRITE(NW,176)                                           GEARO      85
000335      216 IF(AT2-BA2) 309,217,217                                 GEARO      86
000342      309 IF(MN) 620,621,620                                      GEARO      87
000343      621 WRITE(NW,178)                                           GEARO      88
000347          GO TO 217                                               GEARO      89
000352      620 WRITE(NW,179)                                           GEARO      90
000356      217 IF(RM1-RB1) 191,192,192                                 GEARO      91
000363      191 AM1=1.0                                                 GEARO      92
000365          WRITE(NW,118)                                           GEARO      93
000370          GO TO 1920                                              GEARO      94
000373      192 AM1=RM1/RB1                                             GEARO      95
000375     1920 C1=AM1                                                  GEARO      96
000376          AM1=SQRT (AM1*AM1-1.0)-TAN                              GEARO      97
000404          C2=RF1/RB1                                              GEARO      98
000406          PF1=C2                                                  GEARO      99
000407          C1=RM1/RB1                                              GEARO     100
000411          C3=(C1+C2)**2-1.0                                       GEARO     101
000414          IF(C3) 406,406,407                                      GEARO     102
000420      406 C3=0.0                                                  GEARO     103
000421          WRITE(NW,156)                                           GEARO     104
000425          TPD1=0.0                                                GEARO     105
000426          WRITE(NW,156)PD1                                        GEARO     106
000434          GO TO 408                                               GEARO     107
000437      407 PD1=SQRT (C3)                                           GEARO     108
000441          TPD1=ATAN (PD1)                                         GEARO     109
000444      408 IF(RM2-RB2) 193,194,194                                 GEARO     110
000451      193 AM2=1.0                                                 GEARO     111
```

```
000453          WRITE(NW,119)
000456          GO TO 1940
000461      194 AM2=RM2/RB2
000463     1940 C1=AM2
000464          AM2=SQRT (AM2*AM2-1.0)-TAN
000472          C2=RF2/RB2
000474          PF2=C2
000475          C1=RM2/RB2
000477          IF(MN) 456,455,456
000502      455 C2=-C2
000503      456 C3=(C1+C2)**2-1.0
000506          IF(C3) 409,409,410
000510      409 C3=0.0
000511          WRITE(NW,155)
000515          TPD2=0.0
000516          WRITE(NW,155)PD2
000524          GO TO 411
000527      410 PD2=SQRT (C3)
000531          TPD2=ATAN (PD2)
000534      411 K1=1
000535          E1=PF1
000536          E2=PD1
000540          E3=TPD1
000541          E4=RM1
000543          DD=DD1
000544          C1=AM1
000546      201 C2=DD+C1
000550          C1=ATAN (TAN+C1)
000554          C4=C1-C2
000556          C3=E3-E2-DD+TAN
000562          IF(K1-1) 422,422,425
000567      425 IF(MN) 422,421,422
000570      421 C3=-C3
000571          C4=-C4
000573      422 C1=C3+E1
000575          C4=(C1+C4)*0.5
000600          Y=E4*SIN (C4)
000602          X=E4*COS (C4)
000605          IF(K1-1) 202,202,203
000612      202 XM1=X
000613          YM1=Y
000615          K1=K1+1
000617          DD=DD2
000620          C1=AM2
000621          E1=PF2
000623          E2=PD2
000624          E3=TPD2
000626          E4=RM2
000630          GO TO 201
000630      203 XM2=X
000631          YM2=Y
000633          EE=6.2831854/FNJ
000635          CC=EE/FN1
000636          FJ =-FNJ+1.0
000640          RB=RB1
```

```
000641         BR=BR1
000643         BA=BA1
000644         DD=DD1
000646         XM=XM1
000647         YM=YM1
000651         GM=GE1
000652         F=F1
000654         II=1
000655         EP=EP1
000657         WRITE(NW,151)
000662         CALL AJCOH
000663         DO 221 I=1,NN
000667         C1    =XJ(I)
000670         C2    =YJ(I)
000672         FJ1(I)=PJ(I)
000674         C3=CJ(I)
000675         AJ1(I)=AJ(I)
000677         QJ1(I)=QJ(I)
000701         IH1=IH
000702         IP1=IP
000704         QA1(I)=QA(I)
000706         QB1(I)=QB(I)
000710         QC1(I)=QC(I)
000712         IF(C3) 515,515,516
000714     515 WRITE(NW,102)FJ1(I),C3,AJ1(I)
000726         GO TO 221
000731     516 WRITE(NW,102)FJ1(I),C3,AJ1(I),QJ1(I),C1,C2
000751     221 CONTINUE
000756         WRITE(NW,120)XM1,YM1
000765         WRITE(NW,161)
000771         DO 517 I=IH1,IP1
000775     517 WRITE(NW,102)FJ1(I),QA1(I),QB1(I),QC1(I)
001015         DD=DD2
001016         RB=RB2
001017         XM=XM2
001021         YM=YM2
001022         IF(MN) 302,301,302
001024     301 FJ=FNJ
001026         GO TO 310
001026     302 FJ=-FNJ
001030     310 F=F2
001031         EP=EP2
001033         GM=GE2
001034         CC=EE/FN2
001036         II=2
001040         WRITE(NW,152)
001043         CALL AJCOH
001044         L=NN
001046         DO 222 I=1,NN
001051         C4    =XJ(I)
001052         C5    =YJ(I)
001054         IH2=IH
001055         IP2=IP
001057         QA2(I)=QA(I)
001061         QB2(I)=QB(I)
```

```
001063          QC2(I)=QC(I)                                   GEARO    222
001065          FJ2(I)=PJ(I)                                   GEARO    223
001067          C1=AJ(I)                                       GEARO    224
001070          AJ2(L)=C1                                      GEARO    225
001073          C2=QJ(I)                                       GEARO    226
001074          QJ2(L)=C2                                      GEARO    227
001076          IF(C2) 519,518,519                             GEARO    228
001076      518 WRITE(NW,132)FJ2(I),C1                         GEARO    229
001106          GO TO 520                                      GEARO    230
001111      519 WRITE(NW,132)FJ2(I),C1,C2,C4,C5                GEARO    231
001127      520 IF(L-1) 222,222,226                            GEARO    232
001133      226 L=L-1                                          GEARO    233
001135      222 CONTINUE                                       GEARO    234
001140          WRITE(NW,120)XM2,YM2                           GEARO    235
001147          WRITE(NW,163)                                  GEARO    236
001153          DO 521 I=IM2,IP2                               GEARO    237
001157      521 WRITE(NW,102)FJ2(I),QA2(I),QB2(I),QC2(I)       GEARO    238
001177          DO 251 I=1,N                                   GEARO    239
001200          IN=I+N                                         GEARO    240
001201          FJC1(I)=FJ1(IN)                                GEARO    241
001204          AJC1(I)=AJ1(IN)                                GEARO    242
001206          AJC2(I)=AJ2(IN)                                GEARO    243
001210          QJD1(I)=QJ1(I)                                 GEARO    244
001212          QJC1(I)=QJ1(IN)                                GEARO    245
001214          QJC2(I)=QJ2(IN)                                GEARO    246
001216          QJD2(I)=QJ2(I)                                 GEARO    247
001220          CJD1(I)=CJ (I)                                 GEARO    248
001222      251 CJC1(I)=CJ (IN)                                GEARO    249
001226          MUZ=1                                          GEARO    250
001227          MMZ=1                                          GEARO    251
001230      197 CONTINUE                                       MAY1       1
001230          L=NN                                           GEARO    253
001232          DO 415 I=1,N                                   GEARO    254
001233          IN=I+N                                         GEARO    255
001234          UJD1(I)=UJ1(I)                                 GEARO    256
001236          UJC1(I)=UJ1(IN)                                GEARO    257
001241          UJC2(I)=UM2(IN)                                GEARO    258
001243          UJD2(I)=UM2(I)                                 GEARO    259
001245          ZJD1(I)=ZJ1(I)                                 GEARO    260
001247          ZJC1(I)=ZJ1(IN)                                GEARO    261
001251          ZJC2(I)=ZM2(IN)                                GEARO    262
001253          ZJD2(I)=ZM2(I)                                 GEARO    263
001255          QJC(I)=QJC1(I)+UJC1(I)+QJC2(I)+UJC2(I)         GEARO    264
001263          QJD(I)=QJD1(I)+UJD1(I)+QJD2(I)+UJD2(I)         GEARO    265
001273      415 ZJC(I)=ZJC1(I)+ZJC2(I)                         GEARO    266
001301      199 CONTINUE                                       GEARO    267
001301          WRITE(NW,106)                                  GEARO    268
001305          WRITE(NW,102)VPT1,VPT2                         GEARO    269
001317          VP1=VPT1/CS                                    GEARO    270
001322          VP2=VPT2/CS                                    GEARO    271
001324      418 CONTINUE                                       MAY1       2
001324          WRITE(NW,115)                                  GEARO    275
001330          DO 501 I=1,N                                   GEARO    276
001334          WT(I)=WT(N+I)                                  GEARO    277
001337          WN=WT(I)/CS                                    GEARO    278
```

```
001341          IF(WN)214,214,800                                                       GEAR0    279
001343      800 CONTINUE                                                                GEAR0    280
001343          C1=WN**.1                                                               MAY1       3
001347          QD=1.37/FF2*EP12/C1                                                     MAY1       4
001352          ZJD(I)=ZJD1(I)+ZJD2(I)+VP1-VP2                                          GEAR0    281
001360          CCC    =QJC(I)+QD                                                       GEAR0    282
001362          DDD    =QJD(I)+QD                                                       GEAR0    283
001364          C1=CJC1(I)                                                              GEAR0    284
001366          C2=CJD1(I)                                                              GEAR0    285
001367          IF(C1) 256,256,257                                                      GEAR0    286
001371      256 IF(C2) 501,501,258                                                      GEAR0    287
001373      257 IF(C2) 259,259,260                                                      GEAR0    288
001375      259 VJ(I)=ZJC(I)-CCC    *WN                                                 GEAR0    289
001401          WTC(I)=WN*CS                                                            GEAR0    290
001403          WTD=0.0                                                                 GEAR0    291
001404          GO TO 261                                                               GEAR0    292
001405      258 VJ(I)=ZJD(I)-DDD    *WN                                                 GEAR0    293
001411          WTC(I)=0.0                                                              GEAR0    294
001412          WTD=WN*CS                                                               GEAR0    295
001414          GO TO 261                                                               GEAR0    296
001415      260 C3=CCC    *WN+ZJD(I)-ZJC(I)                                             GEAR0    297
001422          C4=DDD    *WN+ZJC(I)-ZJD(I)                                             GEAR0    298
001426          IF(C3) 259,259,262                                                      GEAR0    299
001430      262 IF(C4) 258,258,263                                                      GEAR0    300
001432      263 C1=CCC+DDD                                                              GEAR0    301
001434          C2=CCC    *ZJD(I)+DDD    *ZJC(I)-CCC*DDD*WN                             GEAR0    302
001442          VJ(I)=C2/C1                                                             GEAR0    303
001444          C1=CS/C1                                                                GEAR0    304
001445          WTC(I)=(DDD*WN+ZJC(I)-ZJD(I))*C1                                        GEAR0    305
001452          WTD=(CCC*WN+ZJD(I)-ZJC(I))*C1                                           GEAR0    306
001460      261 EJ1(I)=VJ(I)/CS                                                         GEAR0    307
001463          AJC1(I)=ANG+AJC1(I)                                                     GEAR0    308
001465          WRITE(NW,102)FJC1(I),AJC1(I),EJ1(I),WTC(I),WTD,WN,WT(I),QD              MAY1       5
001511      501 CONTINUE                                                                GEAR0    310
001516          ANG=AJC1(N)                                                             GEAR0    311
001517       24 IF(NUZ-MUZ) 504,504,502                                                 GEAR0    312
001522      502 MUZ=MUZ+1                                                               GEAR0    313
001524          GO TO 199                                                               GEAR0    314
001524      504 MUZ=1                                                                   GEAR0    315
001525          IF(NMZ-MMZ) 214,214,506                                                 GEAR0    316
001530      506 MMZ=MMZ+1                                                               GEAR0    317
001532          GO TO 197                                                               GEAR0    318
001532      214 CONTINUE                                                                GEAR0    319
001532      503 RETURN                                                                  GEAR0    320
001533      102 FORMAT(8E13.5)                                                          MAY1       6
001533      106 FORMAT(//34H INPUT DATA ON TOOTH SPACING ERROR/6X4HVPT19X4HVPT2)        GEAR0    322
001533      110 FORMAT(60H0INPUT LISTING OF PROFILE ERROR AND SUPPLEMENTARY COMPLI      GEAR0    323
               1ANCE/6X2HZ111X2HU111X2HZ211X2HU2)                                       GEAR0    324
001533      112 FORMAT(16H0PRES.ANGLE(DEG))                                             FINAL      7
001533      115 FORMAT(42H0CALCULATED TOOTH MESHING ERRORS AND LOADS//6X3HJC19X4HA      GEAR0    325
               1JC16X11HTANG. ERROR6X3HWTC10X3HWTD11X2HWN11X2HWT10X3HQJD)               MAY1       7
001533      118 FORMAT(74H0DRIVING GEAR INPUT ROOT RADIUS SMALLER THAN BASE CIRCLE      GEAR0    327
               1 RADIUS                         )                                       GEAR0    328
001533      119 FORMAT(74H0DRIVEN  GEAR INPUT ROOT RADIUS SMALLER THAN BASE CIRCLE      GEAR0    329
               1 RADIUS                         )                                       GEAR0    330
```

```
001533      120 FORMAT(48H0COOD. OF EFFECTIVE TOOTH PROFILE AT ROOT CIRCLE11X1HX13 GEARO    331
               1X1HY/52X,2E13.6)                                               GEARO    332
001533      122 FORMAT(/6X3HRP110X3HRB110X3HBA110X3HBR110X3HAT1)               ALG       10
001533      125 FORMAT(66H0 DRIVEN GEAR TEETH ENGAGE UNDER CUT PORTION OF DRIVING  GEARO    334
               1GEAR TEETH//6H  BA1=,  E13.6)                                  GEARO    335
001533      126 FORMAT(66H0 DRIVING GEAR TEETH ENGAGE UNDER CUT PORTION OF DRIVEN  GEARO    336
               1GEAR TEETH//6H  BR1=,  E13.6)                                  GEARO    337
001533      132 FORMAT(  E13.5,13X,4E13.5)                                     GEARO    338
001533      151 FORMAT(/6X2HJ111X3HCJ110X3HAJ18X6HQJ1ABC9X3HXJ110X3HYJ1)       GEARO    339
001533      152 FORMAT(/6X2HJ224X3HAJ28X6HQJ2ABC9X3HXJ210X3HYJ2)               GEARO    340
001533      155 FORMAT(63H0DRIVEN  GEAR INPUT RADIUS TO FILLET CENTER INSIDE BASE  GEARO    341
               1CIRCLE./42H0PROGRAM CONTINUES WITH CORRECT TREATMENT.)          GEARO    342
001533      156 FORMAT(63H0DRIVING GEAR INPUT RADIUS TO FILLET CENTER INSIDE BASE  GEARO    343
               1CIRCLE./42H0PROGRAM CONTINUES WITH CORRECT TREATMENT.)          GEARO    344
001533      159 FORMAT(13X,4E13.5)                                             GEARO    345
001533      161 FORMAT(/6X2HJ110X4HQJ1A9X4HQJ1B9X4HQJ1C)                        GEARO    346
001533      162 FORMAT(/6X3HRP210X3HRB210X3HBA210X3HBR210X3HAT2)               GEARO    347
001533      163 FORMAT(/6X2HJ210X4HQJ2A9X4HQJ2B9X4HQJ2C)                        GEARO    348
001533      170 FORMAT(43H0CALCULATED TOTAL CONTACT COMPLIANCE   QJD=,E13.6)   GEARO    349
001533      171 FORMAT(23H0CALCULATED NORMAL  WN=,  E13.6)                     GEARO    350
001533      174 FORMAT(80H0 ANGLE OF APPROACH ON DRIVING GEAR IS GREATER THAN TOOT GEARO    351
               1H SPACING ANGLE. PROGRAM/25HCONTINUED WITHOUT OVERLAP)          GEARO    352
001533      175 FORMAT(75H0 ANGLE OF RECESS ON DRIVING GEAR IS NOT SMALLER THAN TO GEARO    353
               1OTH SPACING ANGLE. /34H PROGRAM CONTINUED WITHOUT OVERLAP)      GEARO    354
001533      176 FORMAT(80H0 DRIVING GEAR TEETH MESHING ON PROFILE INSIDE OF TIF DI GEARO    355
               1AMETER. PROGRAM CONTINU-/21HED WITHOUT CORRECTION)              GEARO    356
001533      178 FORMAT(80H0 DRIVEN  GEAR TEETH MESHING ON PROFILE OUTSIDE OF TIF D GEARO    357
               1IAMETER. PROGRAM CONTIN-/22HUED WITHOUT CORRECTION)             GEARO    358
001533      179 FORMAT(80H0 DRIVEN  GEAR TEETH MESHING ON PROFILE INSIDE OF TIF DI GEARO    359
               1AMETER. PROGRAM CONTINU-/21HED WITHOUT CORRECTION)              GEARO    360
001533          END                                                            GEARO    361
```

RUN VERSION 2.3 --PSR LEVEL 332--

```
                  SUBROUTINE AJCDH                                               AJCDH
000002            DIMENSION SD(50),CD(50),BIK(50),AIK(50),FLK(50) ,CDC(50)      AJCDH
000002            COMMON PJ(50),CJ(50),QJ(50),AJ(50),XJ(50),YJ(50),             MAY11
                 1A(1500),B(1500),G(3000)                                        MAY11
000002            COMMON DD,BR,BA,FJ,CC,YM,NN,N,FNJ,EP,TAN,RB,GM,F,XM,MN,II,[illegible] AJCDH
000002            COMMON QA(50),QB(50),QC(50),QA1(50),QB1(50),QC1(50),QA2([illegible]QB2(50 AJCDH
                 1),QC2(50),IH,IP                                                AJCDH
000003            DO 106 I=1,NN                                                  AJCDH
000004            QA(I)=0.0                                                      AJCDH
000005            QB(I)=0.0                                                      AJCDH
000006            QC(I)=0.0                                                      AJCDH
000007            QJ(I)=0.0                                                      AJCDH
000010            XJ(I)=0.0                                                      AJCDH
000011        106 YJ(I)=0.0                                                      AJCDH
000014            IF(II-1) 405,405,403                                           AJCDH
000017        405 MM=1.0                                                         AJCDH
000021            GO TO 404                                                      AJCDH
000022        403 MM=MN                                                          AJCDH
000024        404 K=1                                                            AJCDH
000025            DO 501 I=1,NN                                                  AJCDH
000027            AJ(I)=FJ*CC                                                    AJCDH
000031            PJ(I)=FJ                                                       AJCDH
000032            IF(II-1) 412,412,413                                           AJCDH
000035        412 CALL CALCJ(AJ(I),BR,BA,XY)                                     AJCDH
000042            CJ(I)=XY                                                       AJCDH
000044            GO TO 414                                                      AJCDH
000045        413 XY=CDC(I)                                                      AJCDH
000047        414 IF(XY) 503,503,101                                             AJCDH
000051        101 IF(K-1) 102,102,103                                            AJCDH
000054        102 IH=I                                                           AJCDH
000056        103 AX=AJ(I)                                                       AJCDH
000060            DJ=DD+AX                                                       AJCDH
000062            SD(I)=SIN (DJ)                                                 AJCDH
000066            CD(I)=COS (DJ)                                                 AJCDH
000072            C1=ATAN (TAN*AX)                                               AJCDH
000076            C3=COS (C1)                                                    AJCDH
000100            C4=C1-DJ                                                       AJCDH
000102            IF(MM) 402,401,402                                             AJCDH
000104        401 C4=-C4                                                         AJCDH
000105        402 C5=SIN (C4)                                                    AJCDH
000107            C6=COS (C4)                                                    AJCDH
000111            C1=RB/C3                                                       AJCDH
000113            XJ(I)=C1*C6                                                    AJCDH
000116            YJ(I)=C1*C5                                                    AJCDH
000120            IF(K-1) 242,242,243                                            AJCDH
000122        242 BIK(I)=(YJ(I)**3+YM**3)/3.0*F                                  AJCDH
000130            AIK(I)=(YJ(I)+YM)*F                                            AJCDH
000133            FLK(I)=XJ(I)-XM                                                AJCDH
000136            GO TO 504                                                      AJCDH
000136        243 BIK(I)=(YJ(I)**3+YJ(I-1)**3)/3.0*F                             AJCDH
000144            AIK(I)=(YJ(I)+YJ(I-1))*F                                       AJCDH
000147            FLK(I)=XJ(I)-XJ(I-1)                                           AJCDH
000152        504 K=K+1                                                          AJCDH
000154        503 IF(I-NN) 502,501,501                                           AJCDH
```

```
000157      502 IF(MM) 506,505,506                         AJCDH
000160      505 FJ=FJ-1.                                   AJCDH
000162          GO TO 501                                  AJCDH
000163      506 FJ=FJ+1.0                                  AJCDH
000165      501 CONTINUE                                   AJCDH
000170          IF(II-1) 301,301,302                       AJCDH
000172      301 IF(MM) 601,302,601                         AJCDH
000173      601 LL=NN                                      AJCDH
000175          DO 303 I=1,NN                              AJCDH
000176          CDC(I)=CJ(LL)                              AJCDH
000200          IF(LL-1) 303,303,305                       AJCDH
000203      305 LL=LL-1                                    AJCDH
000205      303 CONTINUE                                   AJCDH
000210      302 IP=K+IM-2                                  AJCDH
000213      410 DO 246 L=IM,IP                             AJCDH
000215          E1=0.0                                     AJCDH
000216          E2=0.0                                     AJCDH
000216          E3=0.0                                     AJCDH
000217          E4=0.0                                     AJCDH
000220          EE=XJ(L)-XM                                AJCDH
000223          IM=L                                       AJCDH
000223          IF(MM) 202,203,202                         AJCDH
000225      203 EE=-EE                                     AJCDH
000226      202 DO 245 I=IM,IM                             AJCDH
000230          C1      =XJ(L)-XJ(I)                       AJCDH
000233          C5=FLK(I)                                  AJCDH
000234          IF(MM) 207,208,207                         AJCDH
000236      208 C1=-C1                                     AJCDH
000237          C5=-C5                                     AJCDH
000241      207 C2=C5/BIK(I)                               AJCDH
000243          C3=(C5+3.0*C1)*C5+3.0*C1*C1                AJCDH
000251          E4=E4+C2                                   AJCDH
000253          C4=2.0*C1+C5                               AJCDH
000255          E1=E1+C3*C2                                AJCDH
000260          E2=E2+C4*C2                                AJCDH
000263      245 E3=E3+C5/AIK(I)                            AJCDH
000271          IF(MM) 206,205,206                         AJCDH
000272      205 IM=IM-1                                    AJCDH
000274      206 C1=CD(L)*CD(L)                             AJCDH
000276          C2=SD(L)*YJ(L)                             AJCDH
000300          QA(L) =C1/3.0*E1/EP+(C2*E4-CD(L)*E2)/EP*C2 AJCDH
000312          QB(L) =C1/GM*E3*1.2                        AJCDH
000317          C1=(EE*CD(L)-YJ(L)*SD(L))/YM               AJCDH
000323          QC(L)=C1/EP*1.327/F*C1                     AJCDH
000330      246 QJ(L)=QA(L)+QB(L)+QC(L)                    AJCDH
000336          RETURN                                     AJCDH
000337          END                                        AJCDH
```

RUN VERSION 2.3 --PSR LEVEL 332--

```
                  SUBROUTINE FOUR                                                        FOUR        2
           C      REQUIRES 2*N+1 POINTS  F(I)                                            FOUR        3
           C      POINTS CORRESPOND TO THETA=2*PI/(2*N+1),...,2*PI                       FOUR        4
           C      OUTPUT  A(I),B(I)  REFER TO COSINE AND SINE OF (I-1)*THETA             FOUR        5
000002            COMMON PJ(50),CJ(50),QJ(50),AJ(50),XJ(50),YJ(50),                      FOUR        6
                 1A(1500),B(1500),G(3000)                                                MAY11       6
000002            COMMON DD,BR,BA,FJ,CC,YM,NN,N,FNJ,EP,TAN,RB,GM,F,XM,MN,II,M            FOUR        8
000002            COMMON/GU/NMC,INT,MMM,IPLT,FN1,FN2,RB1,RO1,RO2,RT1,RT2,RM1,RM2,FI,     MAY9        8
                 1T1,T2,F1,F2,RF1,RF2,YE1,YE2,GE1,GE2,POS1,POS2,ANG                      MAY9        9
000002            C=1.0                                                                  FOUR        9
000003            S=0.0                                                                  FOUR       10
000004            M=IFIX(FI)*NMC+NMC/2                                                   MAY9       10
000010            N1=M+1                                                                 FOUR       11
000012            NA=N*NMC                                                               MAY9       11
000014            N2=NA-1                                                                MAY9       12
000015            T1=2./NA                                                               MAY9       13
000020            T2=T1*3.1415927                                                        FOUR       15
000021            C1=COS (T2)                                                            FOUR       16
000023            S1=SIN (T2)                                                            FOUR       17
000026            DO 7 IP=1,N1                                                           FOUR       18
000027            U1=0.0                                                                 FOUR       19
000030            U2=0.0                                                                 FOUR       20
000031            DO 3 I=1,N2                                                            FOUR       21
000032            J=N2-I+2                                                               FOUR       22
000034            U3=G(J)+2.0*C*U1-U2                                                    FOUR       23
000042            U2=U1                                                                  FOUR       24
000043          3 U1=U3                                                                  FOUR       25
000047            A(IP)=T1*(G(1)+C*U1-U2)                                                FOUR       26
000054            B(IP)=T1*S*U1                                                          FOUR       27
000056            AA=A(IP)*C-B(IP)*S                                                     FOUR       28
000062            BB=A(IP)*S+B(IP)*C                                                     FOUR       29
000065            A(IP)=AA                                                               FOUR       30
000067            B(IP)=BB                                                               FOUR       31
000071            Q=C1*C-S1*S                                                            FOUR       32
000074            S=C1*S+S1*C                                                            FOUR       33
000077          7 C=Q                                                                    FOUR       34
000103            RETURN                                                                 FOUR       35
000103            END                                                                    FOUR       36

                  SUBROUTINE CALCJ(C1,C2,C3,C4)                                          CALCJ       2
000007            IF(C3) 240,231,241                                                     CALCJ       3
000011            DATA EHEAD3/4H LB./                                                    CALCJ       4
000011        241 IF(C1) 230,218,218                                                     CALCJ       5
000013        230 IF(ABS (C1)-C3)  220,220,219                                           CALCJ       6
000017        231 IF(C1) 219,218,218                                                     CALCJ       7
000021        240 IF(C1) 219,219,242                                                     CALCJ       8
000023        242 C3=-C3                                                                 CALCJ       9
000024            IF(C1-C3) 219,218,218                                                  CALCJ      10
000026        218 IF(C2-C1) 219,220,220                                                  CALCJ      11
000030        220 C4=1.0                                                                 CALCJ      12
000031            GO TO 221                                                              CALCJ      13
000032        219 C4=0.0                                                                 CALCJ      14
000033        221 RETURN                                                                 CALCJ      15
000034            END                                                                    CALCJ      16
```

RUN VERSION 2.3 --PSR LEVEL 332--

```
                 SUBROUTINE PLT(X,Y,Z,NPTS)                                    PLT          2
000007           DIMENSION Y(3000),X(3000),Z(3000),AXX(4),AYY(4),AZZ(4),ILABX(5),  MAY11     7
                1           ILABY(5),HEAD3(3)                                  PLT          4
000007           COMMON PJ(50),CJ(50),QJ(50),AJ(50),XJ(50),YJ(50),             MAY11        8
                1A(1500),B(1500),G(3000)                                       MAY11        9
000007           COMMON DD,BR,BA,FJ,CC,YM,NN,N,FNJ,EP,TAN,RB,GM,F,XM,MN,II,M   PLT          6
000007           COMMON QA(50),QB(50),QC(50),QA1(50),QB1(50),QC1(50),QA2(50),QB2(50 PLT     7
                1),QC2(50) ,IH,IP                                              PLT          8
000007           COMMON WT(50),HEAD1(6),HEAD2(6)                               MAY1        11
000007           DATA (ILABX(J),J=1,3)/10H     CALCUL,10HATION POIN,2HT /      PLT         10
000007           DATA (ILABY(J),J=1,3)/10HTANGENTIAL,10H ERROR (IN,2H.)/       PLT         11
000007           DATA ILABZ/10HLOAD (LB.)/                                     PLT         12
000007           DATA (HEAD3(I),I=1,2)/10HTANG. FORC,4HE = /                   PLT         13
000007           IN=5                                                          PLT         14
000007           IO=6                                                          PLT         15
000010           ICAL=22                                                       PLT         16
000012           CALL PLOTS(IBUF,4000,ICAL)                                    PLT         17
000014           CALL PLOT(4.,4.5,-3)                                          PLT         18
000017           CALL PLOT(-2.,-4.,3)                                          PLT         19
000022           CALL DASHPT(-2.,6.,.25)                                       PLT         20
000025           CALL SCALE(X,5.,NPTS,+1)                                      PLT         21
000032           Y(NPTS+1)=0.                                                  PLT         22
000036           DO 10 K=1,NPTS                                                PLT         23
000040        10 Y(K)=-Y(K)                                                    PLT         24
000043           CALL SCALE(Y,4.,NPTS+1,+1)                                    PLT         25
000050           Y(NPTS+2)=Y(NPTS+3)                                           PLT         26
000056           CALL SCALE(Z,3.,NPTS,+1)                                      PLT         27
000061           AXX(1)=X(NPTS+1)                                              PLT         28
000065           AXX(2)=X(NPTS+2)                                              PLT         29
000067           AYY(1)=Y(NPTS+1)                                              PLT         30
000071           AYY(2)=Y(NPTS+2)                                              PLT         31
000073           AZZ(1)=Z(NPTS+1)                                              PLT         32
000074           AZZ(2)=Z(NPTS+2)                                              PLT         33
000077           CALL AXIS(0.,0.,ILABX,-22,5.,0.,AXX(1),AXX(2))                PLT         34
000106           CALL AXIS(0.,0.,ILABY,22,4.,90.,0.,AYY(2))                    PLT         35
000116           CALL FLINE(X,Y,-NPTS,1,1,3)                                   PLT         36
000125           CALL PLOT(0.,-4.,-3)                                          PLT         37
000130           CALL AXIS(0.,0.,ILABX,-22, 5.,0.,AXX(1),AXX(2))               PLT         38
000140           CALL AXIS(0.,0.,ILABZ,10,3.,90.,AZZ(1),AZZ(2))                PLT         39
000150           CALL FLINE(X,Z,-NPTS,1,1,11)                                  PLT         40
000157           CALL PLOT(.5,9.5,-3)                                          PLT         41
000162           CALL SYMBOL(0.,0.,.14,HEAD1,0.,40)                            PLT         42
000166           CALL SYMBOL(0.,-.25,.14,HEAD2,0.,40)                          PLT         43
000172           CALL SYMBOL(0.,-.5,.14,HEAD3,0.,14)                           PLT         44
000176           CALL NUMBER(999.,999.,.14,WT,0.,2)                            PLT         45
000202           CALL SYMBOL(999.,999.,.14,EHEAD3,0.,4)                        PLT         46
000206           CALL PLOT(6.,-9.,-3)                                          PLT         47
000211           CALL DASHPT(0.,9.,.25)                                        PLT         48
000214           CALL PLOT(0.,0.,999)                                          PLT         49
000217           DO 20 K=1,NPTS                                                PLT         50
000223        20 Y(K)=-Y(K)                                                    PLT         51
000226           RETURN                                                        PLT         52
000227           END                                                           PLT         53
```

RUN VERSION 2.3 --PSR LEVEL 332--

```
                 SUBROUTINE SPECT
000002           DIMENSION GN(3000),RR(3000),FR(200),GK(200),KK(200),GKK(200)
000002           COMMON PJ(50),CJ(50),QJ(50),AJ(50),XJ(50),YJ(50),
                1A(1500),B(1500),G(3000)
000002           COMMON DD,BR,BA,FJ,CC,YM,NN,N,FNJ,EP,TAN,RB,GM,F,XM,MN,II,M
000002           COMMON/GU/NMC,INT,MMM,IPLT,FN1,FN2,RR1,RO1,RO2,RT1,RT2,RM1,RM2,FI,
                1T1,T2,F1,F2,RF1,RF2,YE1,YE2,GE1,GE2,POS1,POS2,ANG
000002           NR=5
000003           NW=6
           C NWS=1,WS=SPEED OF DRIVING GEAR IN RPM
           C NWS=2,WS=SPEED OF DRIVEN GEAR IN RPM
000004           READ(NR,100) NWS,WS
000014           WS=WS*6.28/60.
000016           FM=FN1*WS/6.28
000020           IF(NWS.EQ.2) FM=FN2*WS/6.28
000024           WRITE(NW,110) FM
000032           FC=FM*N/2.
000035           NT=N*NMC
000037           TR=NMC/FM
000041           H=1./FM/N
000044           FO=1./TR
000046           M=NT/20
000051           SM=M
000052           TMAX=M*H
000055           BE=1./TMAX
000057           WRITE(NW,115)
000062           WRITE(NW,120) FC,FO,BE
000074           WRITE(NW,125)
000100           WRITE(NW,120) H,TR,TMAX,SM
000114           SUM=0.
000115           DO 10 I=1,NT
000117        10 SUM=SUM+G(I)
000123           SA=SUM/NT
000125           DO 20 I=1,NT
000127           GN(I)=G(I)-SA
000132        20 CONTINUE
000134           MM=M+1
000136           DO 30 I=1,MM
000137           IR=I-1
000140           FR(I)=IR*FC/SM
000144           CC=1./(NT-IR)
000147           RR(I)=0.
000151           DO 25 J=1,NT
           C RR(I)=R(I-1)
000153           IF((J+IR).GT.NT) GO TO 30
000157        25 RR(I)=GN(J)*GN(J+IR)+RR(I)
000165        30 RR(I)=RR(I)*CC
000172           MS=M-1
000174           DO 40 K=1,MM
000175           KK(K)=K-1
000177           GK(K)=RR(1)+RR(MM)*(-1.)**KK(K)
000206           SSS=0.
000207           DO 35 JK=1,MS
000211           JJ=JK+1
```

```
RUN VERSION 2.3 --PSR LEVEL 332--                                    SPECT

000212          AA=3.1416*JK*KK(K)/SM                                          MAY11      62
000217       35 SSS=SSS+2.*RR(JJ)*COS(AA)                                      MAY11      63
000230       40 GK(K)=(GK(K)+SSS)*2.*H                                         MAY11      64
000236          GKK(1)=.5*GK(1)+.5*GK(2)                                       MAY11      65
000241          GKK(MM)=.5*GK(M)+.5*GK(MM)                                     MAY11      66
000246          DO 50 LL=2,M                                                   MAY11      67
000247          GKK(LL)=.25*GK(LL-1)+.5*GK(LL)+.25*GK(LL+1)                    MAY11      68
000255       50 CONTINUE                                                       MAY11      69
000260          WRITE(NW,130)                                                  MAY11      70
000264          WRITE(NW,140)                                                  MAY11      71
000270          DO 60 I=1,MM                                                   MAY11      72
000272          SKM=KK(I)*N/(2.*SM)                                            JUNE7       6
000277          WRITE(NW,150)KK(I),FR(I),GK(I),GKK(I),SKM                      JUNE7       7
000314       60 CONTINUE                                                       MAY11      74
000317      100 FORMAT(I5,E13.5)                                               MAY11      75
000317      110 FORMAT(/1X26HMESHING FREQUENCY IN CPS =,E13.5)                 MAY11      76
000317      115 FORMAT(/7X2HFC11X2HFO11X2HBE)                                  MAY11      77
000317      120 FORMAT(8E13.5)                                                 MAY11      78
000317      125 FORMAT(/7X1HH12X2HTR11X4HTMAX9X2HSM)                           MAY11      79
000317      130 FORMAT(/1X31HPOWER SPECTRAL DENSITY FUNCTION)                  MAY11      80
000317      140 FORMAT(/6X,1HK6X2HFR11X2HGK11X3HGKK10X2HKM)                    JUNE7       8
000317      150 FORMAT(I7,3E13.5,F13.5)                                        JUNE7       9
000317          RETURN                                                         MAY11      83
000317          END                                                            MAY11      84
```